STRUCTURAL ORGANIZATION OF PULMONARY SURFACTANT FILMS

by

Bohdana M. Discher

A DISSERTATION

Presented to the Department of Biochemistry and Molecular Biology
and the Oregon Health Sciences University
School of Medicine
in partial fulfillment of
the requirements for the degree of

Doctor of Philosophy

March, 1998

School of Medicine

Oregon Health Sciences University

CERTIFICATE OF APPROVAL

This is to certify that the Ph.D. thesis of

Bohdana M. Discher

has been approved

[redacted]

Professor in charge of thesis

[redacted]

Member

[redacted]

Member

[redacted]

Member

Associate Dean for Graduate Studies

TABLE OF CONTENTS

ACKNOWLEDGMENTS

I would like to acknowledge the following assistance. Dr. Kevin M. Maloney helped with my initial training with Langmuir trough and fluorescence microscopy experiments. William R. Schief was responsible for the Brewster angle microscopy setup and assisted with the BAM imaging and data analysis. Walter Anyan and Heather Helming often helped with the preparations of surfactant fractions. Professors Viola Vogel and David W. Grainger were very helpful with useful suggestions in numerous discussions. Professor Stephen B. Hall helped throughout the thesis project including correcting the grammar and clarity of expression in this thesis.

ABSTRACT

The presence of a very dense, ordered film of pulmonary surfactant may be crucial for normal function of the lung. Surfactant films cover the thin liquid layer that lines the alveolar air spaces. During exhalation the alveolar surface is decreasing and the film is being compressed. To prevent the alveoli from a possible collapse, the compression of pulmonary surfactant has to produce very dense and stable films. The set of studies that embody this thesis first demonstrates and then elucidates the lateral phase separation that occurs during compression of pulmonary surfactant films. The phase separation in films of complete pulmonary surfactant manifests itself through formation of distinct domains. As the film becomes more dense, however, the domains remix with the surrounding phase. To characterize the phase behavior we have used fluorescence microscopy, Brewster angle microscopy, and surface potential measurements. Using a simplified system containing only the purified phospholipids (PPL), we used the variation in the area of the domains in response to added dipalmitoyl phosphatidylcholine (DPPC), the most prevalent component in pulmonary surfactant, to construct a phase diagram. The phase diagram revealed that the domains contain pure DPPC whereas the surrounding regions contain reduced amounts of DPPC along with the other phospholipids, and have the disorganized compressible structure of a fluid phase. The result that the domains in PPL films are DPPC is also supported by their optical thickness and birefringence. The surface pressure at which the domains emerge during compression over a wide range of temperatures suggests that DPPC is the major constituent of the condensed phase in preparations containing more than the surfactant phospholipids. The domains in the PPL films, however, did not remix with the surrounding phase as the film became more dense. To determine the constituents responsible for remixing, we have used surfactant preparations from which the surfactant proteins or neutral lipids were removed. Surfactant proteins were found to reduce the amount of DPPC that enters the domains but to have no effect on miscibility. We have

determined that the remixing is caused by the neutral lipids and that it occurs at or close to a critical point in the phase diagram. Analysis of the interfacial tension between the two phases, which approaches zero at the critical point, suggests that neutral lipids partition into the domains, expanding that phase to allow remixing with the surrounding film. The critical behavior of pulmonary surfactant films suggests that the final phase is not a liquid-condensed DPPC film as it was hypothesized previously but instead a very dense, fluid phase which contains both DPPC and neutral lipids.

CHAPTER 1

INTRODUCTION

Pulmonary surfactant is the mixture of lipids and proteins that covers the thin layer which lines the alveolar air spaces (Fig. 1.1). The major function of pulmonary surfactant is to lower surface tension and in doing so prevent small alveoli from collapsing. The presence of surface-active material in animal lungs was first demonstrated by Pattle (Pattle, 1955). Surfactant deficiency was very soon linked to respiratory failure in premature babies (Avery and Mead, 1959), a condition known today as neonatal respiratory distress syndrome (RDS). RDS is initiated by an inadequate pool of functional surfactant within a structurally and functionally immature lung. Some twenty years later, it was shown that RDS can be treated effectively by administration of exogenous lung surfactant (Fujiwara et al., 1980). Many successful clinical trials have since confirmed that such treatments significantly reduce mortality, morbidity, and other complications associated with RDS including air leaks. Public recognition of these successes came in 1990, when the United States Food and Drug Administration approved lung surfactants for the treatment of premature babies.

There are two general classes of surfactants used for the treatment of RDS: surfactants obtained from mammalian lungs, and surfactants prepared synthetically. A significant effort is directed towards the replacement of natural surfactants by synthetic ones in order to: (1) avoid any possible risk of infection and/or immunological sensitization; and (2) reduce material costs. From the immunological point of view the major concern is contamination of bovine surfactant with prion particles from nervous tissue. Prions are infectious particles (resistant to some sterilizing techniques) which are responsible for slow encephalopathies, some of which have crossed species barriers. Synthetic surfactant has no risk of prion contamination. The high cost of natural surfactant makes it unavailable for treatments of adults with acute RDS (ARDS) who need much

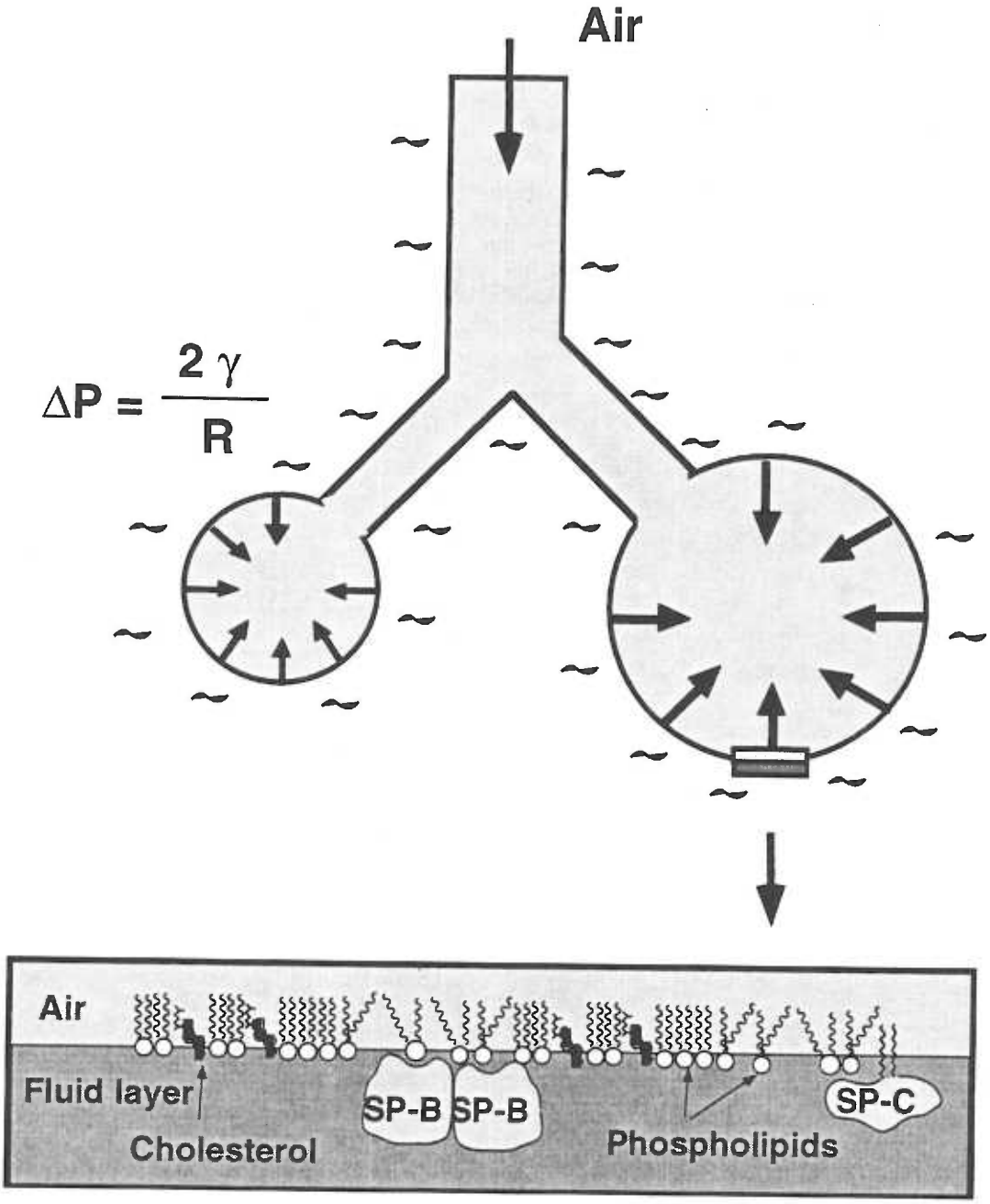

1.1. Pulmonary surfactant is the mixture of phospholipids, neutral lipids, and proteins that covers the thin layer which lines the alveolar air spaces.

higher doses of surfactant than premature newborns. ARDS, formerly called adult RDS, has become a well-recognized disease in adults as well as in children. It results from a number of different causes that lead to injury of the alveolar-capillary membrane, high-permeability pulmonary edema and consequent disruption of the pulmonary surfactant system. Current treatments for ARDS are still inadequate and the reported mortality remains unacceptably high at 40 - 70% (Suchyta et al., 1992). The results from clinical studies in which patients with ARDS were treated with exogenous surfactant are still very limited and controversial. The evaluations of the reports are further complicated by many variables involved in the treatments including (1) the specific surfactant preparation used, (2) the delivery method used (instillation vs. aerosolization), (3) the timing of surfactant treatment over the course of injury, (4) the dose of surfactant administered (Lewis and Veldhuizen, 1995) and (5) different etiologies for ARDS, such as aspiration pneumonia, sepsis, or trauma (Evans et al., 1996). Nevertheless, there is growing supporting evidence for surfactant replacement therapy that comes from studies of ARDS both in children (Evans et al., 1996) and in adults (Gregory et al., 1997). Therefore it is believed that highly effective surfactant that can be synthesized in large quantities might be one of the crucial steps in development of the treatment for ARDS.

The number of synthetic surfactants that have been evaluated in large clinical studies is very limited. The first clinical trial involved administration of pure dipalmitoyl phosphatidylcholine (DPPC) and was unsuccessful (Chu et al., 1967). The second was a 7:3 mixture of DPPC:phosphatidylglycerol, and the last one was a mixture of DPPC, hexadecanol, and tyloxapol (Jobe, 1993). These relatively simple mixtures were found to be less effective in comparison to natural surfactant (Hudak et al., 1997).

In comparison to the evaluated synthetic surfactants, natural surfactant is significantly more complex. The composition of natural pulmonary surfactant is qualitatively similar to the overall composition of cell membranes in that phospholipids, neutral lipids, and proteins are all present. In pulmonary surfactant, phospholipids are the

most prevalent component, accounting for approximately 85% by weight. The majority of phospholipids are phosphatidylcholines (PCs), but unlike PCs in cell membranes (Holub and Kuksis, 1978; Kuksis et al., 1968; Montfoort et al., 1971), in pulmonary surfactant the amount of phosphatidylcholines with both fatty acids fully saturated is unusually high. Almost half of the PCs are saturated (Kahn et al., 1995). Indeed, DPPC, the most abundant component of pulmonary surfactant, is a saturated PC. After PC, the second most abundant phospholipid headgroup is phosphatidylglycerol (PG), which is usually a minor component in animal cell membranes (Caminiti and Young, 1991). The major cell membrane phospholipid headgroups, including phosphatidylethanolamine, phosphatidylserine, and sphingomyelin, are all present in pulmonary surfactant in relatively small quantities.

Neutral lipids in pulmonary surfactant account for about 10% by weight (Poulain and Clements, 1995). The main neutral lipid is cholesterol or a cholesterol derivative. Other neutral lipids include triglycerides, free fatty acids, and trace components (Wright and Clements, 1987). The role of neutral lipid is not clear. Cholesterol is known to interact with the phospholipid's chains and, as a consequence, alter the fluidity of surfactant films. In fact, the content of cholesterol in surfactant is temperature-dependent as is most apparent in reptiles. Cold lizards (18 °C) have significantly elevated levels of cholesterol (Daniels et al., 1995).

At least three different proteins co-isolate with surfactant. These proteins were named SP-A, SP-B, and SP-C in chronological order of their discovery (Possmayer, 1988). A fourth surfactant protein, SP-D, was also found in alveolar lavage but because it does not bind lipids and does not co-isolate with the rest of the surfactant after centrifugation (Kuroki et al., 1991), it is often not considered to be a true surfactant protein. Both SP-A and SP-D are large, multimeric, glycosylated, and water-soluble proteins. They belong to a family of Ca^{2+}-dependent collectins that also includes a mannose-binding protein, complement factor C1q, conglutinin, and collectin-43

(Johansson and Curstedt, 1997). All collectins possess an elongated collagen-like domain and a globular head containing a carbohydrate-recognition domain. SP-A is the most abundant surfactant protein (5-10% by mass) that was considered to be essential for surfactant function. However, recent studies showed that no obvious effects on the respiratory capacity can be observed when its gene is knocked out in mice (Korfhagen et al., 1996). The actual role of SP-A seems to be participation in the lung host defense system (LeVine et al., 1997). Extraction of surfactant excludes SP-A, and none of the samples studied in this thesis include that protein.

Both SP-B and SP-C are involved in rapid adsorption of surfactant phospholipids to the alveolar surface (Haagsman and van Golde, 1991). They are small, extremely hydrophobic proteins. These two proteins can be extracted together with lipids into organic solvents. SP-B is a dimer of molecular weight 17.4 kDa. The SP-C is just 4.2 kDa and it is palmitoylated on two residues. Both SP-B and SP-C are present in significantly smaller amounts than SP-A. For example, in porcine derived surfactant extracted by chloroform/methanol and purified by liquid-gel chromatography to exclude neutral lipids, SP-B constitutes 0.7% (of total mass) and SP-C constitute just 0.4% (Curstedt et al., 1993).

The primary role of lung surfactant is to minimize the surface tension of the air-liquid interface in the alveoli. Pulmonary surfactant is synthesized by specific cells, the type II alveolar epithelial cells, and assembled into lamellar bodies which are secreted by exocytosis into the fluid layer lining the alveoli. After secretion, the pulmonary surfactant components are rapidly adsorbed to the air-fluid interface. Due to the ability of surfactant to reduce surface tension, its presence at the air-fluid interface prevents collapse of the smaller alveoli at the end of exhalation. For a spherical surface, the surface tension is given by the Laplace equation $\Delta p = 2\gamma/R$ where Δp is the difference in pressures between compartments divided by the surface, γ is surface tension, and R is radius of curvature. The equation applies to each alveolus but not all alveoli have the same size. Since alveoli

are connected through airways, any increase in pressure for one alveolus, required to maintain a small radius, rapidly equilibrates with the pressure in alveoli with a large radius. Therefore small alveoli would collapse if the surface tension γ remained constant. A tremendous force would be needed at each breath to re-open collapsed alveoli. Reopening of collapsed alveoli is actually the major problem for the premature infants with RDS. The repeated reopening of collapsed air spaces can damage the epithelium, causing leakage of serum from the capillaries around alveoli into the alveolar space (pulmonary edema). Pulmonary edema can be caused even by effects on hydrostatic pressure due to an increase in surface tension. Higher surface tension would result in shrinkage of alveoli which in turn expands the surrounding interstitial space. That would lead to decreased interstitial pressure and produce a larger hydrostatic pressure gradient across the capillary wall which produces greater flow of fluid out of the capillaries.

DPPC, the most prevalent component of pulmonary surfactant, is believed to be the primary component responsible for the ability to lower surface tension. For a clean air-water interface the interfacial tension is $\gamma_0 = 70$ mN/m, but in the lung, surface tension γ decreases to a value of less than 1 mN/m (Schürch, 1982). DPPC is the only phospholipid which, in single component films, can lower γ so dramatically. The surface pressure Π of compressed DPPC film can reach 70 mN/m. Since $\gamma = \gamma_0 - \Pi$, this surface pressure corresponds very closely to the surface tension observed in the lung. Therefore it is believed that formation of a stable film with highly ordered structure and rigidity of conformationally ordered saturated phospholipids may be crucial for the very low surface tension. This process would require a phase transition from the originally liquid-expanded (LE) phase to either the liquid-condensed (LC) or solid phase. Since many of the remaining surfactant components do not undergo a phase transition but instead irreversibly collapse from the interface when compressed to pressures around 40 - 60 mN/m, it has been hypothesized that the unstable components are selectively excluded or "squeezed-out" from the mixture during compression (Watkins, 1968). Squeeze-out of the unstable

constituents would lead to formation of a highly ordered film that can withstand compression to such high surface pressures without collapse from the interface. Neither the mechanism of squeeze-out nor the characteristics of a presumably ordered phase formed during compression of surfactant films are known.

In any single component film, the formation of the ordered phase can be detected in the compression isotherms which plot pressure (Π) as a function of the average area per molecule (A). The phase transition manifests itself as a discontinuity in the isotherm's slope ($d\Pi/dA$) (Albrecht et al., 1978). In pure DPPC films the phase transition from the conformationally disordered, LE phase to the conformationally ordered, LC phase occurs at Π = 3-5 mN/m at 20 °C, it manifests itself as a plateau on the compression isotherm, and the pressure of this transition increases further with temperature (Albrecht et al., 1978). However, the isotherms for lung surfactant do not exhibit any plateau or kink and so the isotherms do not provide obvious support for a phase transition. On the other hand, the prominent plateau is required only for simple component films, and so the smooth isotherm for the complex mixture of pulmonary surfactant is not helpful in evaluating phase behavior. Therefore the speculated existence of the different phases in pulmonary surfactant remained to be established.

The studies in this thesis are focused on the structure of the interfacial film. We have used two complementary microscopic techniques, fluorescence microscopy and Brewster angle microscopy, to show that phase separation does occur in films of calf lung surfactant extract (CLSE), which contain the full complement of biophysically active components. Fluorescence microscopy distinguishes between different phases on the basis of differences in solubility of fluorescent lipid probes (Fig. 1.2). A more ordered phase has a lower solubility for certain fluorescently labeled lipids that are highly soluble in the disordered, LE phase. Therefore formation of the ordered phase can be detected as dark domains in a bright fluorescent background (Fig. 1.3) (Lösche et al., 1983; McConnell et al., 1984; Peters and Beck, 1983). Brewster angle microscopy (BAM) provides an

alternative method of detecting phase separation (Hénon and Meunier, 1991; Hönig and Möbius, 1991). It distinguishes between regions with different optical thickness, the product of the physical thickness and its refractive index, and so it can detect phases with different molecular densities and/or different refractive indexes. The ordered, tightly packed, phase has higher reflectivity than the LE phase of light polarized in the plane parallel to the interface (p-polarization). Therefore in BAM the formation of the ordered phase can be detected as bright domains in a dark background. Although BAM has somewhat lower spatial resolution, it does not require addition of fluorescently labeled lipids. Therefore it provides an excellent control for the fluorescence experiments to rule out the possibility that the probe alters the system's behavior.

Both microscopic techniques confirmed that the separated phases represent only a gap in the miscibility of the surfactant components during the limited interval of compression. As the film becomes more dense, the two phases remix back into a single phase. To determine the circumstances under which both the phase separation and the remixing occur, we have characterized the phase behavior over a range of pressures and temperatures. The role of the surfactant proteins, the neutral lipids, and the phospholipids other than DPPC in surfactant phase behavior was revealed by comparison of the complete surfactant extract with preparations which lack specific components (Hall et al., 1994). The components were purified by column chromatography and fractions were selected to exclude surfactant proteins and/or neutral lipids. The composition of the domains in films from which both proteins and neutral lipids were removed was determined by construction of a phase diagram. Further supportive evidence about the structure and composition of the domains was obtained from several other studies including (1) the temperature dependence of the domains' appearance, (2) the optical thickness of the two phases, and (3) birefringence of the domains. The analysis of shape, size, density, and total area of the domains for each preparation determined the effects of individual constituents on the phase separation, established what constituent is responsible for the remixing, and revealed that

the remixing occurs due to a critical point. Measurements of surface potentials (Fig. 1.4) allowed us to calculate dipole moment densities of the different phases as well as line tension at the boundaries of the domains under the assumption that neutral lipids partition into only one of the two phases. The results of the calculations qualitatively predict the location of neutral lipids.

Additional introductory material can be found in the beginning of chapters 2, 3, 4, and 5. These chapters are presented as a published paper (Chapter 2) and as manuscripts in preparation for publication.

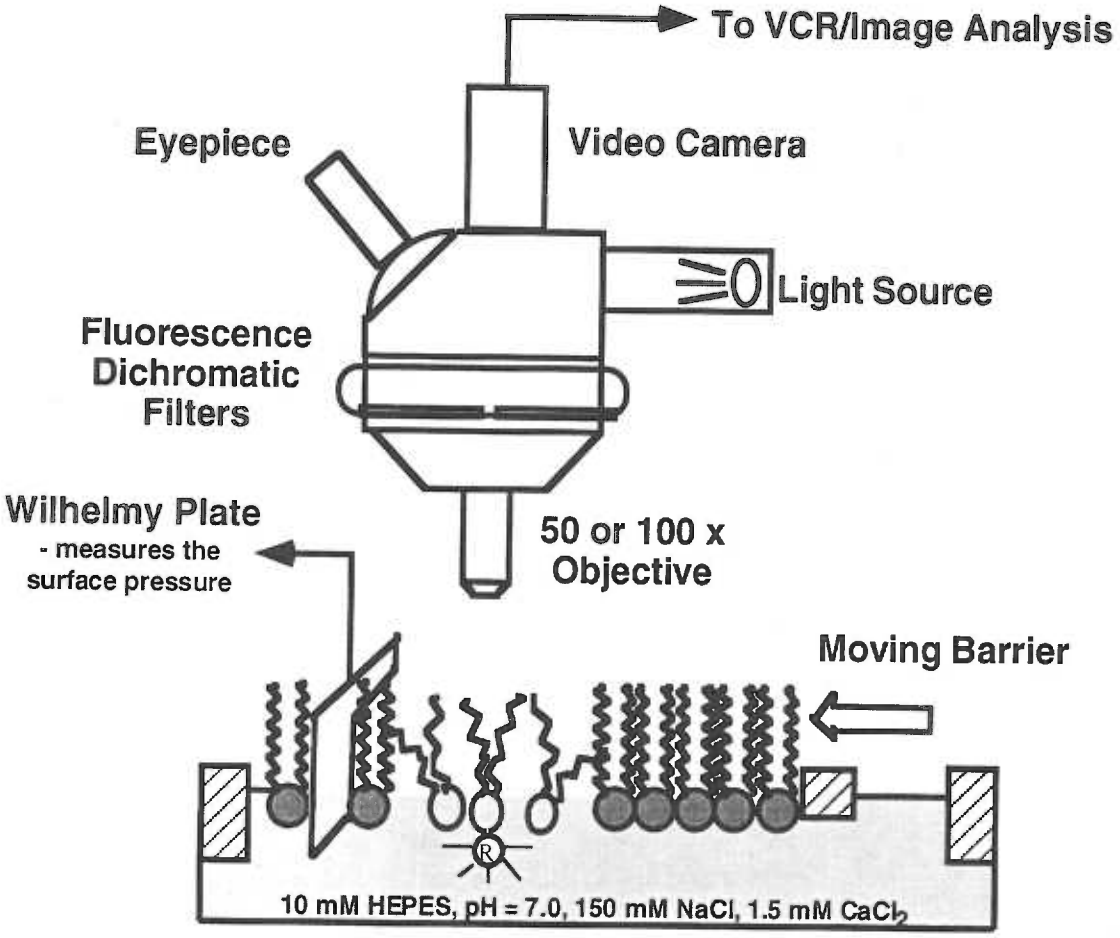

Langmuir Film Balance

1.2. Experimental setup for fluorescence microscopy. Fluorescent microscopy detects different phases based on their solubilities for fluorescently labeled lipids (R).

(1) Laser light containing both polarizations (called p and s-polarization - shown by the arrows) is directed toward the surface at the Brewster angle.

(2) The remaining polarization (p-polarization) hits the surface at the Brewster angle for the clean air-liquid interface.

(3) No light is reflected from the water surface.

(4) Even a single layer of molecules reflects enough light to produce, with a lens, an image on a camera.

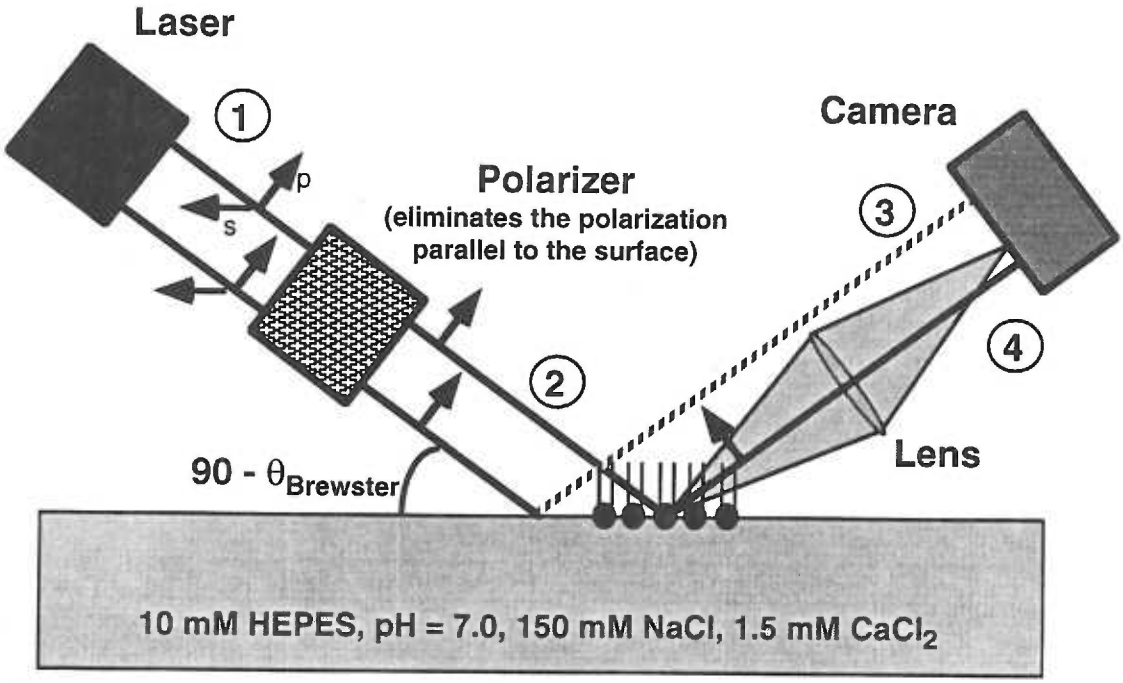

1.3. Experimental setup for Brewster angle microscopy.

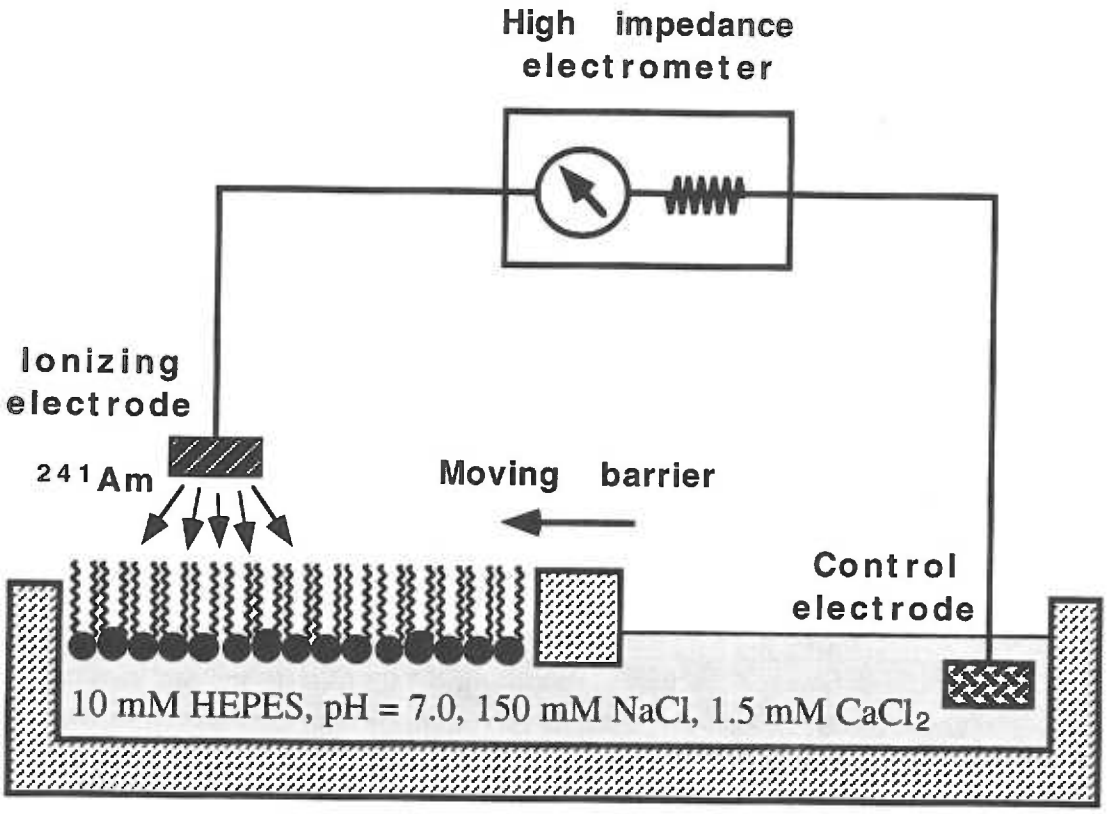

1.4. Experimental setup for surface potential measurements. The layer between the electrode and the air-liquid interface is rendered conducting by coating the electrode with an ionizing source (^{241}Am). The high impedance electrometer then determines the potential difference between the pure air-liquid interface and in the presence of surfactant films.

Biophysical Journal 71: 2583 - 2590, 1996

CHAPTER 2

LATERAL PHASE SEPARATION IN INTERFACIAL FILMS OF PULMONARY SURFACTANT

B.M. Discher[a], K.M. Maloney[b], W.R. Schief Jr.[c],

D.W. Grainger[d], V. Vogel[c] and S.B. Hall[a,e]

Departments of Biochemistry[a] and Medicine[e], Oregon Health Sciences University, Portland, OR 97201

[b]Department of Chemistry, Biochemistry and Molecular Biology, Oregon Graduate Institute of Science & Technology, Portland, OR 97006

[c]Center for Bioengineering, University of Washington, Box 357962, Seattle, WA 98195

[d]Department of Chemistry, Colorado State University, Fort Collins, CO 80523

Address correspondence to:

Stephen B. Hall

Pulmonary and Critical Care Medicine

Mail Code UHN-67

Oregon Health Sciences University

Portland, Oregon 97201-3098

Telephone: (503) 494-6667

Facsimile: (503) 494-6670

e-mail: sbh@ohsu.edu

[b]Current address:

Division of Chemistry and Chemical Engineering, 210-41

California Institute of Technology

Pasadena, California 91125

Running title: Phase separation in lung surfactant films

ABSTRACT

To determine if lateral phase separation occurs in films of pulmonary surfactant, we used epifluorescence microscopy and Brewster angle microscopy (BAM) to study spread films of calf lung surfactant extract (CLSE). Both microscopic methods demonstrated that compression produced domains of liquid-condensed lipids surrounded by a liquid-expanded film. The temperature dependence of the pressure at which domains first emerged for CLSE closely paralleled the behavior of its most prevalent component, dipalmitoyl phosphatidylcholine (DPPC), although the domains appeared at pressures 8-10 mN/m higher than for DPPC over the range of 20-37°C. The total area occupied by the domains at room temperature increased during compression to a maximum value at 35 mN/m. The maximum area of 25 ± 5% of the interface agreed well with the predicted area if all DPPC present in the monolayer was contained in domains. At pressures above 35 mN/m, however, both epifluorescence and BAM showed that the area of the domains decreased dramatically. These studies therefore demonstrate a pressure-dependent gap in the miscibility of surfactant films. The monolayers separate into two phases during compression but remain largely miscible at higher and lower surface pressures.

Key words: surface pressure, epifluorescence, surface tension, Brewster angle microscopy, monolayer films, microstructure

INTRODUCTION

The phase behavior in films of pulmonary surfactant may be critical for normal function of the lung. Pulmonary surfactant is the mix of lipids and proteins that covers the thin liquid layer which lines the alveolar air spaces and minimizes the interfacial tension of the curved surface, preventing alveolar collapse at the end of exhalation. Premature babies born with inadequate amounts of surfactant before the lungs have matured develop the life-threatening injury of the neonatal Respiratory Distress Syndrome caused by repeated collapse and reopening of the small air spaces (Robertson, 1984). Measurements in the lung indicate that the surfactant films achieve extraordinarily dense structures which effectively eliminate interfacial tension when compressed by the shrinking surface area during normal exhalation. Surfactant films in the lung lower interfacial tension, which would be 70 mN/m for a clean air-water interface, to values less than 1 mN/m (Schürch, 1982). Only films with the highly ordered structure and rigidity of the condensed phase seem likely to withstand compression without collapse from the interface to the high surface pressures necessary to achieve this effect.

The compression isotherm of pulmonary surfactant, however, provides no evidence for the formation of liquid-condensed (LC) lipid. In films which contain a single compound, a first-order phase transition produces a discontinuity in the compression isotherm during the liquid expanded (LE)-LC coexistence region. For dipalmitoyl phosphatidylcholine (DPPC), the most prevalent component of pulmonary surfactant, this discontinuity occurs at 3-5 mN/m at 20°C, and shifts to progressively higher surface pressures with increasing temperatures (Albrecht et al., 1978). The isotherms for lung surfactant do not show this characteristic feature, and so provide no support for a phase transition. Prior studies, however, have shown that in mixed films, smooth isotherms do not rule out the presence of phase separation. Nag and Keough have shown with epifluorescence microscopy that binary films of DPPC and dioleoyl phosphatidylcholine

formed a condensed phase despite the absence of any discontinuity in the compression isotherm (Nag and Keough, 1993).

We have used two complimentary microscopic techniques to establish that phase separation does occur in films with the much more complicated composition of pulmonary surfactant. Epifluorescence microscopy distinguishes regions with different packing densities in interfacial monolayers on the basis of differences in solubility of fluorescent lipid probes between ordered domains and the more fluid LE phase (Lösche et al., 1983; McConnell et al., 1984; Peters et al., 1983). Brewster angle microscopy provides an alternate method of detecting phase separation without the need to add exogenous probes, although at somewhat lower spatial resolution (Hénon et al., 1991; Hönig et al., 1991). Our experiments used spread monolayers of extracted calf surfactant (calf lung surfactant extract, CLSE) as a model of the surfactant film in the lung. The spread films provide a system in which the composition and surface concentration of the monolayer are known. The extracts of calf surfactant provide a well characterized mixture which contains the complete mix of surfactant phospholipids, neutral lipids and the two hydrophobic surfactant proteins SP-B and SP-C. It differs in composition from complete surfactant only in the absence of the glycoprotein SP-A (Kendig et al., 1989). The ability of extracted surfactant to adsorb to an air-liquid interface and then undergo compression to high surface pressure is comparable to the performance of complete surfactant (Hall et al., 1992), and it functions well as a therapeutic surfactant in the lung (Jobe, 1993). Our measurements extend over a range of temperatures which includes physiological conditions to determine under what circumstances phase separation occurs in films of pulmonary surfactant.

MATERIALS AND METHODS

Materials:

Extracts of surfactant from calf lungs (calf lung surfactant extract, CLSE) provided by Dr. Edmund Egan of ONY, Inc. (Amherst, NY) and Dr. Robert Notter of the University of Rochester were prepared as described previously (Hall et al., 1992). Surfactant was removed from freshly excised calf lungs by repeated lavage with 150 mM NaCl. Centrifugation at 250 x g for ten minutes removed cells and large debris. Higher speed centrifugation of the resulting supernatant at 12,500 x g for 30 minutes then pelleted the large surfactant aggregates. Following resuspension of the pelleted surfactant, the hydrophobic constituents were extracted into chloroform (Bligh and Dyer, 1959) to yield CLSE.

The composition of the major phospholipid head groups of this mixture is: sphingomyelin, 1% (mol/mol); phosphatidylcholine (PC), 82%; phosphatidylinositol, 3%; phosphatidylethanolamine, 3%; phosphatidylglycerol, 6% (Hall et al., 1994). Ester-linked diacyl compounds constitute 97% of the PCs, of which the four major components are: DPPC, 42%; palmitoyl-palmitoleoyl PC (16:0-16:1), 19%; palmitoyl-oleoyl PC (16:0-18:1), 14%; and palmitoyl-myristoyl PC (16:0-14:0), 13% (Kahn et al., 1995). CLSE also contains approximately 8% (mol/mol) neutral lipid, consisting almost entirely of free cholesterol, and approximately 1% (wt/wt) of the mixture of surfactant proteins SP-B and SP-C (Hall et al., 1994).

The data reported here represent results obtained with a single preparation of CLSE. Experiments with other preparations produced qualitatively equivalent results. Domains appeared, grew, and then abruptly decreased in total area during compression for all preparations. The surface pressure of the maximum area, however, varied by

approximately 5 mN/m. We attributed this variation to measured differences in the composition, particularly in the content of neutral lipid.

DPPC purchased from Sigma (St. Louis, MO) was used without further purification.

Reverse-osmosis grade water for these studies was obtained from purification systems purchased either from Millipore (Bedford, MA) or Barnsteadt (Dubuque, IA) and had resistivity of approximately 18 Mohm·cm. All glassware was acid-cleaned. All solvents were at least reagent-grade and contained no surface active stabilizing agents.

Methods:

A. *Biochemical Assays*:

Phospholipid concentrations were determined by measuring the phosphate content (Ames, 1966) of measured aliquots of extracted material.

B. *Compression Isotherms*

Surface pressure - area (π-A) isotherms of interfacial monolayers were measured on a commercially available trough (KSV-3000, KSV Instruments, Helsinki, Finland). Monolayers were compressed at a rate of 1.0 $Å^2$/phospholipid molecule/minute. The temperature of the trough was regulated with a Lauda RCS circulating bath. Monolayers were created by spreading 80 µl of a 0.95 mM phospholipid stock solution in chloroform at the air-liquid interface. Only the phospholipid concentration of the surfactant solutions was measured, and consequently molecular areas were expressed only in terms of phospholipids with no attempt to correct for the presence of neutral lipid and protein. A 10 minute waiting period before monolayer compression allowed for evaporation of the spreading solvent. The π-A curve reported here was selected from a group of three reproducible isotherms in which deviations in molecular area and surface pressure between

different experiments were less than 2 $Å^2$/phospholipid molecule and 0.4 mN/m respectively. All experiments, including epifluorescence and Brewster angle microscopy as well as compression isotherms, used monolayers spread on a solution of 10 mM Hepes pH 7.0, 150 mM NaCl, and 1.5 mM $CaCl_2$ (HSC).

C. *Epifluorescence Microscopy*

Epifluorescence microscopy used a Zeiss-ACM microscope (Meller, 1988) with a 50x objective to visualize lipid monolayers (Lösche et al., 1983; McConnell et al., 1984; Peters et al., 1983) on the surface of a previously described home-built Wilhelmy balance. The Teflon trough had a surface area of 108 cm^2 and subphase volume of 100 ml (Maloney and Grainger, 1993), the temperature of which was regulated to ± 1°C with water pumped through jackets surrounding the trough. Samples of surfactant preparations containing 1% (mol/mol surfactant phospholipid) of rhodamine-dipalmitoyl phosphatidylethanolamine (Rh-DPPE) labeled at the head group (Molecular Probes, Eugene, OR) were spread in approximately 80 µl of chloroform to give an initial molecular area of 150 $Å^2$/phospholipid molecule. Films were then compressed at 2.8 $Å^2$/phospholipid molecule/minute either to specific surface pressures at which images were recorded on the static film, or until domains appeared in experiments at different temperatures. A Hamamatsu C2400 SIT camera recorded fluorescence images either to VHS video tape for later analysis or directly to computer (Quadra 650, Apple, Inc., Cupertino, CA with LG-3 frame grabber, Scion Corp, Frederick, MD). A C-shaped Teflon mask placed directly in the trough and extending through the interface minimized movement of the monolayer (Grainger et al., 1989; Meller, 1988). Images obtained inside and outside the mask at frequent intervals ensured that the mask created no artifacts.

D. *Brewster Angle Microscopy*

Brewster angle microscopy (BAM) allowed examination of surfactant monolayers without fluorescent probes. Contrast in BAM results from differences in reflectivity to p-polarized light produced by variation in the optical thickness within an interfacial film. The background intensity is suppressed by choosing the angle of incidence to be Brewster's angle for the bare interface, at which no p-polarized light is reflected (Hénon et al., 1991; Hönig et al., 1991).

The BAM was a custom-built apparatus configured to image the surface of a Wilhelmy balance. Light from a 100 mW diode-pumped Nd-YAG laser (Coherent, Santa Clara, CA) was set to p-polarization by a Glan-Thompson polarizer (CVI, Albuquerque, NM; extinction 10^{-6}) prior to incidence on the water surface at 53.12° with respect to the surface normal. A lens system (Spindler & Hoyer, Milford, MA; Zeiss, Thornwood, NY) collected the reflected light and formed an image on a CCD camera (Dage-MTI, Michigan City, IN). For display, the images have been noise-filtered. Since the light collection of the BAM is highly sensitive to the height of the water in the trough, the water level was maintained constant by the regular addition of water to counter the effect of evaporation. Details of this optical setup will be published elsewhere (Schief, et al., to be published). The image from the CCD was captured by a SG-9 Scion capture card (Scion, Frederick, MD) using the program Image from NIH, and viewed directly on the screen of a MacIntosh IIci computer (Apple, Cupertino, CA). Images can be recorded either on-line, or on S-VHS (Mitsubishi, Tokyo, Japan). A graphical programming interface (LabView, National Instruments, Austin, TX) also provided computer control of the Wilhelmy balance. The balance for these studies used a continuous ribbon barrier (Labcon Ltd., Darlington, UK) inserted vertically through the air-liquid interface of buffer contained in a custom-built temperature-regulated Teflon trough.

E. *Image Analysis*

The total area of the domains in epifluorescence images was analyzed using the program Image (NIH, Bethesda, MD). The marked contrast between dark domains and the surrounding fluorescent film allowed direct measurements of the size of all domains in any given microscopic field based on digitally assigned pixel grayscale values. Each data point represents analysis of a minimum of twelve recorded images from four independent experiments. Images were recorded in each experiment from at least three different regions of the monolayer. The fraction of the monolayer occupied by solid domains was calculated by expressing the sum of all domain areas as a percent of the total area analyzed for each experiment, and then averaging the results. Data are expressed as mean ± S.D.

RESULTS

Epifluorescence microscopy demonstrated that compression of films of pulmonary surfactant produces lateral phase separation (Fig. 2.1). Interfacial films composed of the hydrophobic constituents of calf surfactant contained discrete dark domains in an otherwise brightly fluorescent film. Depletion of the fluorescent probe Rh-DPPE in the domains implies different molecular packing from that of the surrounding film. Domains were present on the scale of a few microns at surface pressures of 9 mN/m and above. Formation of these domains produced no discontinuity in the π-A isotherm for CLSE or in its first or second derivative. Plots of the logarithm of the bulk modulus ($-A \cdot \partial\pi/\partial A$) as a function of molecular area were strictly linear with no evidence of the changes in slope which indicate phase separation (Hirshfeld and Seul, 1990). The isotherm remained entirely smooth with compression speeds as low as 0.1 $Å^2$/phospholipid molecule/minute, reduction of temperature to 5°C, or the use of water as subphase rather than buffered electrolyte.

The total area occupied by the domains increased progressively over a broad range of pressures during the initial stages of compression (Fig. 2.2). This behavior is distinct from pure DPPC, for which nonfluorescent domains grow to dominate the interfacial film over the narrow range of surface pressure of the LE - LC coexistence region evident in the compression isotherm (Meller, 1988; Weis and McConnell, 1984). The behavior of the surfactant films was also distinct in that at room temperature, their total area passed through a maximum and then declined rapidly at higher surface pressures (Fig. 2.2). The domains reached a maximum of 25 ± 5% of the total interfacial area at a surface pressure of 35 mN/m, but then fell to 4 ± 1% by 40 mN/m. Most of the individual domains vanished, although a small fraction persisted after decreasing in size. These changes in total area of the domains appeared to represent a true decrease in area rather than simply a loss of fluorescent probe from the interface. The surface film remained brightly fluorescent

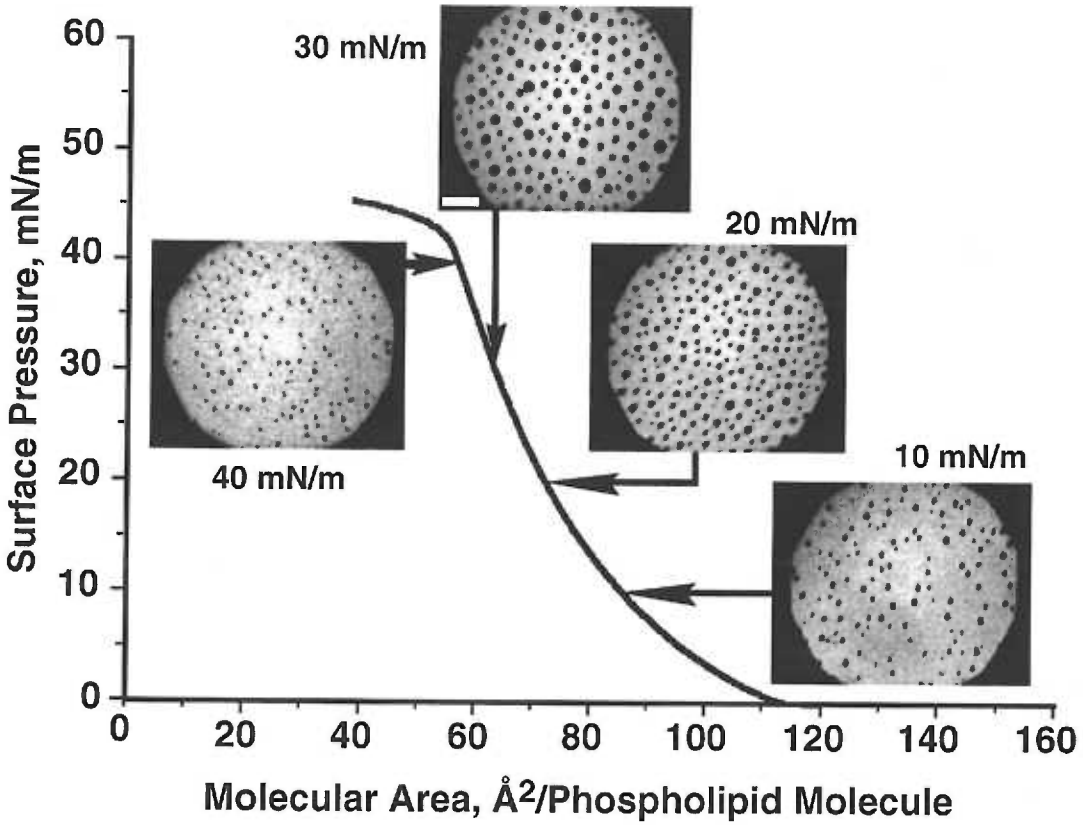

2.1. Surface pressure-area isotherm with epifluorescence micrographs of calf lung surfactant extract (CLSE). Chloroform solutions of preparations containing 1 mol % of rhodamine-DPPE were spread to an initial area of 150 $Å^2$/phospholipid molecule at 20°C on HSC buffered electrolyte. Isotherms were recorded during compression at 1 $Å^2$/phospholipid molecule/minute. Images were obtained in separate experiments from static films following compression at 2.8 $Å^2$/phospholipid molecule/minute to the desired pressure. Representative images are given at 10, 20, 30, and 40 mN/m. Scale bar is 50 μm.

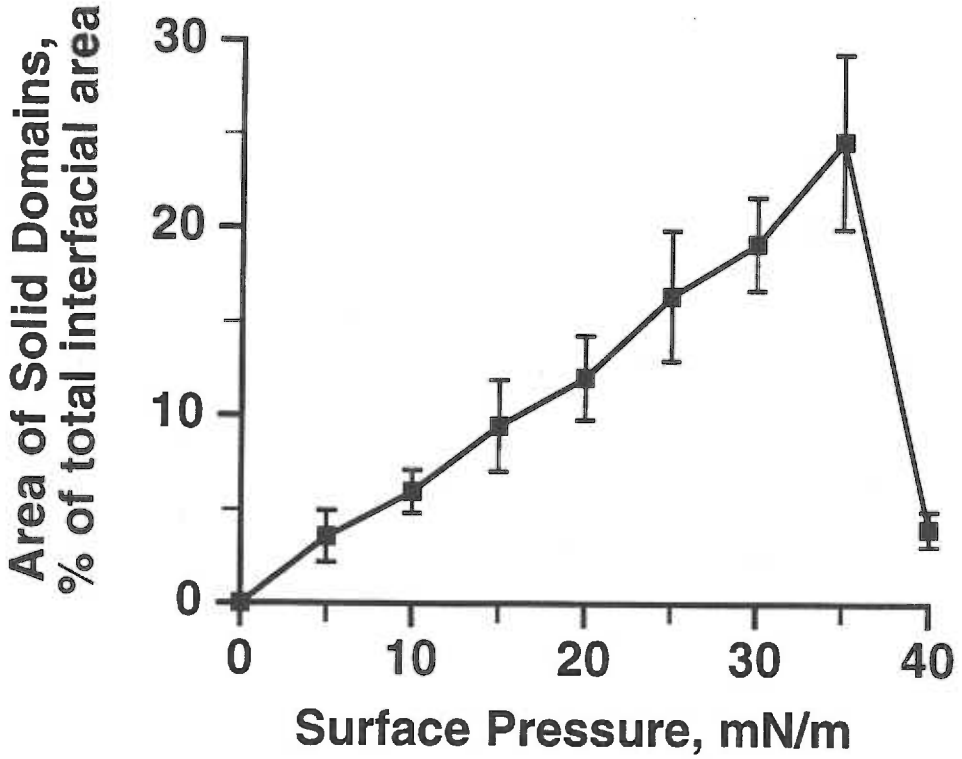

2.2. Variation of total area of condensed domains with surface pressure. Each data point represents mean ± S.D. from analysis of 12 epifluorescence images generated from four independent experiments.

during these changes, making it unlikely that the decrease in area resulted from a loss of probe from the interface and insufficient contrast to distinguish the domains.

Brewster angle microscopy (BAM) demonstrated that the domains visualized by epifluorescence microscopy also exist in the absence of added fluorescent probe and confirmed that the domains are not caused by the presence of the probe (Fig. 2.3). The domains viewed by BAM were bright against a darker background, demonstrating that the optical thickness of the domains was greater than that of the surrounding film. This appearance again suggests a higher packing density in the domains. During compression to high pressures, the contrast between domains and the surrounding film diminished, in large part because of increased reflectivity from the surrounding film. BAM images showed no evidence of domains at pressures approaching 45 mN/m.

The nonfluorescent domains appeared at surface pressures which increased progressively with temperature (Fig. 2.4). The emergence of the domains in CLSE closely paralleled the appearance of condensed phase observed in separate experiments with pure DPPC (Fig. 2.4). The slope of the surface pressure at which domains first appeared as a function of temperature was essentially the same for CLSE and DPPC. The curve for CLSE was shifted to pressures approximately 8-10 mN/m higher than for DPPC. The first appearance of condensed phase in DPPC detected by epifluorescence corresponded exactly to the onset of the LE - LC phase transition in the compression isotherms published previously for this range of temperatures by Albrecht et al. (Albrecht et al., 1978) (Fig. 2.4).

The behavior of both the fluorescent probe and the surfactant limited the range of pressures over which our experiments could be performed. Bright fluorescent spots appeared at pressures above 45 mN/m, suggesting the separation of a distinct phase which is enriched in Rh-DPPE under those conditions. The compression isotherm for pulmonary surfactant also undergoes a prolonged plateau beginning just above 45 mN/m (Keough, 1984), consistent with the upper limit of pressures at which surfactant films exist under

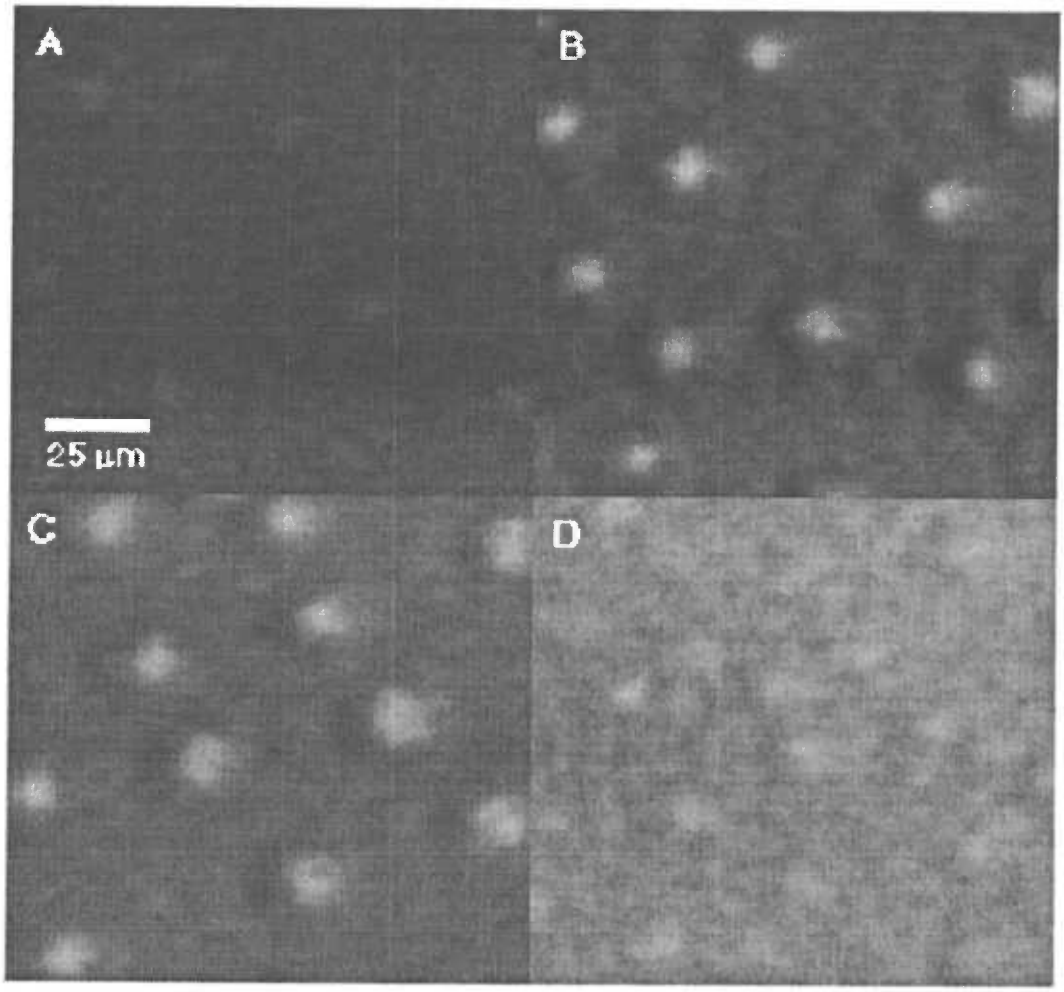

2.3. Brewster angle micrographs of CLSE monolayers. Chloroform solutions of CLSE were spread on HSC buffer at room temperature and compressed to the desired surface pressure. Scale bar represents 25 µm in length. Images were recorded at surface pressures of: A., 10 mN/m; B., 20 mN/m; C., 30 mN/m; D., 41 mN/m. The relative grayscale has been preserved for this sequence of images. The dark and light shadows to the left and right, respectively, of each domain are due to interference of the reflected coherent light at the domain edges.

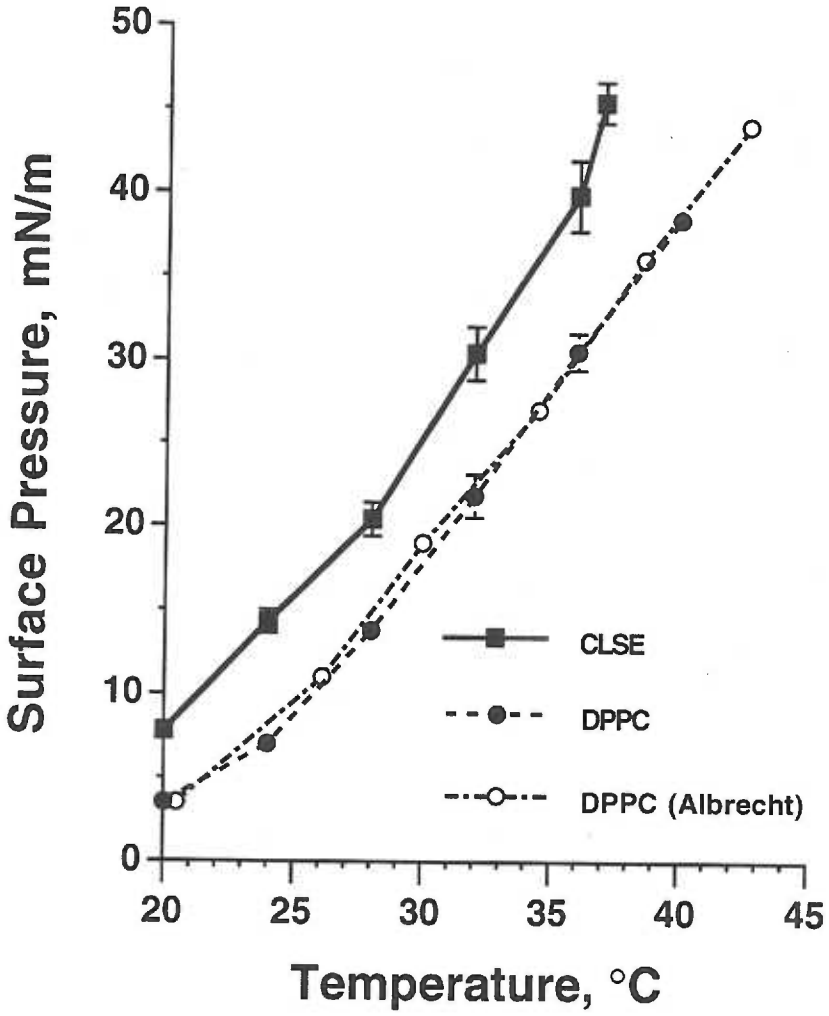

2.4. Temperature dependence of surface pressure at which epifluorescence microscopy first detected domains. Isothermal compressions were conducted at the temperatures indicated to determine the surface pressure at which domains first occurred in epifluorescent images of CLSE. Chloroform solutions were spread to an initial area of 150 $Å^2$/phospholipid molecule and compressed at 2.8 $Å^2$/phospholipid molecule/minute. Data are mean ± S.D. for three experiments.

equilibrium conditions. These constraints established 45 mN/m as the approximate upper end of the range of pressures currently accessible in our experiments.

The surface pressure at which the domains reach their maximum size also varied with temperature. Increasing the temperature from 20° to 24°C shifted the maximum of the total area of the domains above 35 mN/m. At temperatures greater than 24°C, the domains no longer achieved a maximum area within our range of accessible pressures. The total area of the domains at these temperatures continued to increase during compression up to 45 mN/m. Domains persisted up to 37°C, but they appeared just below 45 mN/m at that temperature and consequently the maximum size achieved in our experiments remained quite small (Fig. 2.5). Domains were not seen at temperatures above 37°C.

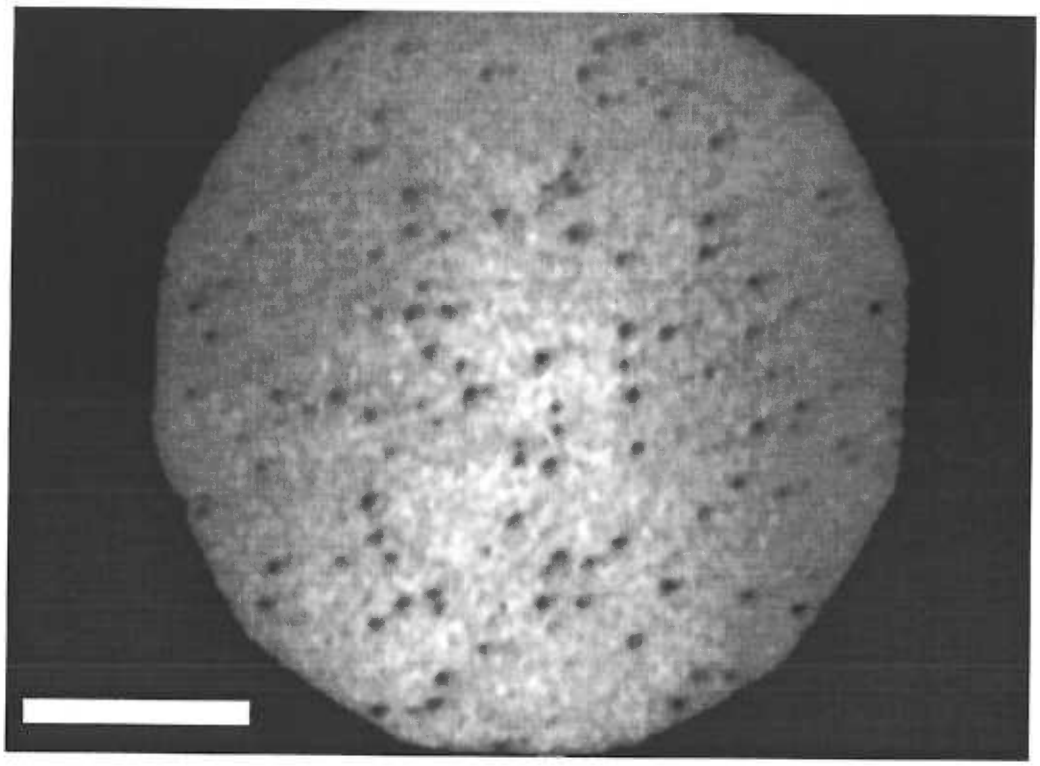

2.5. Epifluorescence micrographs of surfactant preparations at 37°C. Chloroform solutions were spread to 150 $Å^2$/phospholipid molecule on HSC buffer and compressed at 2.8 $Å^2$/phospholipid molecule/minute to 45 mN/m. Scale bar is 50 μm in length.

DISCUSSION

Compression of interfacial monolayers of extracted calf surfactant produces lateral separation of two phases. Both epifluorescence (Fig. 2.1) and Brewster angle microscopy (Fig. 2.3) demonstrate the presence of discrete domains which are distinct from the surrounding film. The domains increase in size over a broad range of surface pressures (Fig. 2.2). At room temperature, however, their area achieves a maximum value and then rapidly declines with further compression (Fig. 2.1-2.3). The surface pressure at which the domains first emerged increased with temperature (Fig. 2.4). Domains persist to 37°C but at that temperature occupy only a limited portion of the interface (Fig. 2.5).

Although we have not provided detailed structural information on the molecular arrangement of components in the domains, we have distinguished regions of more tightly packed constituents. Both methods of microscopy used in these studies rely on structural differences in the surface monolayer to produce contrast (Lösche et al., 1983; McConnell et al., 1984; Peters et al., 1983). Epifluorescence distinguishes areas which differ in the solubility of a fluorescent lipid probe. Tightly packed lipids in the LC phase exclude the large fluorescent chromophore on the probe, which remains soluble in more disorganized LE regions of the film. Prior studies with monolayers containing a single component have shown that the behavior of nonfluorescent domains corresponds exactly to that expected for condensed lipid based on compression isotherms (Knobler, 1990). In the BAM images, reflectivity varies because of differences in refractive index and thickness of the film (Hénon et al., 1991; Hönig et al., 1991). Bright domains in single component films again indicate regions of condensed phase lipid. We are unaware of studies with either method which prove that domains represent condensed phase in films with the compositional complexity of pulmonary surfactant. But the previous results with much simpler monolayers certainly support the hypothesis that the domains in the surfactant films represent highly organized condensed lipids.

The maximum total area occupied by the domains fits well with predictions based on the assumption that they contain only condensed phase DPPC. The fraction of the interfacial area predicted from the composition of CLSE that would be occupied by condensed DPPC closely approximates the actual measurements of the total area covered by domains. The fraction of the interface f_s occupied by domains having a molecular area $\overline{A}_s$ and containing the fraction f of the molecules present is given by

$$\phi_s = f_s \cdot \frac{\overline{A}_s}{\overline{A}}$$

where $\overline{A}$ is the average molecular area for the entire film (Knobler, 1990). DPPC constitutes 30% (mol/mol) of the lipid in CLSE (Kahn et al., 1995). The domains achieved their maximum area when $\overline{A}$ was 60 $Å^2$/molecule. This figure for $\overline{A}$ included lipid molecules but ignored the 1% (wt/wt) content of protein (Hall et al., 1994). The calculated value of f_s then depends on the value of $\overline{A}_s$ assigned from studies of pure DPPC. Compression isotherms indicate that condensed DPPC has a molecular area of 51 $Å^2$/molecule ((Albrecht et al., 1978), and data not shown), which would predict that DPPC in CLSE would occupy 26% of the interface. The value of 43 $Å^2$/molecule obtained by Weis and McConnell (Weis and McConnell, 1985) from their epifluorescence studies would predict 22%. Both calculated values of f_s agree with the measured value of $25 \pm 5\%$ for the maximum area covered by domains.

The domains, however, may well contain components other than DPPC. To the extent that they are in thermodynamic equilibrium with the surrounding film, they are saturated with the other constituents. The surface pressure at which the domains first emerge in CLSE exceeds the value for DPPC by 8-10 mN/m. This difference may reflect the nonideality of the mixed film, but it also could result from the presence of components other than DPPC in the domains. The close proximity over the broad range of temperatures of the pressures at which the domains emerge for DPPC and CLSE does provide further suggestive evidence that DPPC is the most important component of the domains. The LE - LC phase transition for all the other phospholipids is either absent over this range of

temperatures or occurs at pressures well above the values observed here (Kahn et al., 1995). Our data, however, do not exclude the possibility that the domains contain significant levels of other components in addition to the DPPC.

The formation of the domains occurs by a process that is significantly different from the typical first-order phase transition of pure DPPC. The isotherm is smooth without any evidence of a plateau. The domains in CLSE enlarge over a broad range of pressures, extending at room temperature from 9 - 35 mN/m rather than over the narrow LE - LC coexistence region required of a first-order transition and observed for DPPC. Dluhy and coworkers have previously obtained similar results using vibrational spectroscopy (Dluhy et al., 1989). They observed ordering of acyl chains in films of pulmonary surfactant continually over the range of surface pressures from 0-45 mN/m, in marked contrast to the rapid change seen for DPPC between 0 and 10 mN/m. The isotherms for CLSE and DPPC reflect this difference in the behavior of the condensed phase.

The appearance, growth, and disappearance of the domains imply that the miscibility of the constituents of CLSE depends on surface pressure. In this model, enlargement of the domains during compression reflects the progressive separation of DPPC into a condensed phase. The subsequent decrease in total area of the domains observed with further compression at lower temperatures represents remixing of the constituents. Such a gap in miscibility in the phase diagram, with a homogeneous system at low and high pressures separated by a region in which immiscible phases separate, has been seen previously for binary mixtures of DPPC with both cholesterol (Rice and McConnell, 1989; Slotte, 1995; Subramaniam and McConnell, 1987) and dioleoyl phosphatidylcholine (DOPC) (Nag et al., 1993). The decrease in the total area of the domains for DPPC:DOPC was suggested previously to result not from a true decrease in the condensed regions but from a change in the partitioning of the fluorescent probe. Our results with BAM, however, show that the domains also decrease sharply in films which contain no probe, and indicate that the fall in condensed area for CLSE is real.

The remixing of the constituents at high pressures may result from a narrowing of the difference in density of the two phases. Calculations on the molecular area of the film surrounding the domains support this possibility. The condensed domains should be relatively incompressible. If their molecular area changes little during compression, then our results predict that the density of the expanded phase increased significantly. The area per molecule $\overline{A}_f$ for the expanded phase is given by

$$\overline{A}_f = \overline{A} \cdot \frac{(1-\phi_s)}{\left(1-\phi_s \cdot \frac{\overline{A}}{\overline{A}_s}\right)}$$

(Weis et al., 1985). Values of $\overline{A}_f$ calculated from our measurements of $\overline{A}$ and ϕ_s decreased throughout compression. For $\overline{A}_s$ = 51 Å^2/molecule, for instance, obtained from DPPC isotherms (Albrecht et al., 1978), $\overline{A}_f$ decreased from 101 to 57 Å^2/molecule during compression from 5 to 40 mN/m. Our BAM images provide some additional support for this progressive increase in molecular density of the phase that surrounds the domains. The grayscale, and hence the optical thickness, of the domains remained relatively constant during compression while it increased in the surrounding film (Fig. 2.3). The steady increase in the optical thickness of the surrounding film also agrees with the increase in ordering of acyl chains observed by Dluhy and coworkers using vibrational spectroscopy (Dluhy et al., 1989). All of these results suggest that the density of the surrounding film approaches that of the domains. Such a decrease in the difference between the density of the two phases might be sufficient to produce a remixing of the constituents.

Interpretation of the physiological importance of our findings is complicated by the difficulty of extrapolation to experimental conditions not accessible in these studies. Surface pressures in the lung are well above the maximum levels of 45 mN/m which we could study here. Our results, however, do have significant implications for surfactant function, particularly at the upper end of our range of pressures.

One major issue concerns the role of phase separation in the refinement of the surfactant films. The characteristics of monolayers which reach the high surface pressures seen in the lungs suggest that they contain predominantly condensed phase DPPC, which implies a substantial change in composition from the material originally secreted by the alveolar type II cells. In vitro, the compressibility of the surfactant films at high surface pressures approaches that of LC DPPC (Putz et al., 1994). In excised lungs, the temperature dependence of pulmonary mechanics suggests that alveolar films contain LC DPPC (Clements, 1977). The interfacial component of the pulmonary elastic recoil increases abruptly between 40 and 44°C, which correlates well with the melting transition of gel phase DPPC at 41°C. These observations have led to the widely held belief that pulmonary surfactant must undergo substantial refinement of its composition before it can achieve high surface pressures during compression. Refinement could occur during formation of the interfacial film, a process which we have not studied here. The more widely held view, however, has been that compression to surface pressures above equilibrium values selectively eliminates surfactant constituents from the interface. Refinement by this process might proceed via two mechanisms. Constituents might depart from a homogeneous film, which consists of a single phase, according to characteristics of the individual molecules such as their shape. Alternatively, separation of a film into two phases with different collapse pressures could result in refinement. The more disordered LE phase, for instance, might fold from the surface at lower pressures than the condensed phase. This second mechanism, but not the first, requires a separation of two phases. Our studies confirm that phase separation can occur in surfactant films despite the absence of any discontinuity in the compression isotherms. Phase separation, however, occurs only in a narrow regime of temperature and surface pressure. Distinction of these two mechanisms will require studies of phase behavior at the high pressures and dynamic conditions present in the lung.

In summary, compression of films of extracted calf surfactant leads to a partial demixing of the constituents through formation of condensed domains that are surrounded by a less densely packed film. The temperature dependence and area suggest that they contain predominantly but not exclusively DPPC. At lower temperatures, the separation of phases represents a gap in the miscibility of the surfactant film which remains largely homogeneous at higher and lower surface pressures.

ACKNOWLEDGMENTS

The authors thank Dr. Edmund Egan of ONY, Inc. and Dr. Robert Notter of the University of Rochester for samples of extracted calf surfactant. These studies were supported by the American Lung Association of Oregon (DWG and SBH), the Whitaker Foundation (DWG, SBH, and VV), and HL 03502 (SBH). The costs of publication were provided by the family and friends of Vern McKee. BMD was supported in part by a fellowship from the Tartar Trust. WRS was supported as a predoctoral fellow by NIH training grants in Biotechnology (GM 08437) and Molecular Biophysics (GM 08268).

CHAPTER 3

ANALYSIS OF THE COMPOSITION AND STRUCTURE OF SEPARATED PHASES IN INTERFACIAL MONOLAYERS OF PULMONARY SURFACTANT PHOSPHOLIPIDS

Bohdana M. Discher[a], William R. Schief Jr.[b], Viola Vogel[b],
David W. Grainger[c], and Stephen B. Hall[a,d]

Departments of Biochemistry and Molecular Biology[a], Physiology and Pharmacology[d], and Medicine[d], Oregon Health Sciences University, Portland, OR 97201

[b]Department of Bioengineering, University of Washington, Seattle, WA 98195

[c]Department of Chemistry, Colorado State University, Fort Collins, CO 80523

Address correspondence to:

Stephen B. Hall

Mail Code UHN-67

Oregon Health Sciences University

Portland, Oregon 97201-3098

Telephone: (503) 494-6667

Facsimile: (503) 494-6670

e-mail: sbh@ohsu.edu

Running title: DPPC in Monolayers of Pulmonary Surfactant Phospholipids.

ABSTRACT

Compression of pulmonary surfactant films leads to a film phase separation. The characteristics of the separated phase suggest that it contains mainly DPPC. We have performed studies on the phase behavior of the purified phospholipids (PPL) to determine the exact composition. Variation of the condensed phase detected by fluorescence microscopy in monolayers containing different amounts of DPPC allowed us to construct a phase diagram verifying that the separated phase contains only DPPC whereas the surrounding phase contains both DPPC and the other phospholipids. Using BAM we have confirmed that the separated domains in films of pulmonary phospholipids possess the same anisotropy and reflectivity of p-polarized light as the liquid-condensed phase in films of pure DPPC.

Key words: epifluorescence
Brewster angle microscopy
dipalmitoyl phosphatidylcholine
anisotropy
lung
phase separation
surface tension
surface active agents
membrane lipids
biophysics

INTRODUCTION

The structure of the interfacial film of pulmonary surfactant is a critical determinant of its physiological function. Pulmonary surfactant is the mix of lipids and proteins that coats the alveolar air spaces. By forming a film on the thin liquid layer that lines the alveoli, pulmonary surfactant lowers interfacial tension and stabilizes the air spaces against collapse at low volumes. The ability of the surfactant film to perform this function depends on the structural stability of the interfacial film. During the expiratory phase of the respiratory cycle, the decreasing alveolar surface area compresses the surfactant film, and measurements in the lung indicate that its surface pressure achieves high values approaching 70 mN/m (Schürch, 1982). Surfactant's physiological function then depends on the formation of a film that remains stable at such high pressures without collapse from the interface. Most investigators have attributed the film's stability to the presence of a highly ordered liquid-condensed (LC) phase (Keough, 1992). The most prevalent component of surfactant, dipalmitoyl phosphatidylcholine (DPPC), occurs as the LC phase in single-component films and can achieve the pressures measured in the lung. This constituent, however, represents only 30% of complete surfactant (Kahn et al., 1995), and both the structure and the composition of the functional film in situ remain uncertain.

We have undertaken studies of the phase behavior of surfactant monolayers at pressures below the equilibrium spreading pressures of approximately 45 mN/m. Phase behavior under these conditions provides important information for understanding the development of the structure and composition of the functional film at higher pressures. Our studies emphasize the full complexity of the surfactant mixture both to complement results with the simple model systems used by others (e.g., Lipp et al., 1996; Nag et al., 1993) and because the diverse set of components may be functionally important. We previously used microscopic methods to demonstrate phase separation in monolayers of extracted calf surfactant (calf lung surfactant extract, CLSE) (Chapter 2). Both

fluorescence microscopy and Brewster angle microscopy (BAM) demonstrated that at intermediate surface pressures, condensed domains separate from the surrounding fluid phase. Several characteristics suggested that the domains were enriched in DPPC.

In the studies reported here, we have extended our prior investigations by considering the phase behavior of the purified phospholipids (PPL) obtained by removing the proteins and neutral lipids from calf surfactant (Hall et al., 1994). Fluorescence microscopy and BAM of compressed monolayers again demonstrate phase separation. To obtain compositional information, we have studied the variation of the phase areas in mixtures containing different amounts of DPPC. In addition to adding DPPC to PPL, a mixture of synthetic phospholipids also replicated the composition of PPL without DPPC. Quantitative BAM provided structural information. Our results provide a self-consistent picture indicating that the condensed domains contain essentially pure DPPC.

MATERIALS AND METHODS

Materials:

Phosphatidylglycerol (PG) derived from egg yolk lecithin and DPPC were obtained from Sigma Chemical Company (St. Louis, MO) and used without further characterization or purification. The following compounds were purchased from Avanti Polar Lipids (Alabaster, AL): rhodamine-dipalmitoyl phosphatidylethanolamine (Rh-DPPE) labeled at the head group N-(Lissamine rhodamine B sulfonyl)-1,2-dihexadecanoyl-sn-glycero-3-phosphoethanolamine; 1-palmitoyl-2-myristoyl-sn-glycero-3-phosphocholine (PMPC); 1-palmitoyl-2-oleoyl-sn-glycero-3-phosphocholine (POPC); 1-palmitoyl-2-palmitoleoyl-sn-3-phosphocholine (PPoPC).

The purified phospholipids (PPL) were separated from extracts of calf surfactant (calf lung surfactant extract, CLSE) provided by either Dr. Edmund Egan of ONY, Inc. (Amherst, NY) or Dr. Robert Notter of the University of Rochester (Rochester, NY). CLSE is obtained by lavaging freshly excised calf lungs, removing cells from the lavage fluid by low speed centrifugation, pelleting the large surfactant aggregates from the cell-free lavage at 12,500 x g for thirty minutes, and extracting the resuspended pellet (Hall et al., 1992). Column chromatography then separates the CLSE into distinct peaks for the surfactant proteins, phospholipids and neutral lipids (Takahashi and Fujiwara, 1986). Pooling the appropriate fractions provides the PPL (Hall et al., 1994). The original published protocol used a column that incompletely separated the proteins from the phospholipids and required two passes through the column to obtain PPL. Substitution of a longer column accomplishes the complete separation during a single elution.

An approximate replica of PPL containing its major constituents was prepared using commercially available phospholipids. Native PPL contains 33 mol% DPPC, 15% PPoPC, 11% POPC, 10% PMPC, and 9% anionic phospholipids consisting of a complex

mixture of phosphatidylinositols and phosphatidylglycerols (Kahn et al., 1995). The remaining constituents are present in amounts less than a few percent. The mixture of synthetic compounds contained 11 mol% PG derived from egg yolk lecithin (Sigma Chemical Company, St. Louis, MO), 19% PPoPC, 14% POPC, 13% PMPC, and 42% DPPC to preserve the ratios of these components with each other. This mixture was also prepared without DPPC but with the ratios of all other components preserved. PG converted from egg lecithin provided a readily available source of anionic phospholipids with pairs of mixed acyl groups to substitute for the anionic compounds in pulmonary surfactant.

The subphase for all experiments contained 10 mM Hepes pH 7.0, 150 mM NaCl, 1.5 mM $CaCl_2$ (HSC). Water for these studies was first distilled and then purified by using systems obtained from Millipore (Bedford, MA) or Barnstead (Dubuque, IA). All glassware was acid-cleaned. All solvents were at least reagent-grade and contained no surface active stabilizing agents.

Methods:

Biochemical assays:

Phospholipid concentrations were determined by measuring the phosphate content (Ames, 1966) of measured aliquots.

Fluorescence microscopy:

These studies used a Nikon epifluorescence microscope focused on the surface of a Wilhelmy balance. The microscope contains infinity optics and a 100x super long working distance objective assembled on a custom-built stand. The Wilhelmy balance confines films within a constant perimeter vertical Teflon ribbon (Labcon, Darlington, UK) that linearly varies the confined area by reconfiguration of the ribbon. The maximum area is

532 cm^2, and the subphase volume is approximately one liter. A computer controls movement of the barrier and processes measurements of the surface pressure and surface area via the graphical interface program LabView (National Instruments, Austin, TX). Phospholipid solutions in chloroform contained 0.1 mol% Rh-DPPE unless specified otherwise. Solutions were spread in volumes of approximately 80 µl to an initial molecular area of 120 $Å^2$/molecule. After ten minutes to allow for evaporation of the solvent, films were compressed at 3 $Å^2$/molecule/minute.

Images were recorded on each apparatus by a Hamamatsu C2400 SIT camera, and then either recorded by VCR for later analysis or captured directly to computer (Macintosh IIci, Apple, Cupertino, CA) via frame grabber (LG-3, Scion Corp., Frederick, MD). A C-shaped Teflon mask placed directly in the subphase minimized movement of the monolayer. Images recorded inside and outside the mask ensured that it created no artifacts. Images were captured and analyzed using the program Image (NIH, Bethesda, MD). The fraction of interfacial area occupied by the nonfluorescent domains was calculated by counting pixels with grayscale above and below assigned threshold values.

Brewster angle microscopy:

Brewster angle microscopy examined films containing no extraneous fluorescent probe. BAM derives contrast from differences in reflectivity of structures within a film to p-polarized light incident at Brewster's angle for the clean air-water interface (Hönig et al., 1991). The previously described home-built instrument (Chapter 2) used in these studies was configured to image the surface of the same Wilhelmy balance used for fluorescence measurements. P-polarized light incident at 53.12° on the air-water interface reflected through an analyzing polarizer of variable orientation to a lens system and onto a CCD camera. The orientation of the analyzing polarizer varied from p-polarization to detect anisotropy in the reflected images. Images from the camera were captured by computer. Reproducible measurements of relative grayscale on a scale of 256 required the careful

maintenance of the interface at a constant level relative to the optical components. Grayscale values are linearly proportional to the reflectance of interfacial structures to p-polarized light, and were reproducible between experiments to within ± 5-15 unit. Data shown here are representative of at least three experiments.

Statistics:

Data are stated as mean ± S.D. unless stated otherwise. The standard error of the slope and intercept for linear fits of the area of each phase to the mol fraction of DPPC (Figure 9) were calculated using the program Igor Pro (WaveMetrics, Lake Oswego, OR).

RESULTS

Compression of PPL monolayers induced the separation of two phases. Both fluorescence microscopy and BAM distinguished domains that appeared in films at approximately 6 mN/m and grew as surface pressure increased. The domains were dark by fluorescence microscopy, demonstrating exclusion of the fluorescent probe from these areas (Fig. 3.1). In BAM, domains appeared bright, indicating greater optical thickness than the surrounding film (Fig. 3.2). These characteristic appearances both suggested that domains represented more condensed regions of the film. The isotherm for PPL was entirely smooth, and showed no plateau or kink to correspond with the phase transition evident by microscopy (Fig. 3.1).

The initial shape of the domains represented nonequilibrium forms (Fig. 3.1). The nonfluorescent areas were highly convoluted (Fig. 3.1), unlike the circular domains observed with CLSE (Chapter 2). After equilibration for several hours, the domains converted to circular shapes (Fig. 3.3). The total nonfluorescent area, however, changed only slightly with time, decreasing 5% over 6 hours.

The surface pressure at which fluorescence microscopy first detected the domains varied with temperature (Fig. 3.4). We have previously demonstrated for CLSE that domains appeared at pressures which closely paralleled values for pure DPPC (Chapter 2). PPL produced values that fell between DPPC and CLSE over the full range of temperatures from 20 to 40°C.

These several characteristics suggested that the domains in PPL were similar in structure and packing density to LC DPPC. To determine the extent to which the area of condensed phase responded to changes in the content of DPPC, we prepared mixtures of PPL with different amounts of DPPC. The nonfluorescent fraction of the interface increased with added DPPC (Fig. 3.5). Domains appeared between 4-6 mN/m in all mixtures of PPL with DPPC and then grew to a maximum area at 30-35 mN/m before

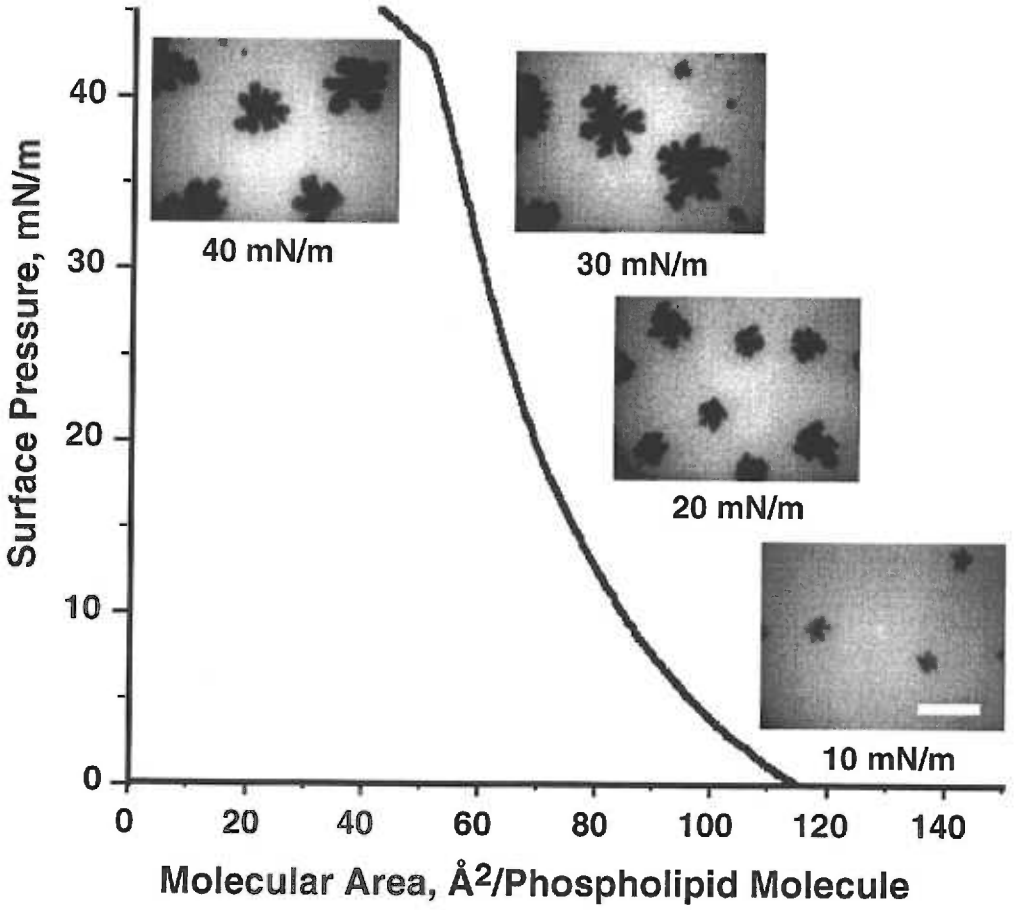

3.1. Surface pressure-area isotherms with epifluorescence images for purified phospholipids (PPL) from calf surfactant. Chloroform solutions of PPL containing 0.1% Rh-DPPE were spread to an initial molecular area of 150 $Å^2$/molecule on a subphase of HSC at 20°C. Isotherms were recorded during continuous compression at 3 $Å^2$/molecule/min. Fluorescence images were recorded in separate experiments from static films after compression at the same rate to the designated pressure. Images are representative of greater than 50 experiments. Scale bar represents 50 μm.

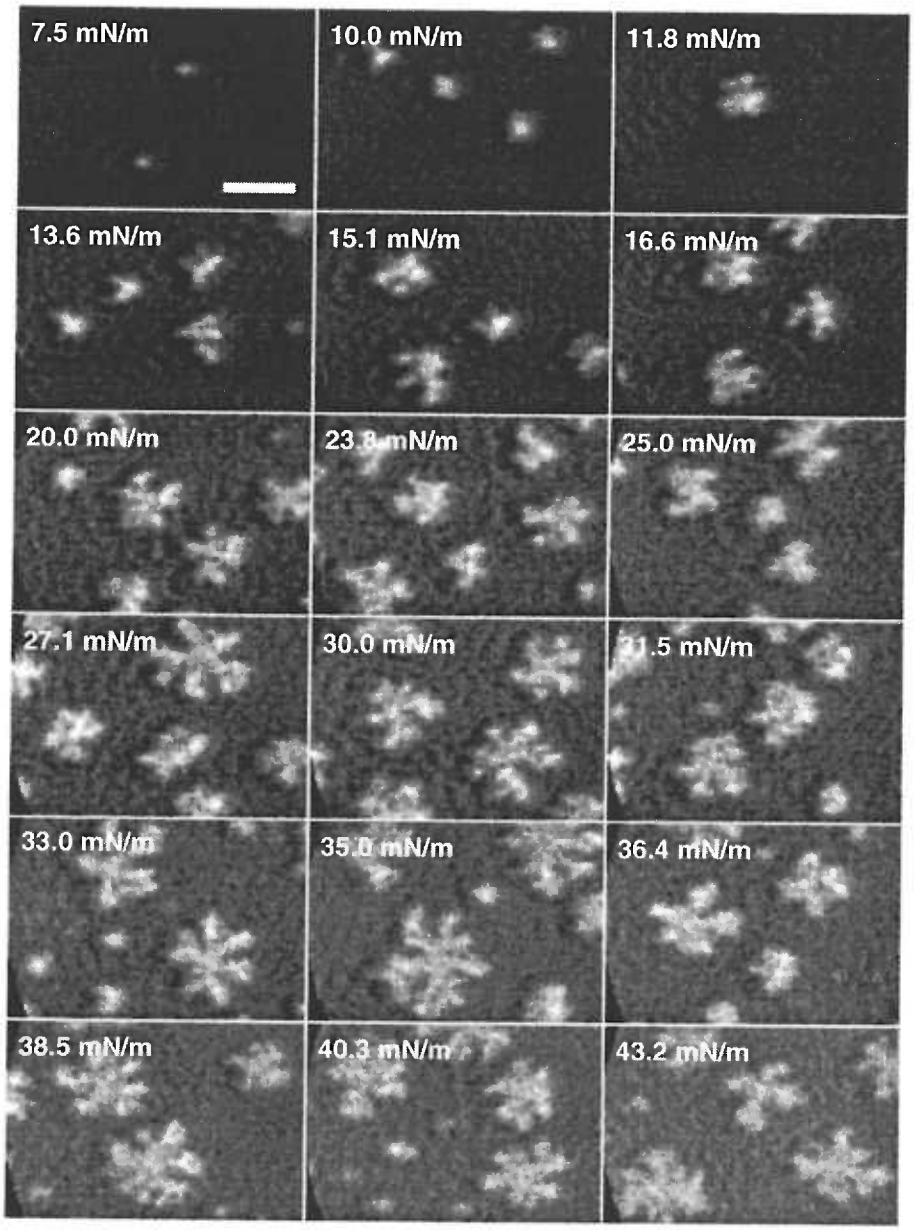

3.2. Brewster angle micrographs of PPL monolayers. Solutions of PPL in chloroform were spread on a subphase of HSC at room temperature and compressed at 3 $Å^2$/molecule to the surface pressures indicated. Scale bar is 50 μm.

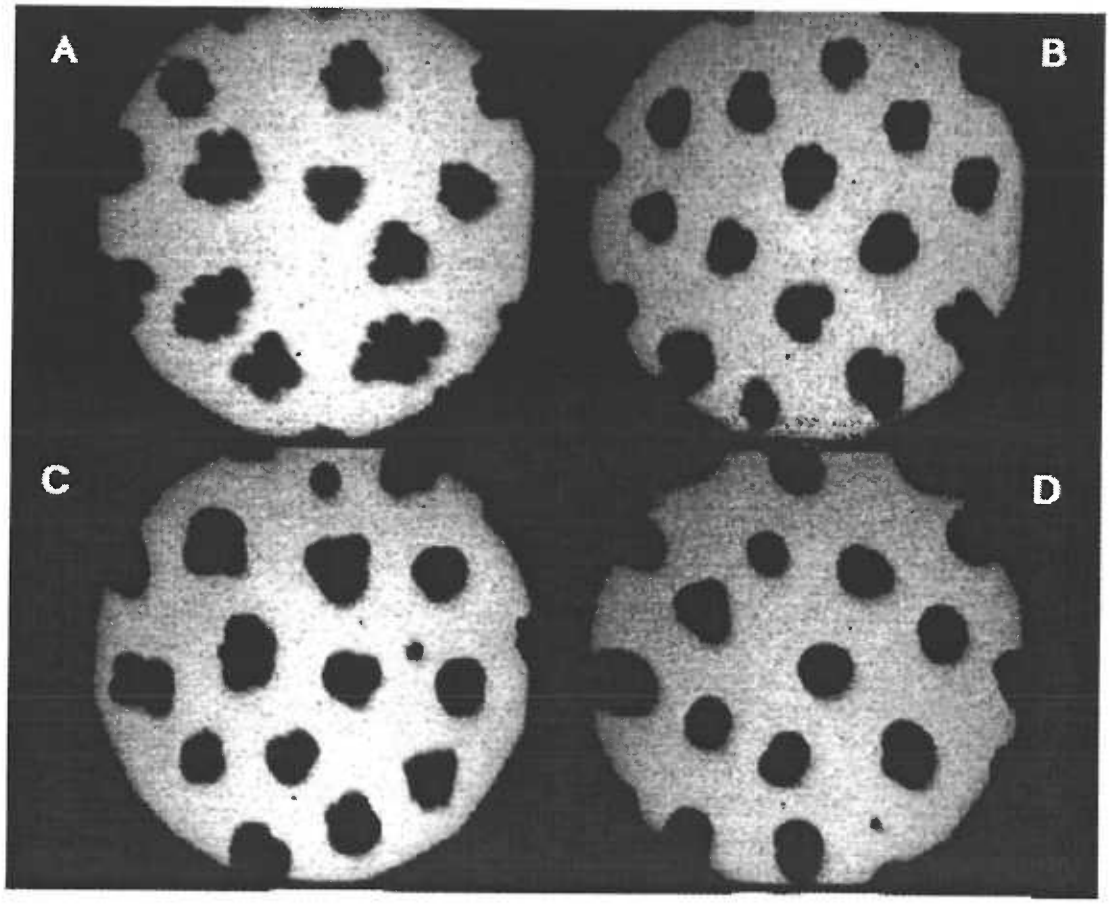

3.3. Variation of the shape of domains with time at 25 mN/m. Films of PPL containing 1% (mol:mol) Rh-DPPE were spread to an initial area of 150 $Å^2$/molecule and compressed at 2.8 $Å^2$/molecule/minute to 25 mN/m. Images of the static films were then recorded at the following number of hours after cessation of compression: A, 0; B, 2.5; C, 3.5; D, 6.5.

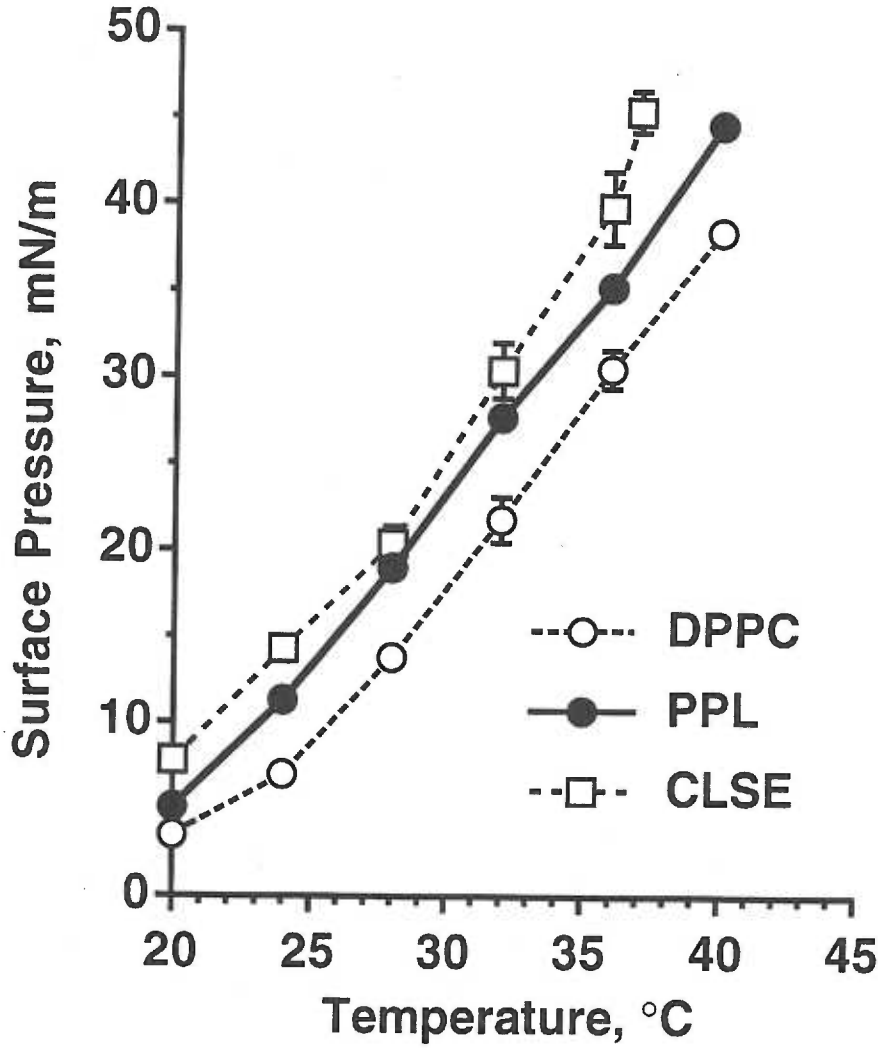

3.4. Temperature dependence of surface pressure at which domains first emerged. Isothermal compressions conducted at the temperatures indicated determined the surface pressures at which the domains first became apparent by fluorescence microscopy in monolayers of PPL (filled symbols). Chloroform solutions containing 1% Rh-DPPE were spread to an initial area of 150 $Å^2$/molecule and compressed at 2.8$Å^2$/molecule/minute. Data are mean ± S.D. For comparison, open symbols are measurements for CLSE and DPPC (Chapter 2).

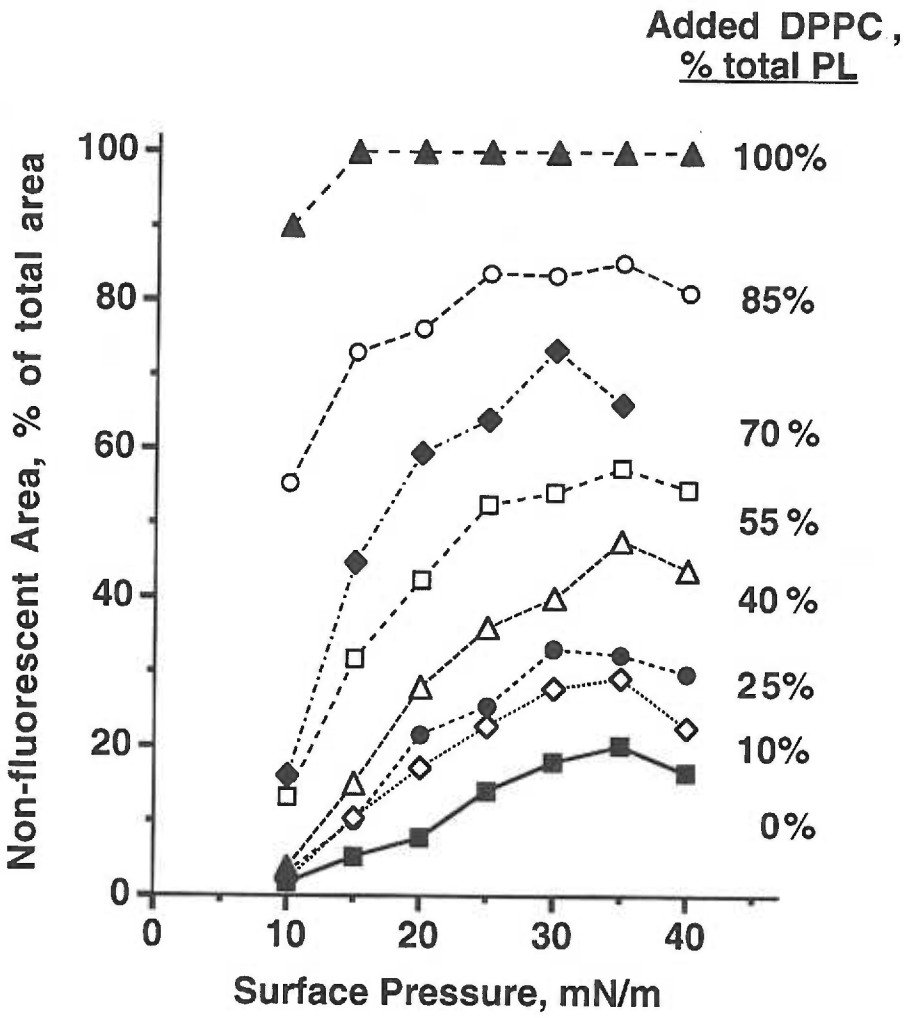

3.5. Variation of nonfluorescent area with surface pressure for different mixtures of PPL with added DPPC. Images obtained on static films were analyzed to determine the percentage of the interface occupied by the nonfluorescent domains. DPPC-PPL mixtures are described in terms of the amount of added DPPC expressed as the fraction of total phospholipid. At least three images were analyzed from different parts of the film in each of four experiments to obtain each data point.

declining at 40 mN/m. At each surface pressure for which fluorescence micrographs were obtained, more DPPC produced a larger nonfluorescent area. We also tested a replica of PPL prepared from commercially available individual phospholipids to determine if domains would appear in the absence of DPPC. PPL contains four major phosphatidylcholines that constitute approximately 70% of the mixture (Kahn et al., 1995). Films containing these components in the appropriate ratios with PG produced nonfluorescent domains. When DPPC was omitted from these mixtures, microscopy detected no such separation of phases (the experiments that involved reconstruction of the surfactant film were performed by Heather Helming and Carolyn Sousa).

The added DPPC produced a linear change in the area occupied by each phase at surface pressures above 20 mN/m. We obtained the areas for the condensed domains and the surrounding monolayer from the fraction of the interface ϕ occupied by the phase, obtained from the fluorescence micrographs (Fig. 3.5), multiplied by the average molecular area $\tilde{A}$ for the entire film, obtained from the compression isotherms (Fig. 3.6). These areas for each phase then represent the absolute area, uncorrected for the number of molecules in the phase, despite having units of molecular area because normalization is for molecules in the film rather than in the individual phase. For each surface pressure, the areas $\phi_c \cdot \tilde{A}$ and $\phi_f \cdot \tilde{A}$ of the condensed and fluid phases respectively for the different mixtures were plotted as a function of mol fraction of DPPC (Fig. 3.7). The response of phase area to DPPC changed with surface pressure. At 10 and 15 mN/m, the response was nonlinear, with the area of each phase initially changing little with added DPPC but then increasing steeply. At higher pressures, however, the area covered by the fluorescent and nonfluorescent regions varied with the mol fraction of DPPC along a straight line (Fig. 3.7).

BAM also provided further information concerning the structure of the two phases. During compression of PPL, the domains and surrounding film produced different behavior of the grayscale. For the domains, the grayscale remained constant while the surrounding film became progressively brighter. This observation was apparent

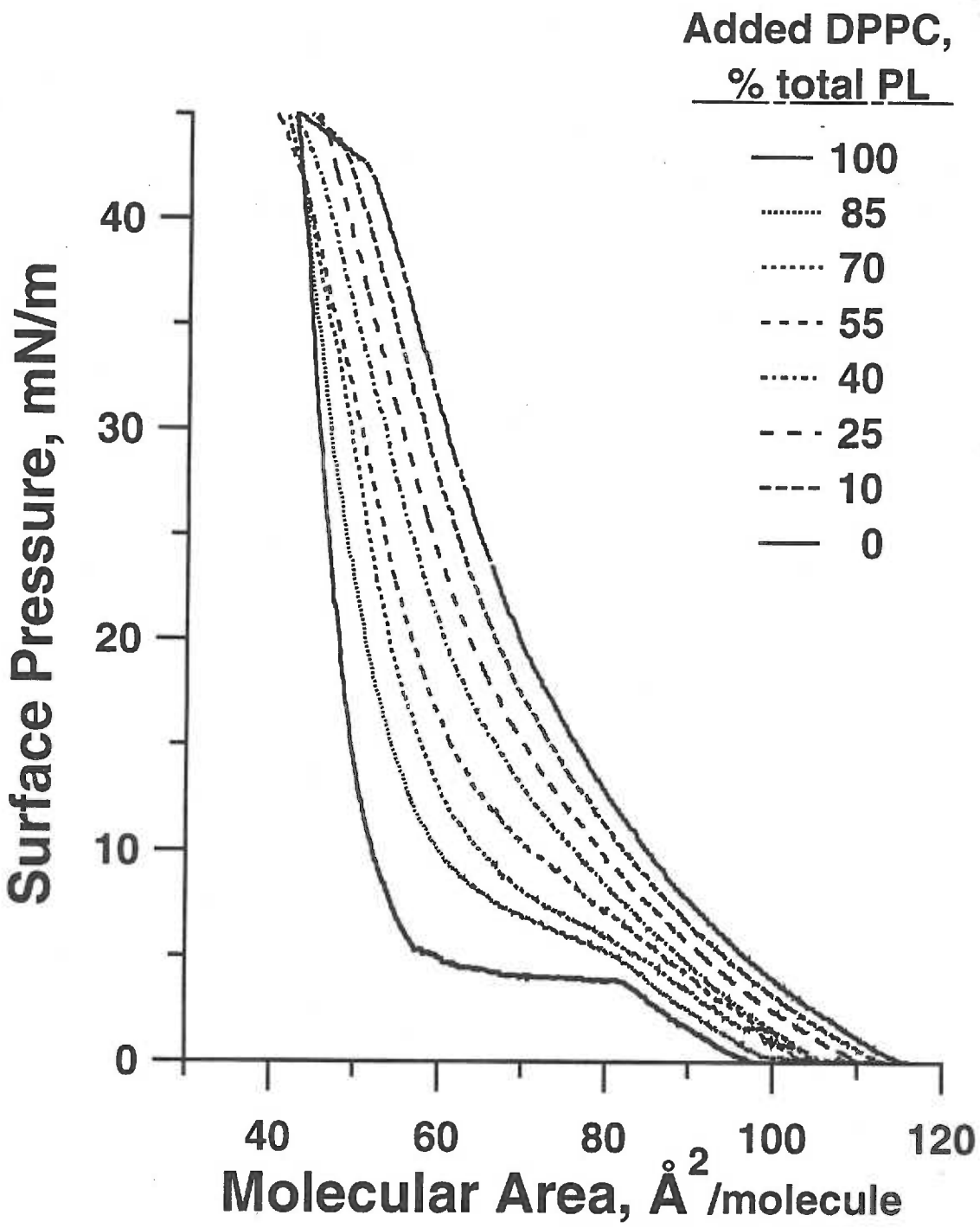

3.6. Compression isotherms for mixtures of PPL and DPPC. Mixtures were spread from chloroform solution to 120 $Å^2$/molecule on a subphase of HSC and compressed continuously at 3 $Å^2$/molecule/min.

3.7. Variation of the area of each phase with different levels of added DPPC at incremental surface pressures. A, area of the nonfluorescent domains; B, area of the surrounding fluorescent film. Areas were calculated as the product of the fraction of the interface occupied by each phase, ϕ_c or $(1 - \phi_c)$, times $\tilde{A}$, the average molecular area of the film. X^{DPPC}(added) on the top axis is the mol fraction of the DPPC added to the DPPC-PPL mixtures. X^{DPPC}(total) is the mol fraction of total DPPC, including DPPC endogenous to PPL using the previously determined content of 33% DPPC in PPL (Kahn, 1995). The line in each case represents the linear least squares fit to the data. For clarity of presentation, areas are offset above the data for the surface pressure with the lowest areas. The increment in area was 10 $Å^2$/molecule for every 5 mN/m above 10 mN/m up to 30 mN/m, and the 15 $Å^2$/molecule for each subsequent 5 mN/m.

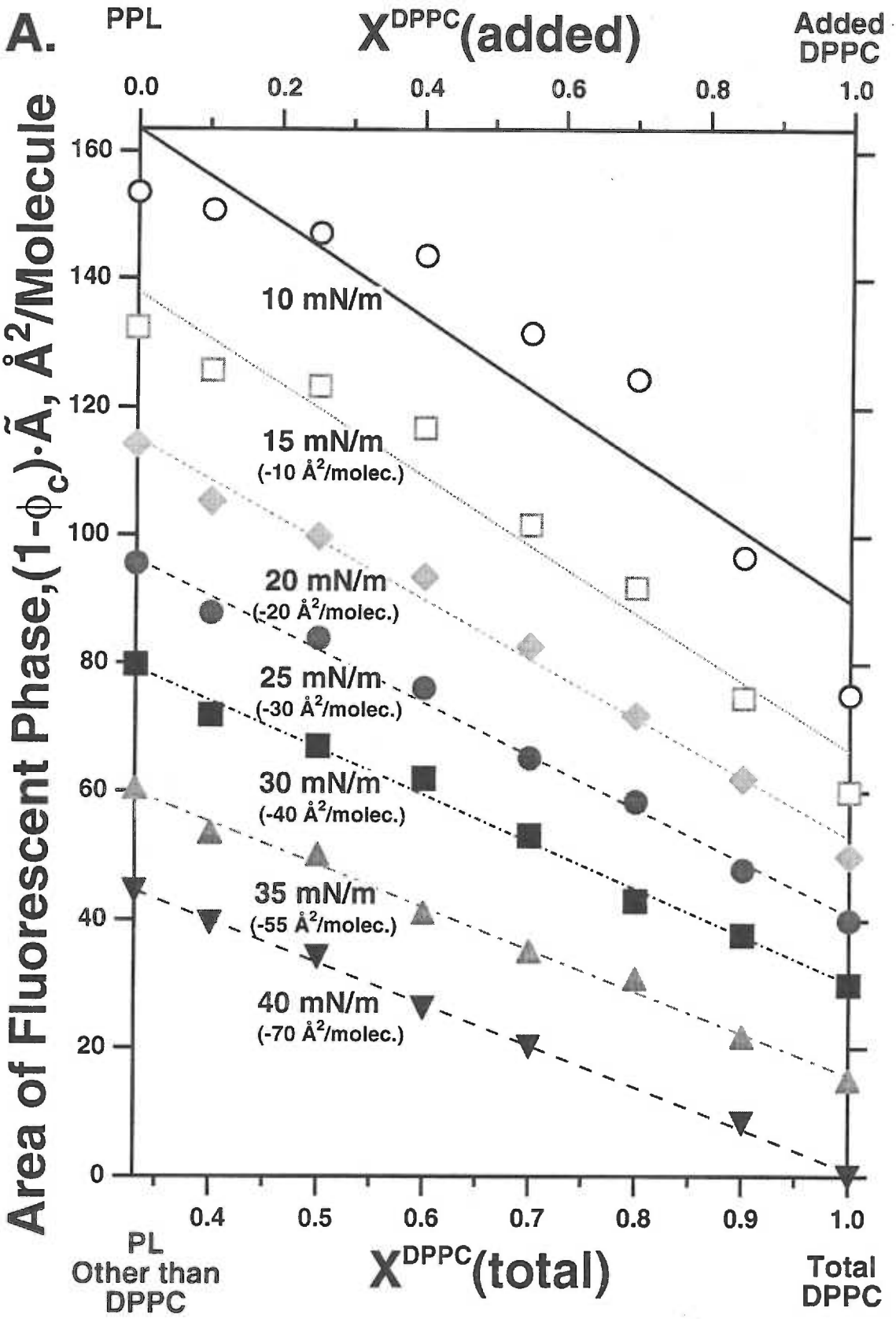
A.
PPL
X^{DPPC}(added)
Added DPPC
0.0
0.2
0.4
0.6
0.8
1.0
160
140
120
100
80
60
40
20
0
Area of Fluorescent Phase,$(1-\phi_c)\cdot\tilde{A}$, Å^2/Molecule
10 mN/m
15 mN/m
(-10 Å^2/molec.)
20 mN/m
(-20 Å^2/molec.)
25 mN/m
(-30 Å^2/molec.)
30 mN/m
(-40 Å^2/molec.)
35 mN/m
(-55 Å^2/molec.)
40 mN/m
(-70 Å^2/molec.)
0.4
0.5
0.6
0.7
0.8
0.9
1.0
PL Other than DPPC
X^{DPPC}(total)
Total DPPC

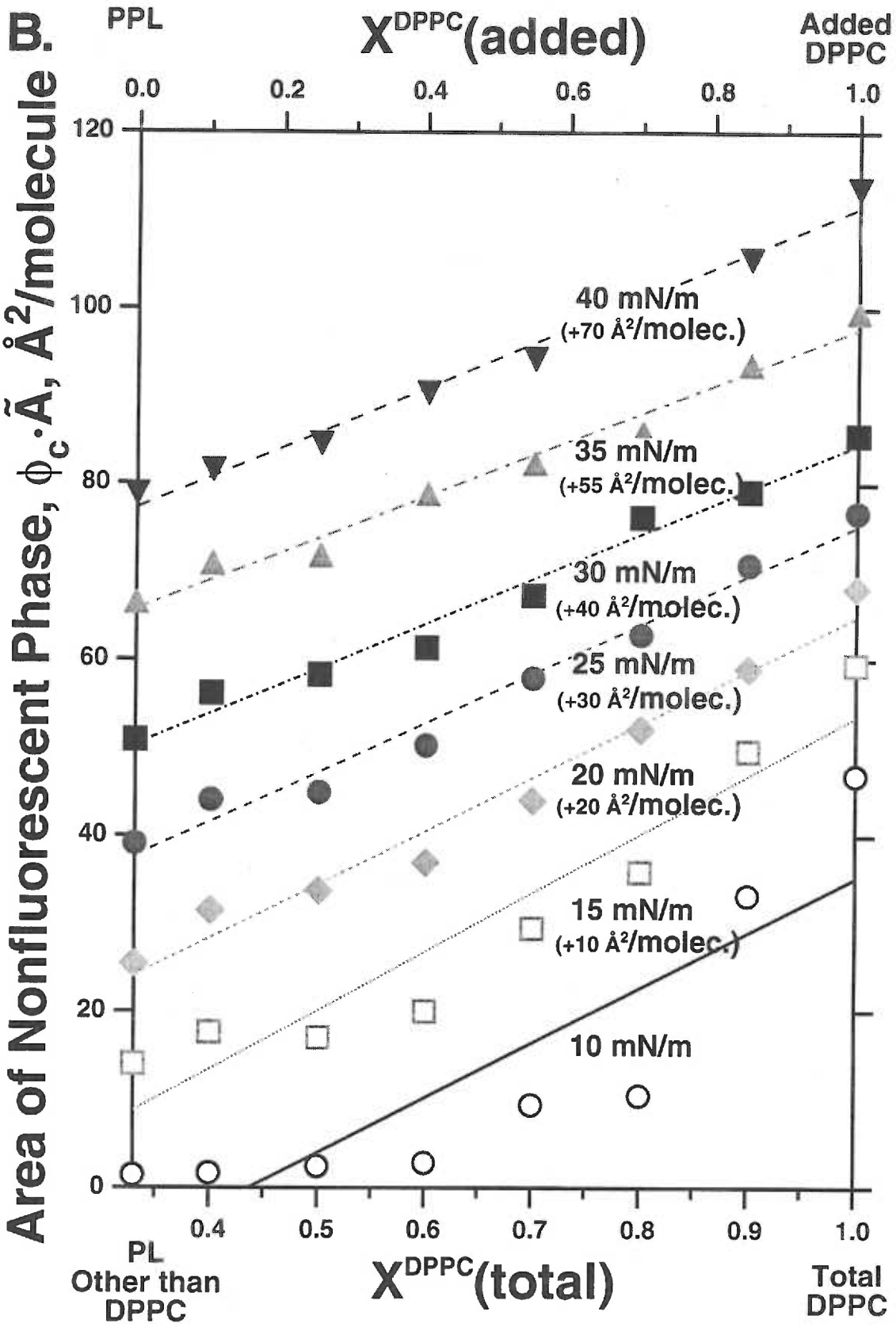
B.
PPL
X^{DPPC}(added)
Added DPPC
0.0
0.2
0.4
0.6
0.8
1.0
120
100
80
60
40
20
0
Area of Nonfluorescent Phase, $\phi_c \cdot \tilde{A}$, Å²/molecule
40 mN/m
(+70 Å²/molec.)
35 mN/m
(+55 Å²/molec.)
30 mN/m
(+40 Å²/molec.)
25 mN/m
(+30 Å²/molec.)
20 mN/m
(+20 Å²/molec.)
15 mN/m
(+10 Å²/molec.)
10 mN/m
0.4
0.5
0.6
0.7
0.8
0.9
1.0
PL
Other than
DPPC
X^{DPPC}(total)
Total
DPPC

qualitatively from the micrographs (Fig. 3.2), but analysis of grayscale values provided quantitative documentation as well (Fig. 3.8). Grayscale values were reproducible between experiments to within 5-15 units. For PPL, the domains produced grayscale values that varied only between 110 and 144 a.u. during compression from 8 to 41 mN/m. The LC phase for pure DPPC had similarly constant values, with grayscale falling in the range of 120 - 145 during the coexistence region. Two DPPC-PPL mixtures containing 50 and 70% DPPC were also tested, for which domains showed similar behavior.

The brightness of the surrounding film, however, increased with increasing surface pressure. The liquid expanded (LE) phase in films of pure DPPC produced the expected constant grayscale during compression at constant surface pressure across the coexistence region. For films containing PPL, however, the grayscale from these regions surrounding the domains increased progressively with surface pressure. For PPL itself, values increased from 21 at 0 mN/m to 67 at 41 mN/m. The mixed films containing DPPC added to PPL behaved similarly. Grayscale increased at similar rates as a function of surface pressure for all three films, producing slopes of 1.0 for PPL, 1.1 for 50% DPPC and 1.3 for 70% DPPC. Variation of the DPPC content in the films with PPL therefore had little effect on grayscale for either the domains or the surrounding film.

BAM also allows measurements of the anisotropy of the film. Anisotropy occurs when the hydrocarbon chains in a given region tilt not randomly but such that their projection in the interfacial plane has a net alignment. An analyzing polarizer in the reflected beam allows detection of the anisotropy. Light incident on the monolayer is polarized in the plane perpendicular to the interface, and so rotations of the analyzer in opposite directions from the plane of polarization will detect net alignment in the interfacial plane. Experiments detected anisotropy for the domains in both DPPC and PPL (Fig. 3.9). Intensities within regions of the domains were preserved for analyzer rotations in one direction and attenuated for opposite rotations. For the domains of DPPC, the variation between the different regions was continuous during progression along the triskelion arms,

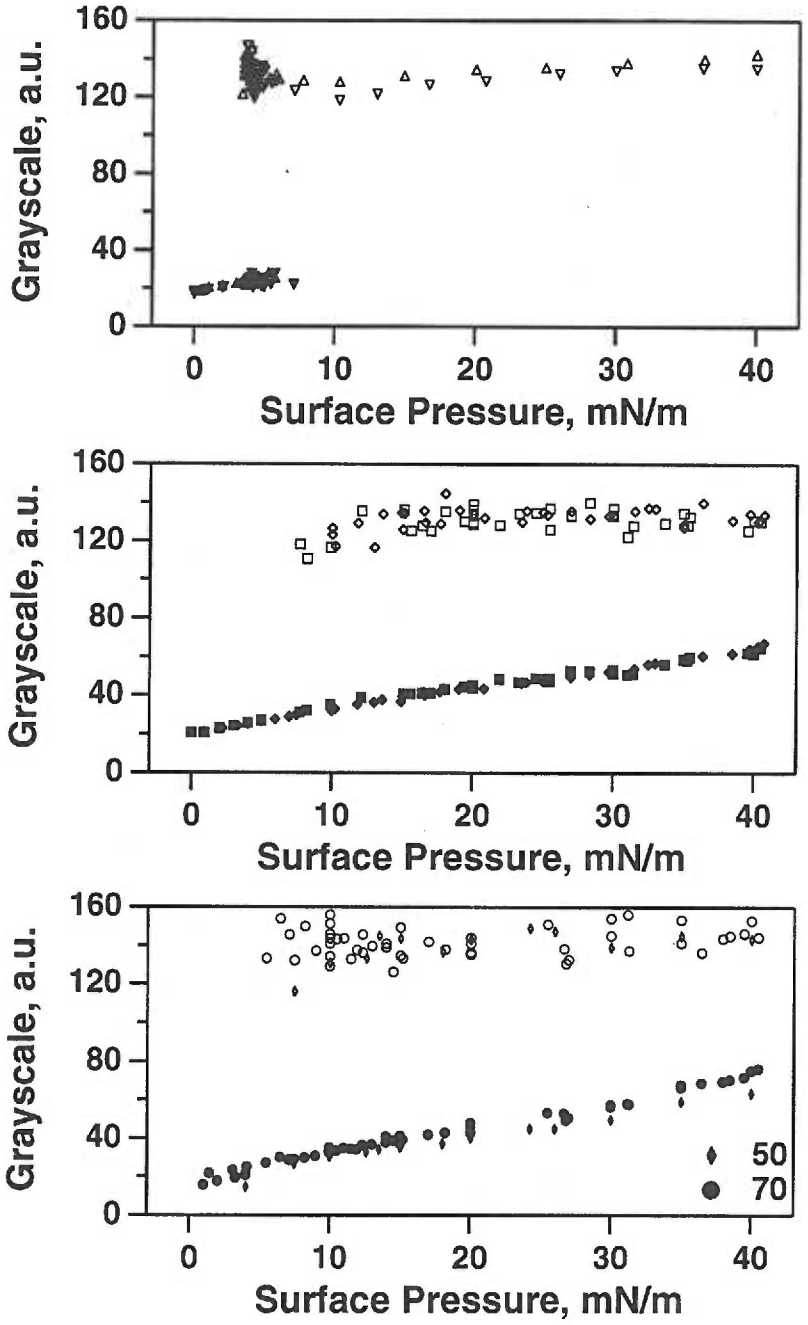

3.8. Variation of grayscale in Brewster angle micrographs. Chloroform solutions of phospholipids were spread on HSC subphase to an initial molecular area of at least 120 $Å^2$/molecule. Films were compressed at 1.4 $Å^2$/molecule/minute. Grayscale values were obtained for different regions of the film for the following components: A, DPPC; B, PPL; C, mixtures of DPPC and PPL containing a total of 50% and 70% total DPPC. The open symbols indicate the domains, the full symbol the surrounding phase. Each experiment is represented by different symbol.

A.

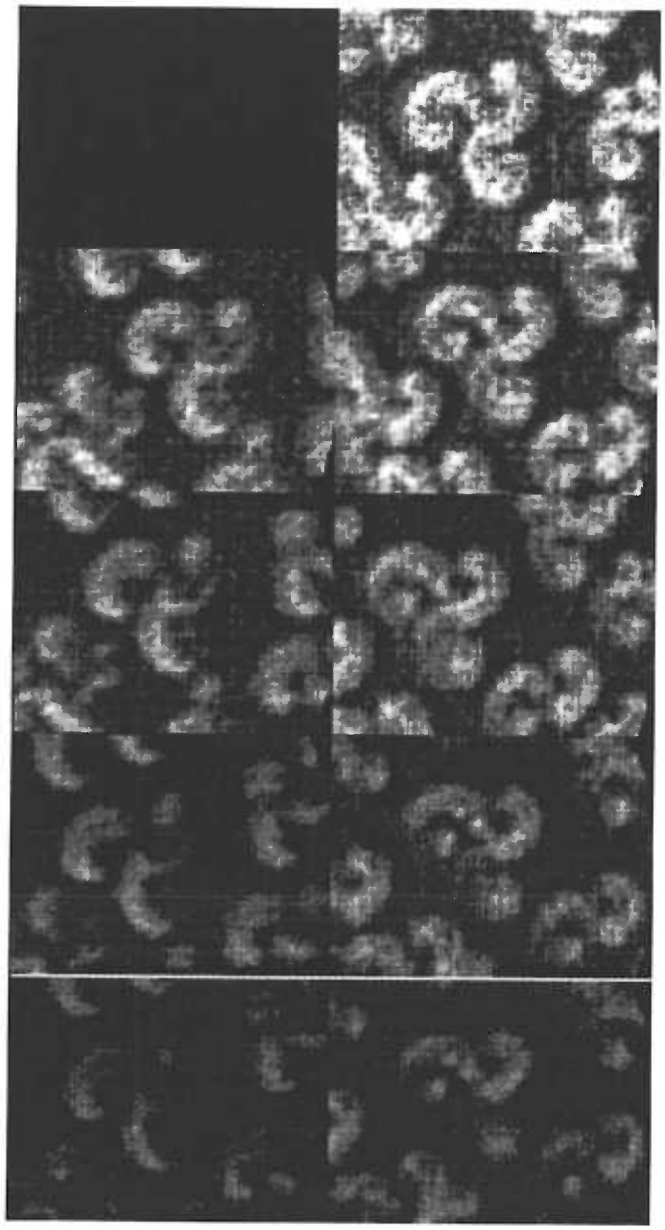

3.9. Anisotropy in Brewster angle micrographs. P-polarized light incident at 53.12° on the air-water interface reflected through an analyzing polarizer of variable orientation to a lens system and onto a CCD camera. The angle of the analyzer relative to p polarization is given for each micrograph. A. DPPC at 5 mN/m, with the following polarizer settings (top to bottom): 0°; 180°; ± 27.5°; ± 37.5°; ± 47.5°; ± 57.5°. B. PPL at 30 mN/m with the following polarizer settings (top to bottom): 0°; 180°; ± 25°; ± 35°; ± 45°; ± 55°.

B.

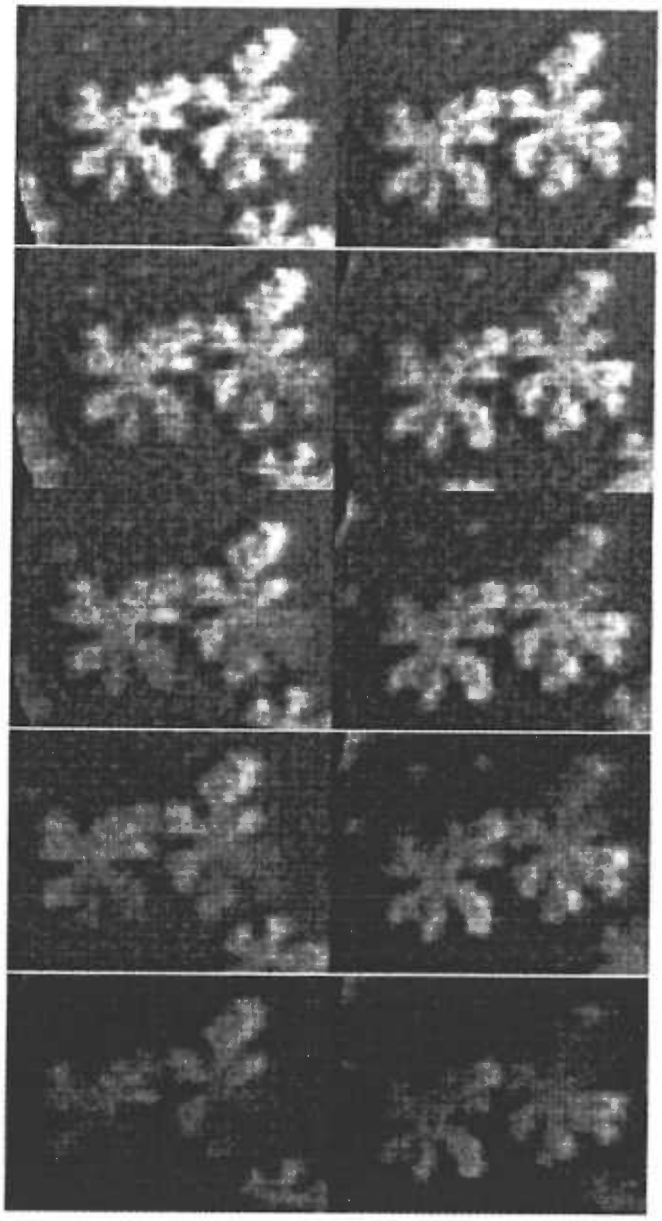

consistent with the expected progressive variation in the direction of tilt for the condensed molecules. The progressive variation was less evident in the irregularly shaped domains for PPL, but opposite analyzer rotations again showed regions with opposite effects on reflected intensity, indicating alignment of compounds within the interfacial plane. In contrast, the film surrounding the domains showed no anisotropy. Rotation of the analyzer through the angle α reduced the grayscale for these regions by $\cos^2\alpha$, as expected for an isotropic phase.

DISCUSSION

Our results show that compression of monolayers containing the complete set of pulmonary surfactant phospholipids leads at intermediate surface pressures to the separation of two phases. Our measurements provide information on both the structure and composition of each phase, and indicate that the domains represent a condensed phase containing only DPPC surrounded by a fluid phase with the other phospholipids. We will first discuss the implications of the fluorescence measurements on the composition of each phase, and then the structural information provided by BAM.

The fluorescence measurements on the area for the two phases in mixtures of PPL with different amounts of DPPC provide information directly related to composition. Analysis of the data requires an expression relating phase area to composition. If the total number of molecules in the film is n, and the number for the condensed and fluid phases are n_c and n_f respectively, then

$$n = n_c + n_f$$

Our complex mixture contains numerous constituents, each of which can partition differently between the two phases. At any given surface pressure for the mol fraction X^i of the constituent i in the complete film, if X_c^i and X_f^i are its mol fractions for the two phases, then

$$n \cdot X = n_c \cdot X_c^i + n_f \cdot X_f^i.$$

This relationship leads directly to the lever rule,

$$\frac{n_c}{n_f} = \frac{(X^i - X_f^i)}{(X_c^i - X^i)}$$

and also provides a relationship between the fraction f of all molecules in each phase and composition:

$$f_c \equiv n_c/n = \frac{(X^i - X_f^i)}{(X_c^i - X_f^i)}$$

In terms of our experimental measurements, the area of the condensed phase is given by

$$\phi_c \cdot \tilde{A} = f_c \cdot \tilde{A}_c$$

where ϕ_c is the fraction of the interface occupied by the condensed phase, $\tilde{A}$ is the molecular area of the entire film, and $\tilde{A}_c$ is the average molecular area within the condensed phase (Knobler, 1990). Substitution then yields

$$\phi_c \cdot \tilde{A} = \tilde{A}_c \cdot \frac{(X^i - X_f^i)}{(X_c^i - X_f^i)} \qquad (1)$$

for the condensed phase and

$$\phi_f \cdot \tilde{A} = (1 - \phi_c) \cdot \tilde{A}$$
$$= \tilde{A}_f \cdot \frac{(X_c^i - X^i)}{(X_c^i - X_f^i)} \qquad (2)$$

for the fluid phase. These expressions then relate the areas of each phase to the compositions for any particular constituent at a fixed surface pressure. For phase areas that vary linearly with X^i, this relationship then provides a simple approach for calculating the composition of each phase. According to equation (1), the slope for plots of $\phi_c \cdot \tilde{A}$ versus X^i will be $\tilde{A}_c/(X_c^i - X_f^i)$ and the intercept is $-\tilde{A}_c \cdot X_f^i/(X_c^i - X_f^i)$. The ratio of -intercept /slope then provides X_f^i. From equation (2), the comparable ratio for plots of $\phi_f \cdot \tilde{A}$ yields X_c^i. This method then determines the content of component i in each phase at a given surface pressure.

Our experimental data show that the areas for each phase do vary linearly with the mol fraction of DPPC. Above 15 mN/m, $\phi_c \cdot \tilde{A}$ and $\phi_f \cdot \tilde{A}$ both fit well to a linear relationship with X^{DPPC} (Fig. 3.7). The ratio of -intercept/slope for these data then provide values of X_c^{DPPC} and X_f^{DPPC} at each of the surface pressures above 15 mN/m. This analysis then allows construction of a simple phase diagram (Fig. 3.10). The surface pressures at which the domains first emerged for the different mixtures define the lower boundary of the coexistence region. The compositions obtained at specific surface pressures from the plots of $\phi \cdot \tilde{A}$ vs. X^{DPPC} for each phase define the lateral boundaries. The values from this analysis indicate that fluid phase contains mostly phospholipids other than DPPC. The

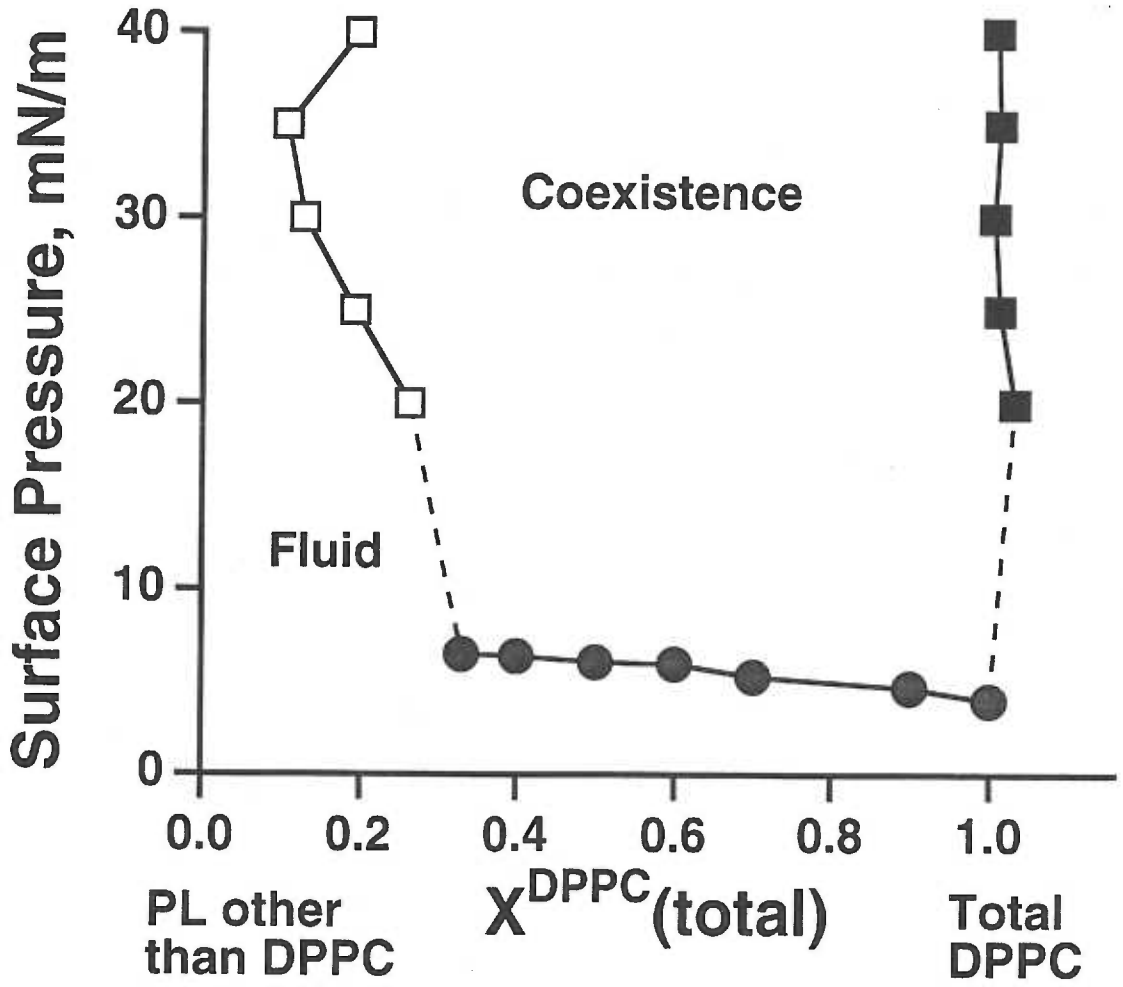

3.10. Phase diagram for PPL. X^{DPPC}(total) is the mol fraction of total DPPC, including material both added and endogenous to PPL at 20 °C. Gray circles are points determined directly from the surface pressures at which domains first emerged for the different mixtures. Squares are data obtained from the variation for the different PPL-DPPC mixtures of the nonfluorescent (filled squares) and fluorescent (empty squares) phase (Fig. 3.9). Data at 10 and 15 mN/m, where the relationship between phase area and content of DPPC were nonlinear, are omitted from this diagram. Dotted lines instead connect the two sets of established points. "Fluid" indicates the region of the homogeneously fluorescent monolayer. "Coexistence" indicates the conditions under which nonfluorescent domains are present together with the surrounding fluorescent monolayer.

limited content of DPPC in this phase falls from 26% at 20 mN/m to a minimum of 11% at 35 mN/m before increasing to 20% at 40 mN/m. The condensed domains contain only DPPC.

This analysis also provides values for the molecular areas of each phase (Fig. 3.11). Given the calculated values of X_c and X_f, equations (1) and (2) provide a value of $\tilde{A}_c$ and $\tilde{A}_f$ for each mixture and each surface pressure at which measurements were made. Because the composition of each phase is fixed, the molecular areas must also be constant, and so the values of $\tilde{A}_c$ and $\tilde{A}_f$ were averaged at each surface pressure for the different mixtures. These average values of $\tilde{A}_c$ and $\tilde{A}_f$ at different surface pressures then provide compression isotherms for each phase (Fig. 3.11). The curves behave as expected from the phase diagram. The domains of DPPC had molecular areas that fit well with isotherms for films of pure DPPC. The surrounding film, which contains the same phospholipids as PPL except for a reduced content of DPPC, had areas shifted to slightly larger values than PPL. These data agree with the phase diagram to present a self-consistent view of the phase behavior of our system, and indicate that the domains contain only DPPC.

The areas for each phase versus the mol fraction of DPPC clearly deviate from linearity at surface pressures 10 and 15 mN/m. We believe that the non-linearity of those data is a non-equilibrium phenomenon related to the fact that the initial formation of DPPC domains even in pure DPPC films does not obey the lever rule with respect to the molecular areas under the same experimental conditions (Klopfer and Vanderlick, 1996) and therefore our analysis is not suitable for those lower pressures.

Brewster angle micrographs provide information more directly related to the structure of the different phases. Grayscale, for instance, indicates the optical thickness of the film. Measurements for the domains indicate that they have the same grayscale values as LC DPPC, and also that these values were similarly invariant during compression over a range of surface pressures. The constant optical thickness indicated by these measurements shows that the PPL domains, like the LC DPPC, are incompressible, and further

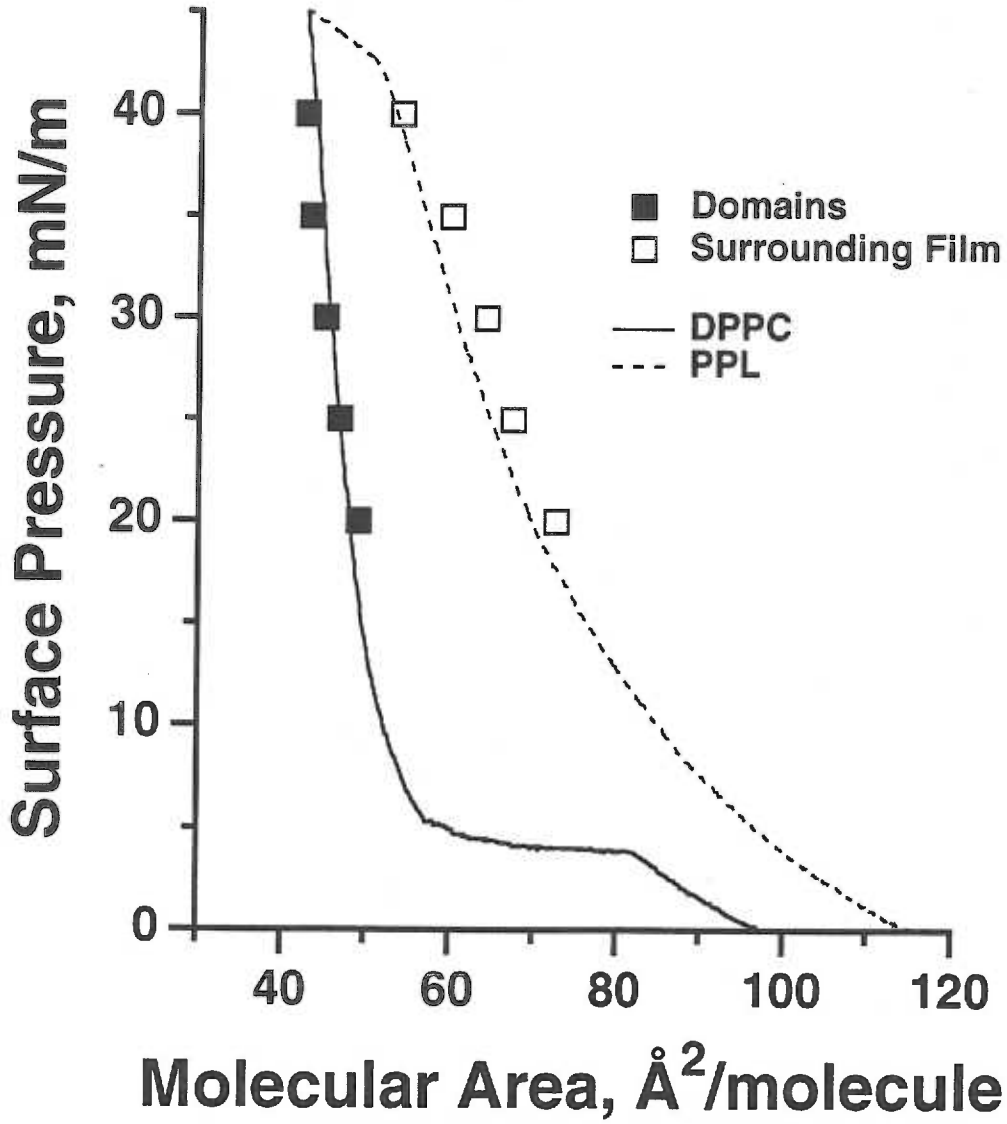

3.11. Isotherm for each phase in mixed monolayers of DPPC-PPL at 20 °C. Values of the molecular area for each phase were calculated from the phase diagram and microscopic measurements and averaged over the series of DPPC-PPL mixtures at each surface pressure. Filled symbols give values for the domains, and empty symbols for the surrounding film. Isotherms for pure DPPC and for PPL are shown for comparison.

establishes behavior expected of a condensed phase. In contrast, the grayscale values for the regions surrounding the domains in the PPL films were lower than LC DPPC, and they varied with surface pressure. The compressibility of these regions again fits with the characteristics expected of a fluid phase. In mixtures of DPPC and PPL, the similar grayscale values and rate of variation with surface pressure for each phase indicate that the optical thickness and compressibility are independent of the film's composition. This structural information of course does not specify the composition of the two phases. It is, however, entirely consistent with the behavior expected from the compositions indicated by the fluorescence measurements.

Optical anisotropy provides further evidence that the domains and surrounding film represent condensed and fluid phases respectively. The anisotropy observed for the bright domains in the PPL films indicate a net alignment of constituents within the interfacial plane, consistent with the organized structure expected for a condensed phase. The optical isotropy of regions surrounding the domains demonstrates the random alignment expected for a fluid phase. These results again fit with behavior predicted for the composition indicated by the fluorescence measurements. The pattern of anisotropy, however, for the domains in PPL and DPPC raises the possibility that their compositions could still be slightly different. The chiral structure of DPPC leads to the chiral shape of the LC domains in the coexistence region. Careful inspection of the micrographs shows the gradual shift in anisotropy along the triskelion arms that indicates the expected progressive rotation of the molecular alignment. For the PPL domains, however, the alignment instead seems to change discretely. Individual extrusions from the domains seem to vary in brightness together, with different analyzer orientations causing a uniform variation without the gradation across the projection that would suggest progressive shift in the direction of tilt. This finding raises the possibility of the presence in the PPL domains of compounds other than DPPC. The error for the compositions calculated from the fluorescence measurements certainly allows for that possibility. Nevertheless, the domains in the PPL films are

forming in a significantly different electrostatic field due to the different composition of the surrounding phase, and that factor can have an impact on the molecular organization. Specifically, the tilt of the molecules at the boundaries of domains during their formation can be reduced due to larger electrostatic interaction with the molecules in the LE phase. Since the observed difference in the patterns of anisotropy between DPPC and PPL is quite subtle and not necessarily related to the different composition, we consider that the suggestion of compounds other than DPPC in the PPL domains is inconclusive.

Our findings have direct physiological relevance in that they provide a mechanism by which the composition of the surfactant film might undergo refinement. Although only 30% of the constituents in CLSE are DPPC (Kahn et al., 1995), the mechanical characteristics of the functional film suggest that it consists predominantly of that single compound. The widely held squeeze-out hypothesis contends that other components are eliminated from the monolayer by compression above equilibrium pressures (Watkins, 1968). Although direct evidence to demonstrate refinement remains lacking, our finding that as much as 61% of the DPPC separates into a pure LC phase for PPL suggests that such a process could occur on the basis of the separated phases. Domains demonstrated previously in films of complete extracts of surfactant are also likely to contain predominantly DPPC. Measurements with labeled SP-C suggest that proteins probably occur outside the domains (Nag et al., 1996; Nag et al., 1997). Cholesterol can mix with DPPC in the condensed phase (Albrecht et al., 1981) but only to a very limited extent, and in the partitioning between the two surfactant phases, the content of the domains seems likely to be even lower. The condensed domains also seem likely to be more stable above equilibrium spreading pressure than the surrounding fluid phase. We have not measured relative stabilities, but the known characteristics of the two phases makes this likely. Separation of DPPC into a highly refined and more stable phase could then provide the basis by which a refined film occurs.

In summary, fluorescence microscopy and BAM show that monolayers containing the complete mix of phospholipids from calf surfactant separate into two phases during compression at the air-water interface. Discrete domains contain only DPPC, and have the incompressible ordered structure expected of a condensed phase. The surrounding regions contain reduced amounts of DPPC along with the other phospholipids, and have the disorganized compressible structure of a fluid phase.

ACKNOWLEDGMENTS

The authors gratefully acknowledge the gift of extracted calf surfactant by Dr. Edmund Egan of ONY, Inc. and Dr. Robert Notter of the University of Rochester. Heather Helming assisted in the preparation of samples of PPL. This research was supported by funds from the National Institutes of Health (HL 03502 and 54209), the Whitaker Foundation, and the American Lung Association of Oregon. BMD was supported in part by a fellowship from the Tartar Trust. WRS was supported as a predoctoral fellow by NIH training grants in Biotechnology (GM 08437) and Molecular Biophysics (GM 08268).

CHAPTER 4

NEUTRAL LIPIDS CAUSE REMIXING OF SEPARATED PHASES IN INTERFACIAL MONOLAYERS OF PULMONARY SURFACTANT

Bohdana M. Discher[a], Kevin M. Maloney[b], David W. Grainger[c],

and Stephen B. Hall[a,d]

Departments of Biochemistry and Molecular Biology[a], Physiology and Pharmacology[d],

and Medicine[d], Oregon Health Sciences University, Portland, OR 97201

[b]Department of Chemistry, Biochemistry and Molecular Biology,

Oregon Graduate Institute of Science & Technology, Portland, OR 97006

[c]Department of Chemistry, Colorado State University, Fort Collins, CO 80523

Address correspondence to:

Stephen B. Hall

Mail Code UHN-67

Oregon Health Sciences University

Portland, Oregon 97201-3098

Telephone: (503) 494-7680

Facsimile: (503) 494-6670

e-mail: sbh@ohsu.edu

Running title: Critical point in pulmonary surfactant films induced by neutral lipids.

ABSTRACT

We have previously shown that although films of pulmonary surfactant initially separate during compression into two phases, these remix when the films become more dense. In the studies reported here, we have used fluorescence microscopy to determine the role of the different surfactant constituents in the remixing of the separated phases. The complete mixture of pulmonary surfactant components was separated by column chromatography into the following three fractions: the purified phospholipids (PPL); surfactant protein and phospholipids (SP&PL); and the neutral and phospholipids (N&PL). Nonfluorescent domains emerged and grew during compression of films containing each preparation despite entirely smooth isotherms. The domains in N&PL abruptly decreased in area from a maximum of 26 ± 3% of the interface at 25 mN/m to 4 ± 2% at 30 mN/m. In contrast, PPL reached a maximum of 20 ± 2% at 35 mN/m, but decreased only slightly to 17 ± 2% at 40 mN/m. The nonfluorescent area in SP&PL increased continuously to 17 ± 1% at 40 mN/m. The nonfluorescent phase was dispersed into a larger number of smaller domains for both N&PL and SP&PL relative to PPL, consistent with a reduction in interfacial tension between the two phases. Continuous observation showed that the initially circular domains in N&PL became highly distorted just prior to remixing with the surrounding film. This shape transition indicates that the remixing caused by the neutral lipids occurs at or close to a critical point in the phase diagram.

Key words: critical point
surfactant proteins
dipalmitoyl phosphatidylcholine
cholesterol
line tension
epifluorescence
monolayer
surface tension

INTRODUCTION

Interfacial films of pulmonary surfactant cover the thin liquid layer that lines the small air spaces of the lung. During exhalation, when the films are compressed due to the decreasing surface area, the surfactant lowers surface tension to remarkably low levels (Schürch, 1982). Only highly ordered films seem likely to withstand compression to the very high densities implied by these measurements without collapse from the interface. In single component systems, more than half of the surfactant constituents form liquid-expanded (LE) films that are not stable at the interface at the surface pressures required for the extremely low surface tensions. Therefore these components must be either eliminated from the interface during compression or reorganized together into a stable structure. Since the formation of a very stable film requires that its characteristics must undergo dramatic change, phase behavior is likely to be a critical determinant of the function of pulmonary surfactant.

We have reported previously that phase separation does occur in films of pulmonary surfactant (Chapter 2). The discrete domains that emerged during compression of extracted calf surfactant (calf lung surfactant extract, CLSE) acquired several properties characteristic of liquid condensed (LC) dipalmitoyl phosphatidylcholine (DPPC). In a simplified system, containing only the purified phospholipids (PPL) obtained from pulmonary surfactant, we have shown that the domains do contain pure DPPC (Chapter 3). Several other aspects, however, of the phase behavior for the complete CLSE mixture differed from the purified phospholipids. The most remarkable difference is the miscibility of the two phases. Although there was similarity in the emergence and growth of domains

for PPL and CLSE during initial compression to a maximum area, in PPL the domains then decreased minimally in size, but in CLSE they quickly remixed with the rest of the film.

In the studies reported here we have compared preparations of calf surfactant that lack specific components (Hall et al., 1994) to determine what constituents are responsible for the remixing in films of CLSE. Our results show that remixing occurs in the presence of the neutral lipids, but not in their absence. Careful observation of the film during remixing revealed large distortions of the domain's shape prior to their disappearance. The distortions indicate that line tension in these films is quite low, and that remixing occurs at a critical point.

MATERIALS AND METHODS

Materials:

Extracted calf surfactant (calf lung surfactant extract, CLSE), prepared as described previously (Hall et al., 1992), was obtained from Dr. Edmund Egan of ONY, Inc. (Amherst, NY) and Dr. Robert Notter of the University of Rochester. CLSE was fractionated to exclude specific components using column chromatography by a slight modification of a previously published protocol (Hall et al., 1994). Gel permeation chromatography separates the proteins, phospholipids, and neutral lipids into distinct peaks (Takahashi et al., 1986). Pooling selected fractions provides preparations which contain the purified phospholipids (PPL), the neutral and phospholipids (N&PL), and the surfactant proteins and phospholipids (SP&PL) (Fig. 4.1). Each of these preparations then contains the complete set of surfactant phospholipids with or without the surfactant proteins and neutral lipids. Although in the original protocol (Hall et al., 1994) the protein and phospholipid peaks overlapped, a longer column achieved complete separation on a single pass for the materials studied here. Preparations were eluted from the LH-20 matrix (LKB-Pharmacia, NJ) with a solvent of acidified chloroform-methanol (0.1 N $HCl:CHCl_3:CH_3OH$; 1:9:9 v:v:v) (Bizzozero et al., 1982; Takahashi et al., 1986), followed by extraction of the constituents into chloroform (Bligh et al., 1959). Samples of SP&PL suffered variable losses of proteins and were supplemented with protein purified separately to obtain the protein/phospholipid ratio found for CLSE (Hall et al., 1994). Experiments reported here that compared preparations used material derived from a

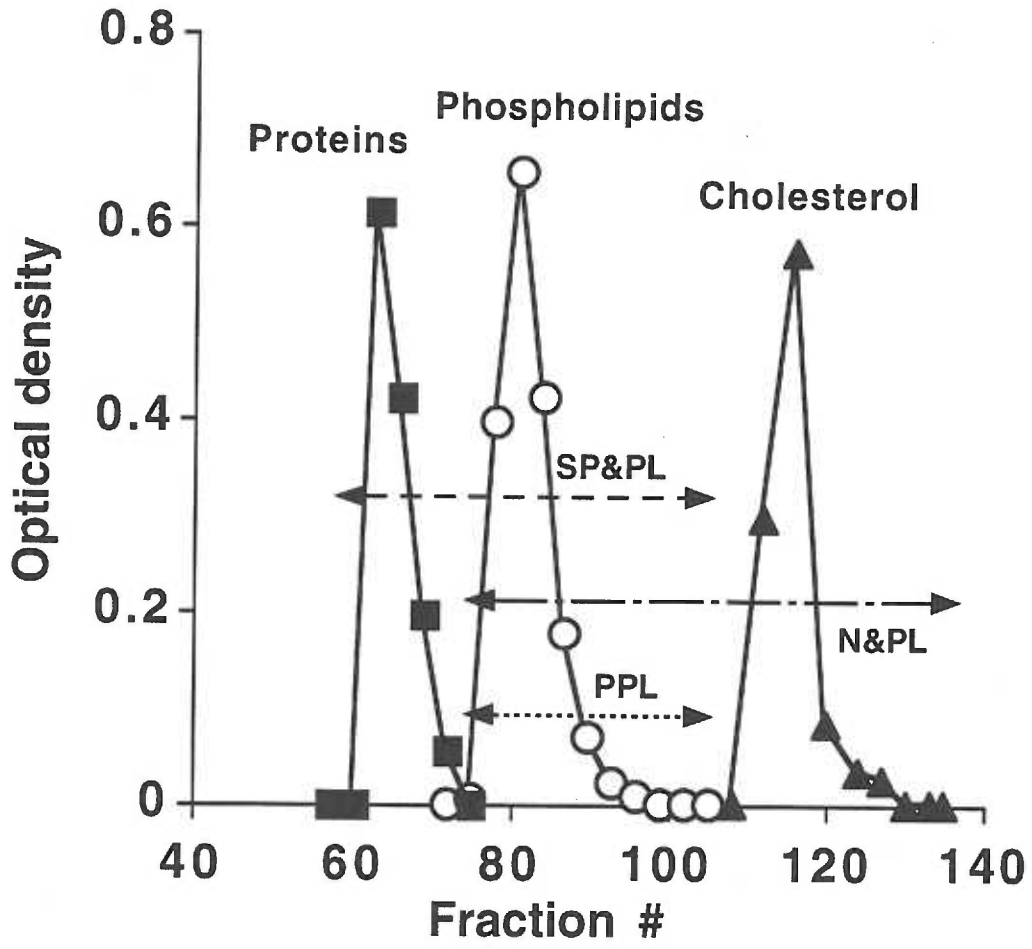

4.1. Separation of components from CLSE with LH-20 column chromatography. 500 µl of sample was injected into the column and eluted with chloroform:methanol:0.1 N HCl 95:95:10 (v/v/v) at 12 ml/hour into fractions collected every 15 minutes. Fractions were assayed for protein (filled squares), phospholipid (open circles), and cholesterol (filled triangles). Horizontal lines indicate the fractions that were collected to obtain different preparations of surfactant components: SP&PL, surfactant proteins and phospholipids; N&PL, neutral and phospholipids; and PPL, purified phospholipids.

common batch of CLSE. The separate experiments with N&PL that monitored the shape transition immediately prior to remixing used a batch different from the material for the other experiments. Results with different batches were qualitatively similar, although variables such as the surface pressure at which the separated phases remixed did vary.

DPPC was obtained from Avanti Polar Lipids, Inc. (Alabaster, AL) and used without further analysis or purification. N-(Lissamine rhodamine B sulfonyl)-1,2-dihexadecanoyl-sn-glycero-3-phosphoethanolamine (Rhodamine-DPPE) was purchased from either Avanti Polar Lipids (Alabaster, AL) or Molecular Probes (Eugene, OR).

Reverse-osmosis grade water for these studies was obtained from purification systems purchased either from Millipore (Bedford, MA) or Barnstead (Dubuque, IA) and had resistivity of approximately 18 Mohm·cm. All glassware was acid-cleaned. All solvents were at least reagent-grade and contained no surface active stabilizing agents.

Methods:

A. *Biochemical Assays*:

Phospholipid concentrations were determined by measuring the phosphate content (Ames, 1966) of measured aliquots of extracted material. Protein assays used the amido black method of Kaplan and Pedersen (Kaplan and Pedersen, 1989), with bovine serum albumin as a standard. Cholesterol (free and esterified) was measured by reduction with ferrous sulfate (Searcy and Bergquist, 1960).

B. *Compression Isotherms*

Surface pressure (π) - area (A) isotherms of interfacial monolayers were measured for PPL, SP&PL and N&PL on a commercially available trough (KSV-3000, KSV Instruments, Helsinki, Finland). Monolayers were compressed at a rate of 1.0 $Å^2$/phospholipid molecule/minute. Water pumped through the base of the trough regulated subphase temperature. Monolayers were created by spreading stock solutions in chloroform at the air-liquid interface. A 10 minute waiting period before beginning compression allowed for evaporation of the spreading solvent. π-A curves reported in Figure 4.2 were selected from a group of three reproducible isotherms in which deviations in molecular area and surface pressure between different experiments were less than 2 $Å^2$/phospholipid molecule and 0.4 mN/m respectively. Molecular areas were expressed in terms only of phospholipid for reasons of simplicity and accuracy, with no attempt to correct for the presence of neutral lipid and protein. All experiments used a subphase of 10 mM Hepes pH 7.0, 150 mM NaCl, and 1.5 mM $CaCl_2$ (HSC).

C. *Epifluorescence Microscopy*

Epifluorescence microscopy monitored phase separation during compression of the different monolayers. All studies used no more than 1% (mol/mol surfactant phospholipid) Rhodamine-DPPE. Samples were spread from chloroform to an initial molecular area of 150 $Å^2$/phospholipid molecule. The films were compressed at 2.8 $Å^2$/phospholipid molecule/minute. Measurements of the nonfluorescent area used a previously described home-built Wilhelmy balance (Maloney et al., 1993) and a Zeiss-ACM microscope (Meller, 1988) with a 50x objective. Images in experiments that compared the different preparations

were obtained from static films at specific surface pressures 10 minutes after stopping compression to allow for equilibration within the film. Experiments concerning the shape transition in N&PL also obtained images from static films, but with shorter periods of equilibration. The fluorescent images were recorded by Hamamatsu C2400 SIT camera to either to VHS video tape for later analysis or directly to computer (Quadra 650, Apple, Inc., Cupertino, CA with LG-3 frame grabber, Scion Corp, Frederick, MD). A C-shaped Teflon mask placed directly in the trough and extending through the interface minimized movement of the monolayer (Grainger et al., 1989; Meller, 1988). Images obtained inside and outside the mask at frequent intervals ensured that the film remained comparable in both locations.

D. *Image Analysis*

The total area, number and individual size of the domains in epifluorescence images were analyzed using the program Image (NIH, Bethesda, MD). The marked contrast between dark domains and the surrounding fluorescent film facilitated counting and allowed direct measurements of the size of all domains in any given microscopic field based on digitally assigned pixel gray-scale values. Each data point represents analysis of a minimum of three images recorded from different regions of the monolayer for each of four independent experiments.

The density of domains was calculated as the number per image divided by the area of an image. Average densities were again obtained from at least three images for each of four experiments. The software provided a count of the number and individual area of all domains in each image analyzed. The density of domains and their distribution among the

different sizes were calculated from these data. Histograms for the size of individual domains were constructed using area intervals adjusted for the range of sizes observed for the different samples. Domains which were interrupted by the aperture of the microscope for which the true area was unknown were not included. The normalized frequency for the different areas was obtained by dividing the number of domains in any specific interval by the total number analyzed.

The nonfluorescent fraction of the monolayer was calculated as the sum of the area occupied by the individual domains observed in an image expressed as the percentage of its total area.

Data are expressed as mean ± S.D.

RESULTS

The phases that initially separate during compression of pulmonary surfactant films again become miscible later at higher molecular densities (Chapter 2). The basis for the remixing is unknown. To determine what constituents are responsible for this phenomenon, we have analyzed the behavior of surfactant preparations that lacked the surfactant proteins and/or the neutral lipids. Column chromatography separated CLSE into distinct peaks containing the surfactant proteins, the phospholipids, and the neutral lipids. Collection of appropriate fractions provided preparations containing the purified phospholipids (PPL) alone, the surfactant proteins and phospholipids (SP&PL), or the neutral and phospholipid (N&PL) (Fig. 4.1) (Hall et al., 1994). The behavior of films containing the different preparations was then compared to the complete surfactant and to the purified phospholipids which lack both of these components.

The surface pressure-area isotherms for the different preparations were similar to each other (Fig. 4.2) and to the curve for CLSE (Chapter 2). The isotherm for CLSE is a continuous smooth curve (Chapter 2) that shows no discontinuity suggestive of the plateau observed for DPPC (Chapter 3) which corresponds to the transition from the liquid-expanded (LE) to the liquid-condensed (LC) phase. The isotherms for PPL, SP&PL, and N&PL all showed similarly smooth isotherms without evidence of any discontinuity below 40 mN/m.

We have used fluorescence microscopy to follow phase behavior during compression on a Wilhelmy balance. Fluorescence microscopy on static films at specific surface pressures detected the formation of nonfluorescent domains in all the studied fractions (Fig. 4.2). The subfractions behaved similarly to CLSE during initial compression, with domains emerging between 5 and 10 mN/m and then increasing in size

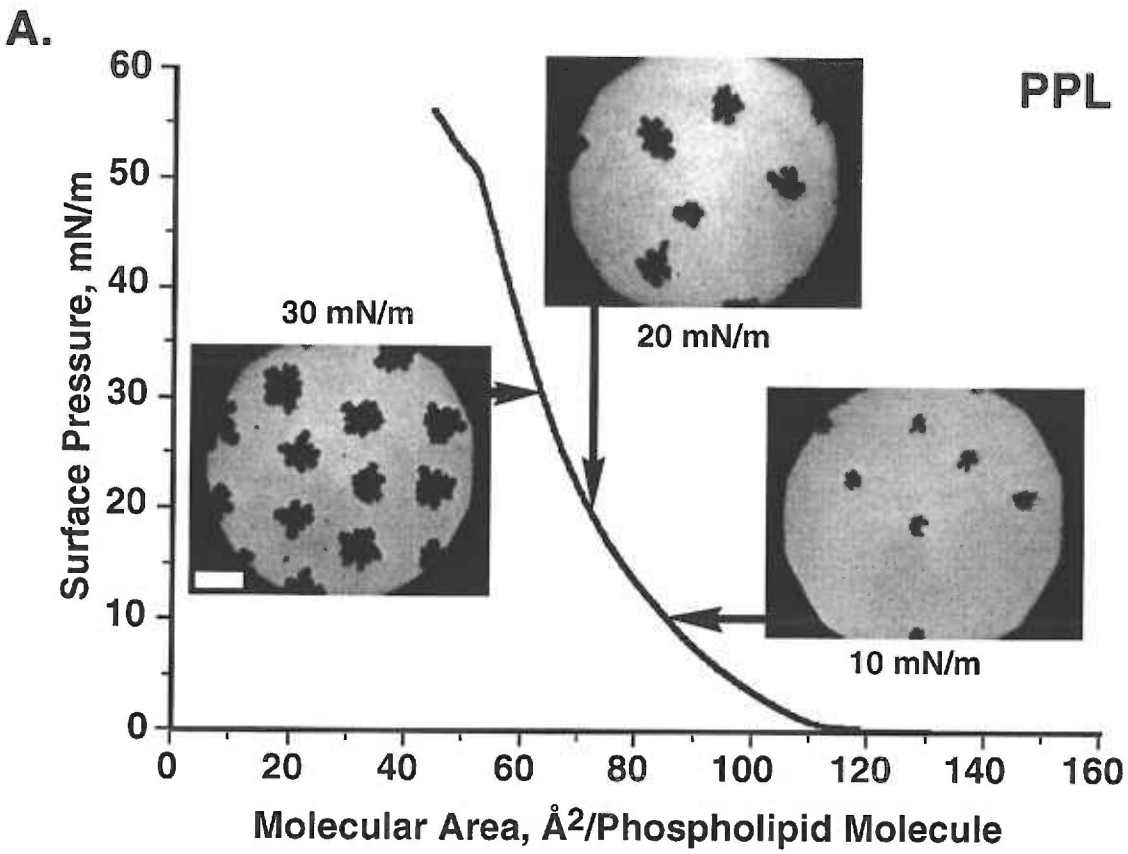

4.2. Surface pressure-area isotherm with epifluorescence micrographs of films containing: A, PPL; B, SP&PL; and C, N&PL. Chloroform solutions of preparations containing 1% (mole/mole) rhodamine-DPPE were spread at 20°C on HSC. Images were obtained from static films following compression at 2.8 Å^2/phospholipid molecule/minute to the desired pressure. Representative images are given at the specified surface pressures. Scale bar is 50 μm. Isotherms were obtained in separate experiments for the preparations without the addition of rhodamine-DPPE during compression at 1 Å^2/phospholipid molecule/minute.

B.

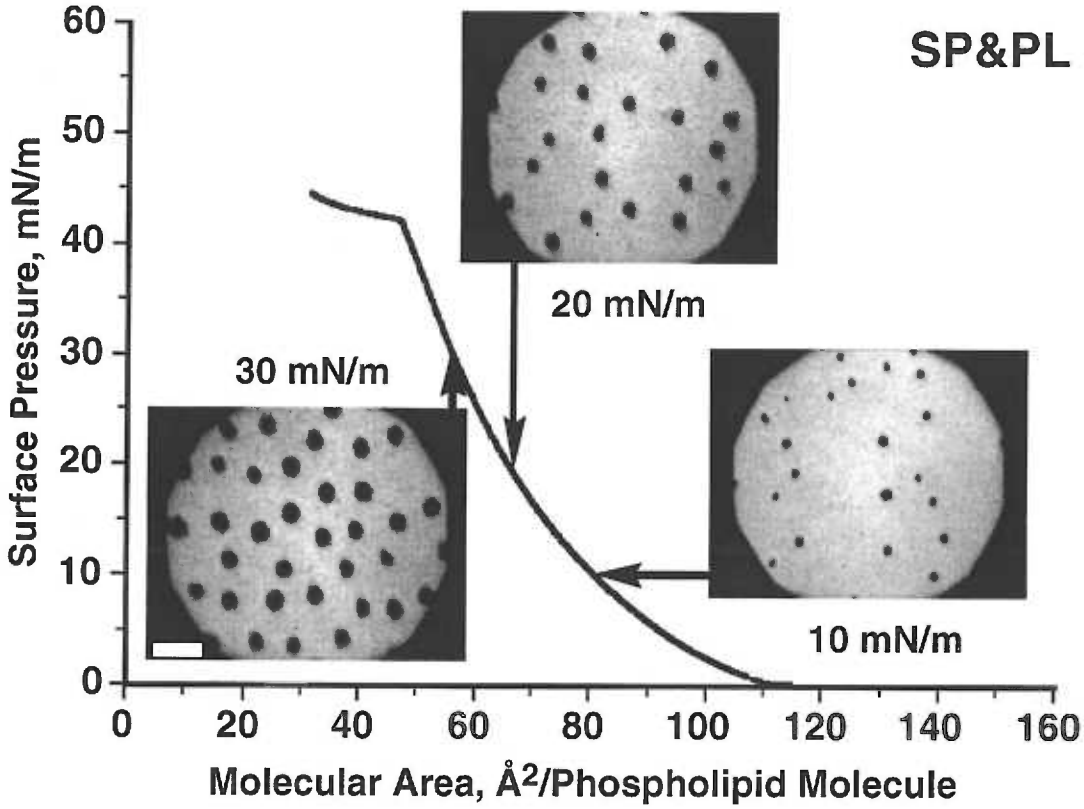
SP&PL
Surface Pressure, mN/m
60
50
40
30
20
10
0
0
20
40
60
80
100
120
140
160
Molecular Area, Å2/Phospholipid Molecule
20 mN/m
30 mN/m
10 mN/m

C.

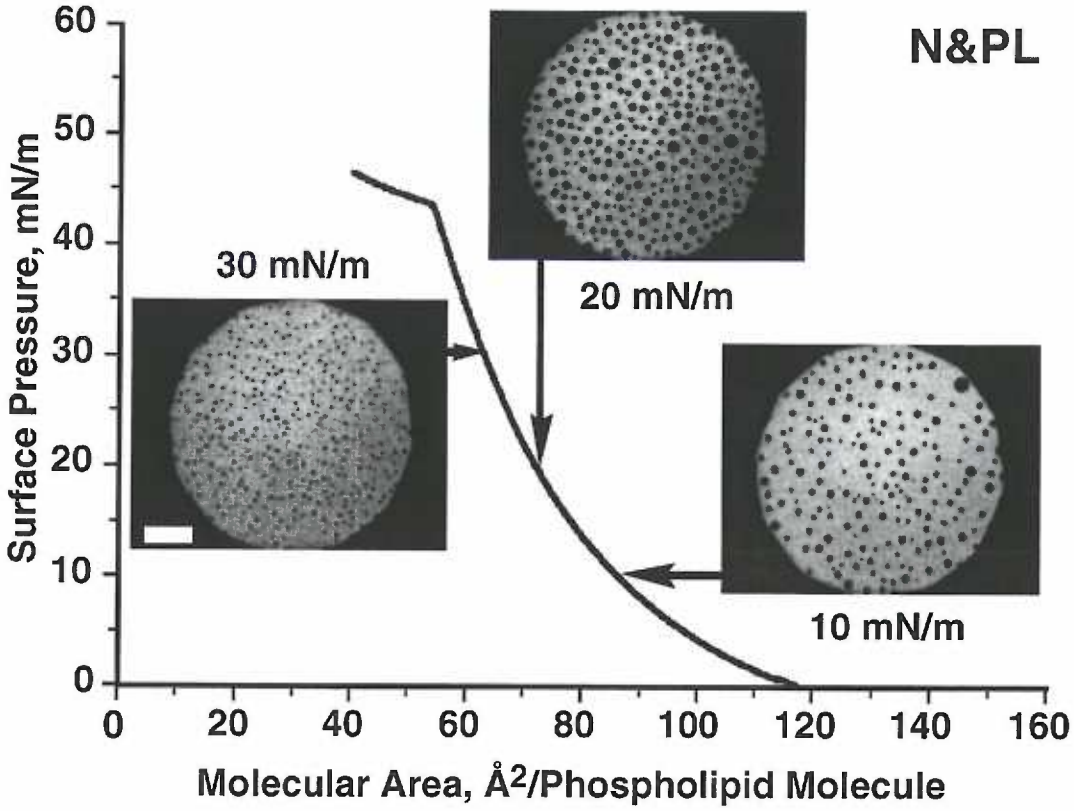
N&PL
30 mN/m
20 mN/m
10 mN/m
Surface Pressure, mN/m
0
10
20
30
40
50
60
0
20
40
60
80
100
120
140
160
Molecular Area, Å2/Phospholipid Molecule

over a broad range of surface pressures. The domains in PPL films initially had shapes substantially different from the circular forms in CLSE (Fig. 4.2A). These, however, represented nonequilibrium structures. In films of PPL held at fixed surface pressures over a period of hours, the domains gradually changed to more regular shapes. Many domains adopted the kidney-bean contour characteristic of domains in pure DPPC (Chapter 3). The domains in both N&PL and SP&PL were circular.

Measurements of the nonfluorescent area allowed quantitative comparison among the different preparations (Fig. 4.3). The total nonfluorescent areas for PPL and CLSE were reasonably comparable at all pressures up to 35 mN/m, at which CLSE occupied 25 ± 5% of the interface and PPL 20 ± 2% (Fig. 4.3). N&PL produced the largest nonfluorescent phase, reaching 26 ± 3% of the interface at a pressure of 25 mN/m for which CLSE occupied only 16 ± 3%. Domains in SP&PL occupied a significantly smaller interfacial area, reaching only 16 ± 1% at 35 mN/m. Relative to PPL, the additional presence of the neutral lipid in N&PL and the proteins in SP&PL then produced opposite effects on the nonfluorescent area.

Only domains in the films of N&PL underwent the remixing observed previously. The nonfluorescent area for this preparation abruptly declined between 25 and 30 mN/m to 4 ± 2%. The magnitude of the decrease in nonfluorescent area in N&PL was similar to the change observed previously for CLSE, which dropped from 25 ±5% to 4 ± 2% of the interface between measurements 5 mN/m apart (Chapter 2). The domains in the PPL films also passed through a maximum area at 35 mN/m, but the subsequent decrease was only 3%, and the nonfluorescent phases remained distinct. The total area of the SP&PL domains was increasing during the entire compression and reached a maximum of 17 ± 1%

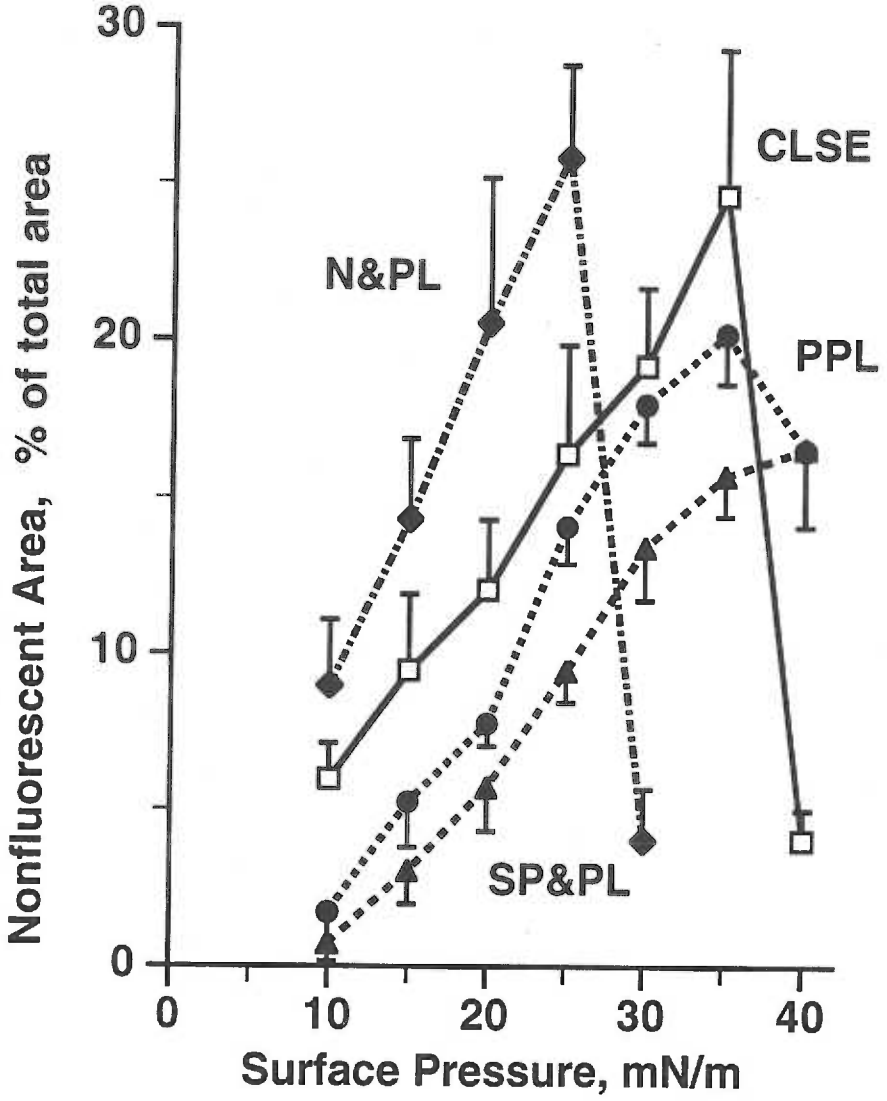

4.3. Variation of total area of condensed domains with surface pressure. Total area of the domains is expressed as the fraction of the total image area analyzed. Mean ± S.D. At least three images were analyzed at each surface pressure for each of four experiments.

at 40 mN/m. Remixing therefore occurred in both preparations that contain the neutral lipids, but not in the two from which they had been removed.

The distribution of the nonfluorescent area into domains of different sizes also differed among the different preparations. PPL, for instance, produced small numbers of large domains (Figs. 4.4 and 4.5). In N&PL, the additional presence of the neutral lipids instead yielded a much larger number of smaller domains. At 20 mN/m, for instance, the most frequent size for domains in PPL was 250 μm^2 but only 10 μm^2 for N&PL. The density of domains was $(12.9 \pm 5.0) \times 10^3$ domains/mm^2 for N&PL, but only $(0.5 \pm 0.2) \times 10^3/mm^2$ for PPL. In SP&PL, the non-fluorescence phase was also distributed among smaller domains than in PPL, but the difference was less than for N&PL. The most frequent size at 20 mN/m was 45 μm^2 for SP&PL, with a density of domains at $(1.1 \pm 0.2) \times 10^3/mm^2$. CLSE produced a distribution more similar to N&PL, with the most frequent size occurring at 10 μm^2 for 20 mN/m with a density of $(9.2 \pm 2.7) \times 10^3$ domains /mm^2. The additional presence of the neutral lipids and the proteins in the different preparations then both lead to distribution of the nonfluorescent area among more numerous domains, with the neutral lipids causing the greater effect.

Our initial experiments monitored films at specific predetermined surface pressures. To characterize the process of remixing more thoroughly, we also conducted experiments on N&PL in which compression was halted according to the appearance of the film. Domains underwent a dramatic change in shape before dissolving into the surrounding film (Fig. 4.6). The original circular shape (Fig. 4.6A) became first slightly elongated (Fig. 4.6B) and then progressively distorted, adopting highly irregular profiles (Fig. 4.6C), before dissipating into the surrounding film. We used N&PL for these experiments rather

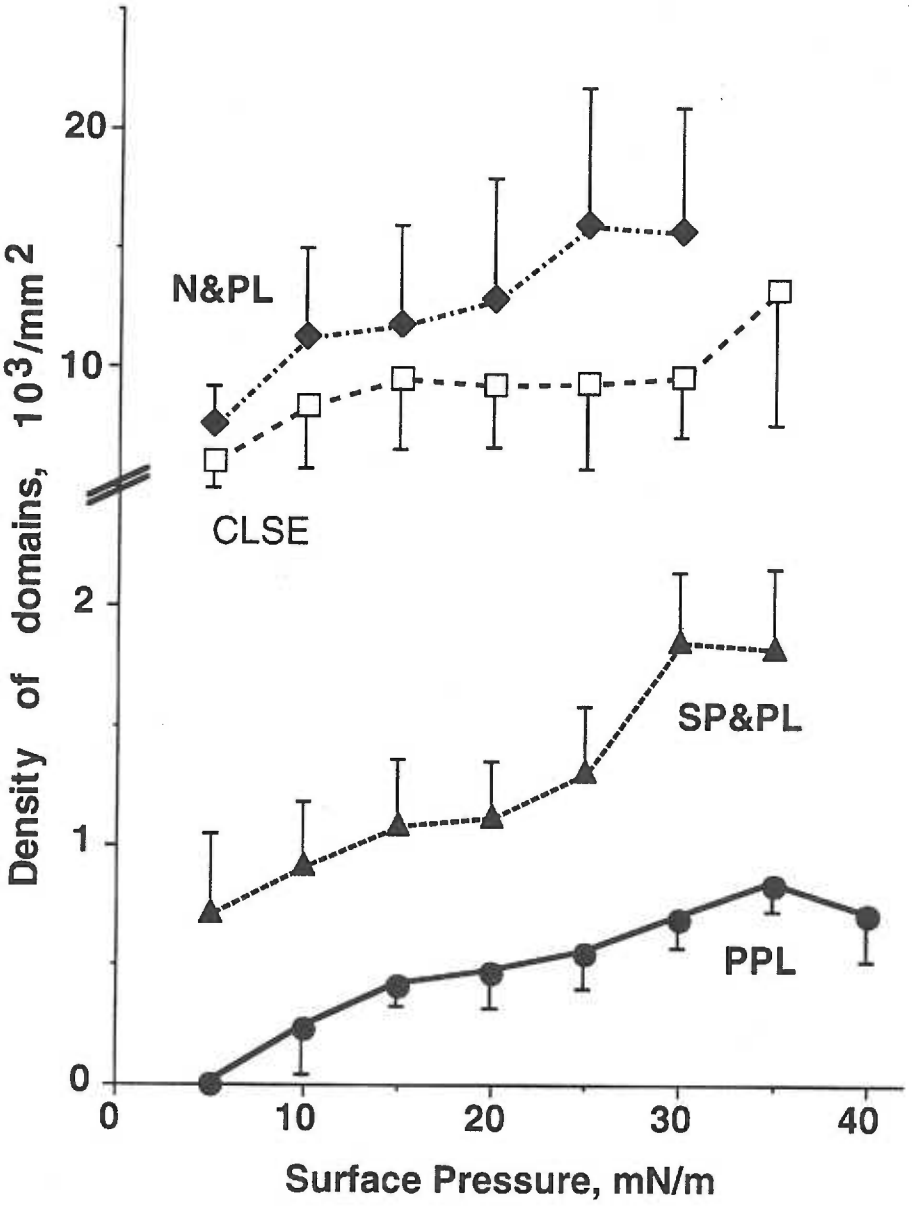

4.4. Density of domains, in terms of number per area, in different preparations of surfactant components. The preparations were spread and compressed to specific surface pressures. Images were recorded from static films at the pressures indicated. The number of domains was counted from three images at each surface pressure for each preparation in four experiments. Mean ± S.D.

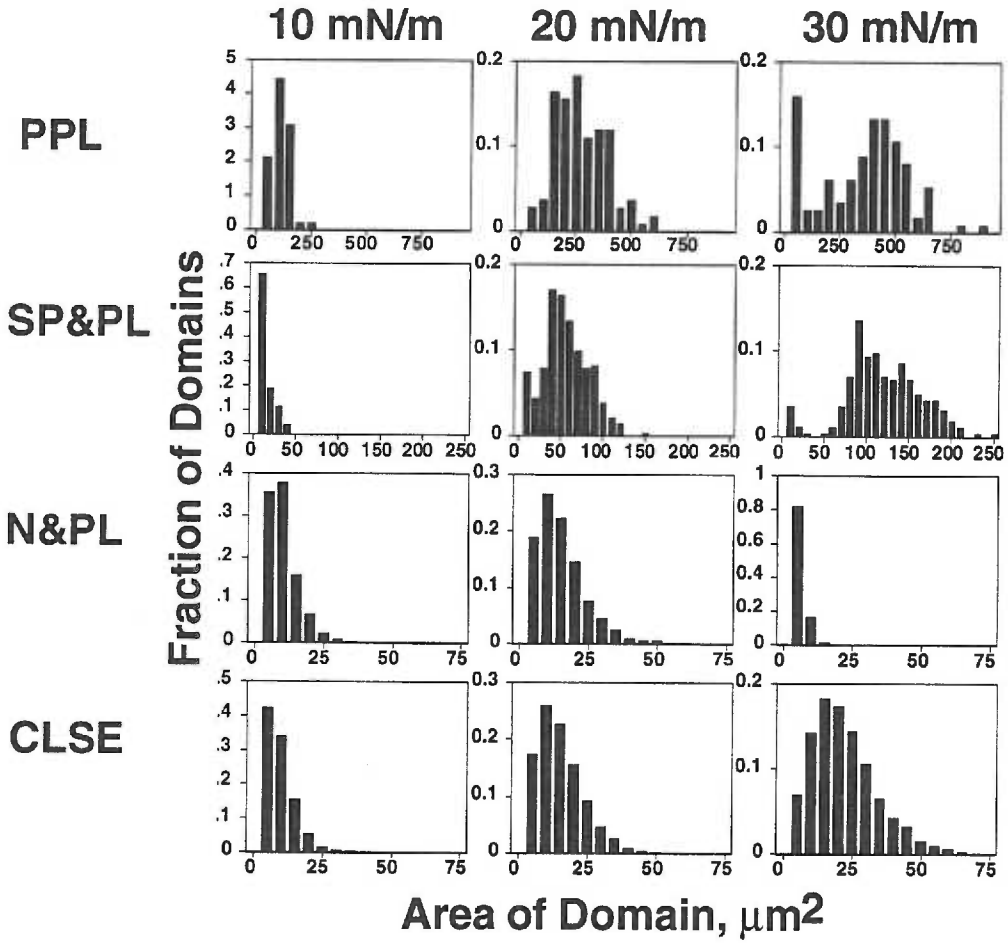

4.5. Size distribution of domains in monolayers of surfactant constituents. Results are expressed as the fraction of domains analyzed that occurred within specific ranges of size. The different preparations produced different maximum sizes, and required the following different intervals in size for this analysis: 5 μm^2 for CLSE and N&PL; 10 μm^2 for SP&PL; and 50 μm^2 for PPL. Results at each surface pressure were averaged from at least three images from each of four experiments.

A.

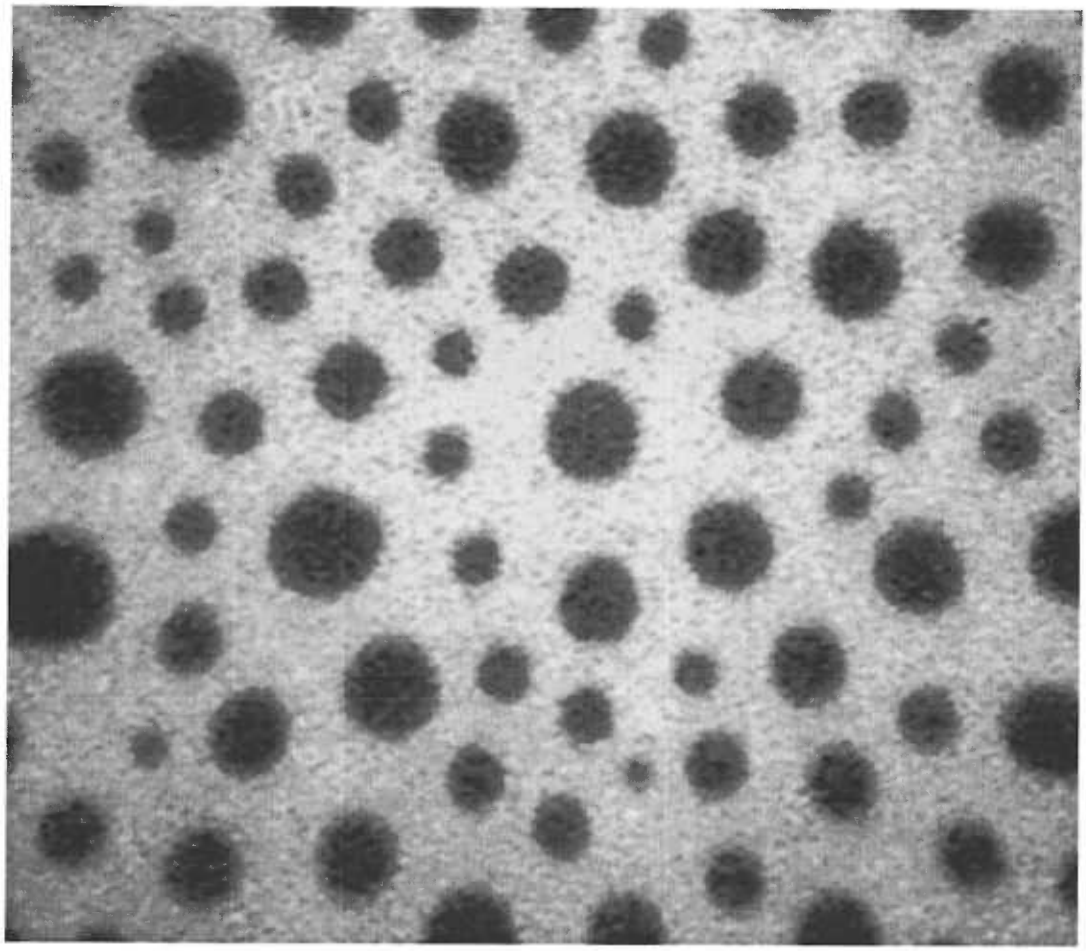

4.6. Fluorescence images of films containing N&PL. Films were spread in chloroform and compressed at 2.8 $Å^2$/phospholipid/minute until microscopy suggested the beginning of the shape transition. Images were then recorded from static films at the following surface pressures: A, 30 mN/m; B, 31 mN/m; C, 31 mN/m with compression of the film from Fig. 4.6B only to overcome the small decay in surface pressure after the cessation of compression.

B.

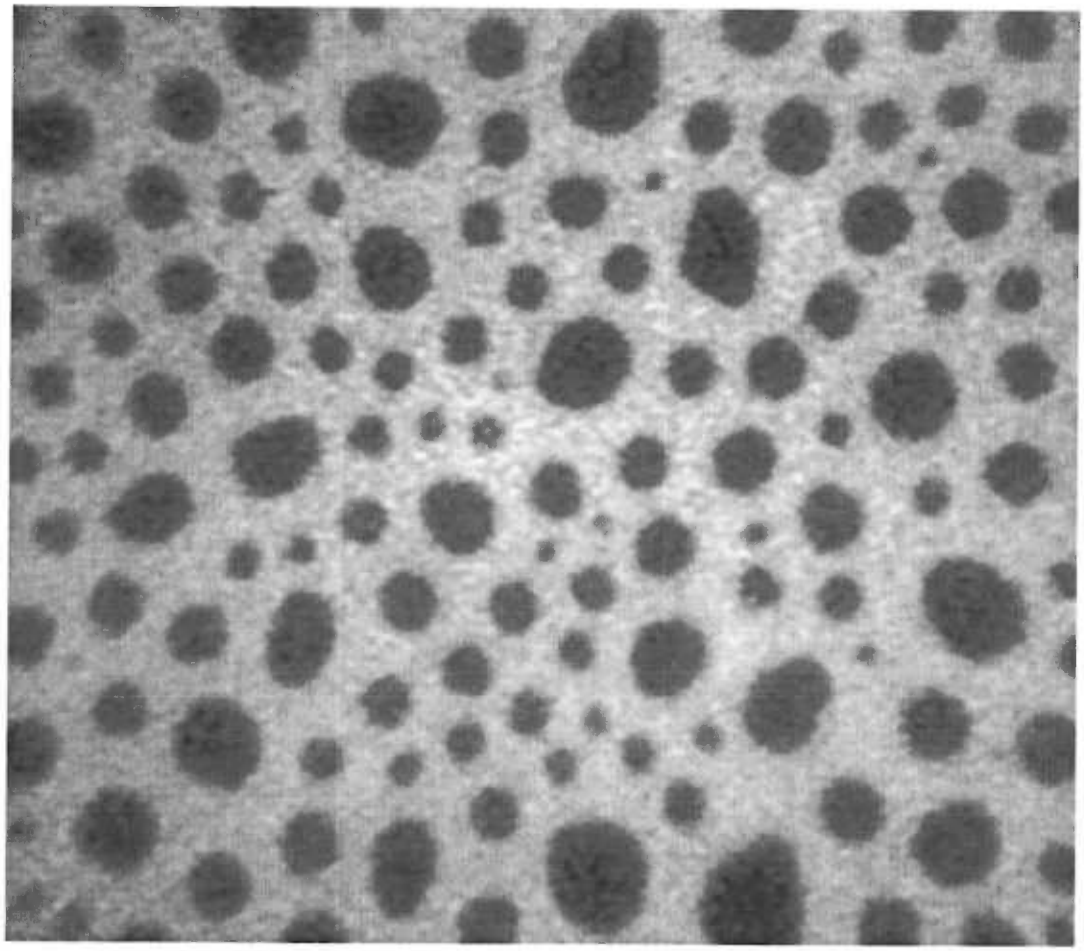

C.

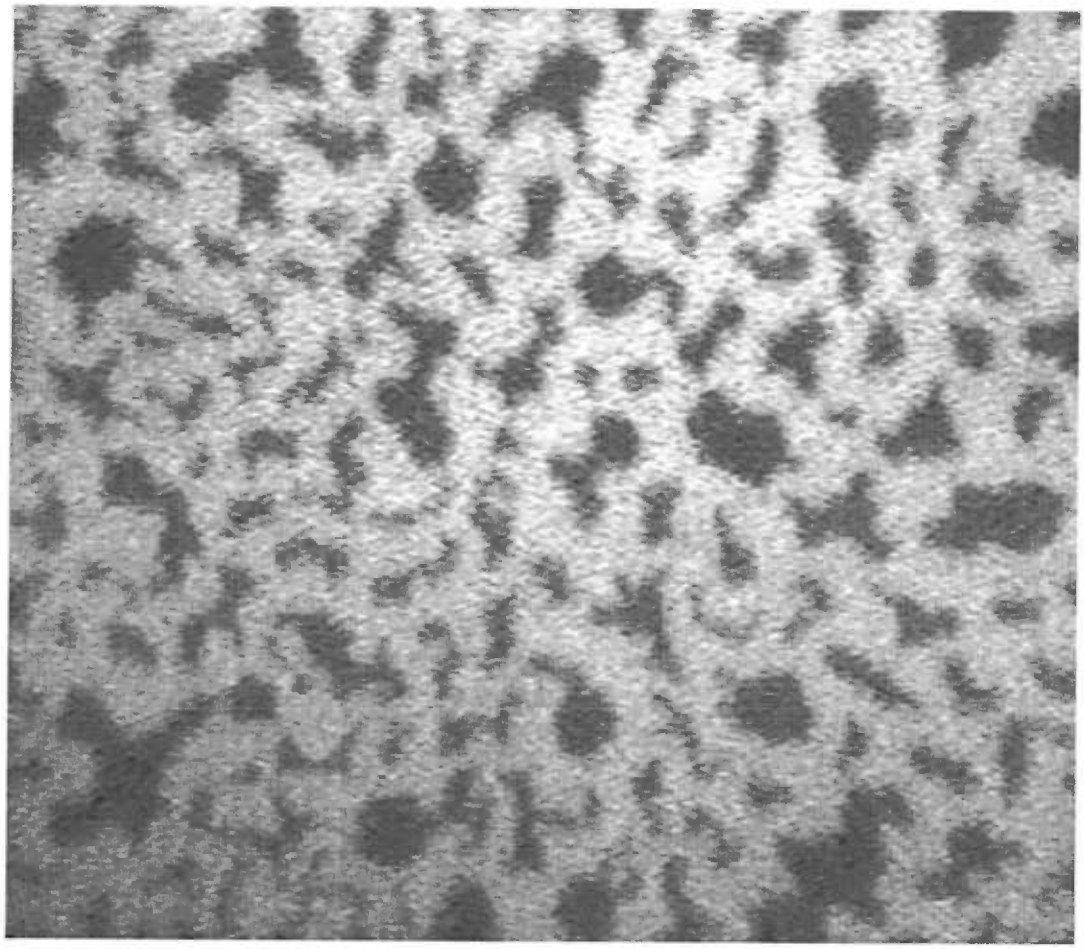

than CLSE because remixing occurred at a lower surface pressure. Films of N&PL, but not CLSE, underwent a complete transition to produce a single homogeneously fluorescent phase below the surface pressures at which the fluorescent probe dissociates from the monolayer. The preparation of N&PL used in these experiments differed from the material used in the early comparative studies, and remixing occurred at a higher surface pressure, reflecting our general finding that this phenomenon occurs at slightly different points during compression for different lots of material. This distinctive transformation of shapes, however, was a characteristic finding for all films in which remixing occurred.

DISCUSSION

These studies show that neutral lipids cause remixing of separated phases in interfacial films of pulmonary surfactant. We have found previously that compression of interfacial monolayers containing CLSE produced separation of a condensed phase from the surrounding film. Domains of this phase increased in size during compression, but then abruptly remixed with the surrounding film. In these experiments, we asked which components of the complex mixture that comprises pulmonary surfactant contribute to the remixing. Our approach has been to use preparations containing the complete mix of surfactant phospholipids, but without the surfactant proteins and/or the neutral lipids. The domains in PPL, which contains only the phospholipids, do decrease in size to a very limited extent. Just as has been shown previously for binary mixtures of DPPC and DOPC (Nag et al., 1993), the nonfluorescent area in PPL achieves a maximum value and then declines slightly. This behavior, however, differs significantly from the much greater decrease observed for CLSE over a narrow range of surface pressure. Only N&PL produces a similarly abrupt drop in the nonfluorescent area. The domains in SP&PL increase continuously during compression. The condensed phase then remixes in both preparations, N&PL and CLSE, that contain the neutral lipids, but in neither PPL nor SP&PL from which they are absent.

The domains in N&PL undergo a dramatic change in shape just prior to remixing. The initially circular domains become first mildly elongated and then grossly distorted into highly irregular shapes before the condensed phase dissolves into the surrounding film (Fig. 4.6). The shape transition shows that the remixing occurs at or at least very close to a critical point.

A critical point is defined as the conditions in a phase diagram at which separation for two coexisting phases in equilibrium terminates (Rowlinson and Widom, 1982). For

monolayers consisting of a single phospholipid the critical point can be determined from the second derivative of the compression isotherms obtained at critical temperature where $d^2\Pi/d^2\tilde{A}=0$ (Fig. 4.6) (Albrecht, 1978). The absence of any discontinuity in the compression isotherms of pulmonary surfactant films which resulted from the complexity of the mixture impeded such analysis.

However, the critical point has long been studied extensively in many other systems and it turned out that critical phenomena observed in many different materials near various kinds of critical points have quite a few features in common. The phenomena observed near a critical point are referred to as critical phenomena and the variable which differs for the two phases is referred to as the order parameter. The most well-known critical point is liquid-gas critical point of H_2O with density being the order parameter. Examples of other order parameters of materials with well studied critical points are the magnetization for the ferromagnetic critical point for iron, the sublattice magnetization for the antiferromagnetic critical point for FeF2, or the electron pair amplitude for the superconductivity critical point for lead. Critical behavior has been also demonstrated previously in binary mixtures pertinent to the surfactant films such as dimyristoyl phosphatidylcholine (DMPC) and cholesterol (Hirshfeld et al., 1990; Seul and Samon, 1990; Subramaniam et al., 1987) or DPPC-cholesterol (Rice et al., 1989; Slotte, 1995). In these binary mixtures the critical point occurs well below the values at which remixing occurs here. Our preparations, however, are far from binary mixtures. Two thirds of the phospholipids are compounds other than DPPC, and these other constituents are likely to explain the difference in critical pressures. Considerably smaller amounts of phospholipid elevate the critical pressure of the DMPC-cholesterol mixture to the range of remixing in our experiments (Hagen and

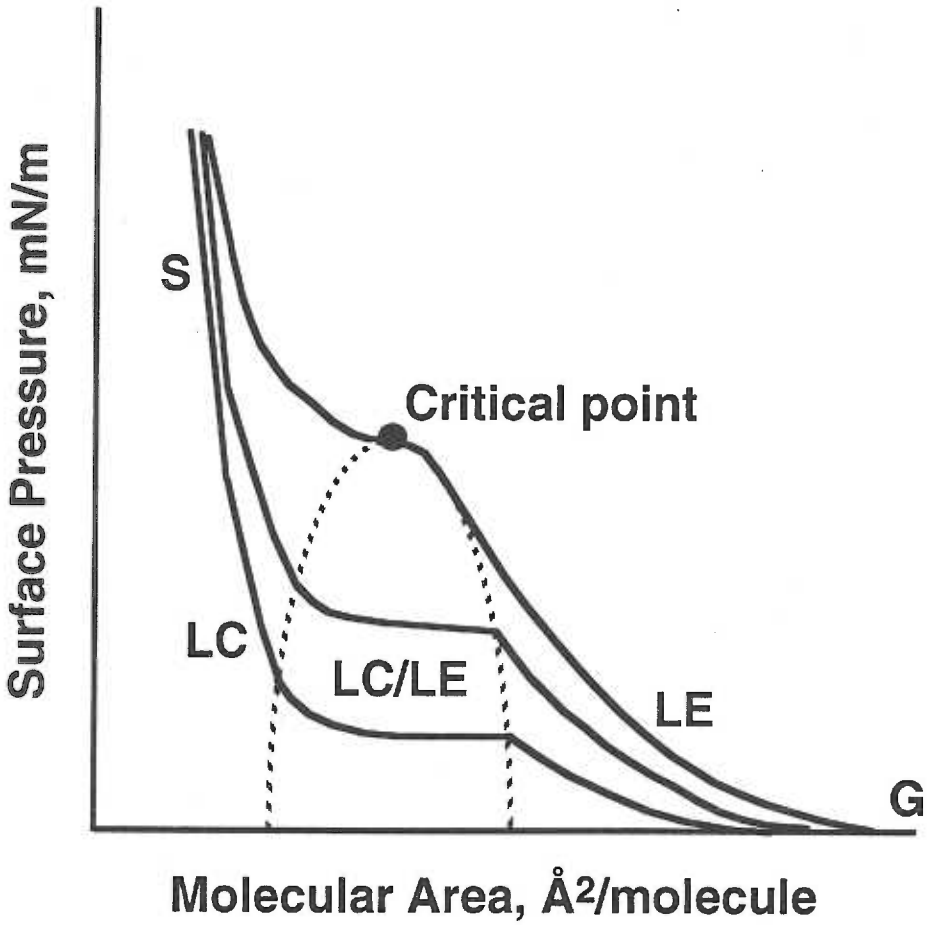

4.7. Schematic representation of pressure-area phase diagram and critical point of phospholipid monolayer. The three different curves represent isotherms at three different temperatures. The upper curve is isotherm at the critical temperature. The dashed line marks the boundary of the coexistence region for the LE and LC phases. The different phases are gas (G), liquid-expanded (LE), liquid-condensed (LC) and solid (S).

McConnell, 1996). The simple model systems therefore fit with our results that a critical point explains the remixing in the complete biological mixture of pulmonary surfactant.

Typical features of systems near critical point are large-scale fluctuations of the order parameter and very long relaxation times. The large scale fluctuations occur because the order parameter for the two distinct phases approaches each other and therefore the interfacial tension between the two phases, or line tension, must become zero at the critical point. Very low line tension is unable to maintain the original circular shape of the domains and large fluctuations, characteristic of the critical point, occur. The phases are changing without any discontinuity of state with minimal changes in conditions at the critical point, as occurs in our system. Most of the nonfluorescent phase remixes during a very small increase in surface pressure. The existence of small domains at surface pressure 5 mN/m above the onset of remixing agrees with the very long relaxation times that is often referred to as "critical slowing down" (Ma, 1982).

The distribution of the condensed phase among the domains in the different preparations provides further information about the effect of neutral lipids. The size of the domains to some extent reflects line tension. Under equilibrium conditions, the conflicting influences of line tension and electrostatic effects determine the size. Line tension tends to minimize the total interfacial perimeter by producing a smaller number of larger domains. In contrast, the electrostatic repulsion among the greater density of dipoles within the domains tends to disperse the condensed components into a larger number of smaller domains. In the surfactant preparations, the neutral lipids produce smaller domains. Whether or not the surfactant proteins are present, the addition of neutral lipids increases the number and decreases the size of the nonfluorescent domains. If the neutral lipids do

not increase the difference in dipole moment density between the two phases, then the smaller domains suggest lower line tension. The effect of the neutral lipids on the size of the domains therefore suggests that they move line tension in a direction consistent with their induction of a critical point.

The neutral lipids must alter substantially the characteristics of at least one of the two separated phases to generate a critical point. The characteristics of the two phases must become the same at the critical point, and so the neutral lipids must produce a major change in the properties of at least one of the two phases in the film containing only phospholipid. Comparison of the nonfluorescent areas for the different preparations suggests that the major effect is on the condensed domains. The additional presence of the neutral lipids produces a greater nonfluorescent area in N&PL relative to PPL and in CLSE relative to SP&PL. The total nonfluorescent area is greater for N&PL than for PPL at all surface pressures up to 25 mN/m. The same effect occurs for CLSE and SP&PL in preparations containing the proteins. Partitioning of the neutral lipids into the domains would explain the enlargement of the condensed area. Prior studies suggest, however, that the maximum content of cholesterol in condensed DPPC should be quite limited. Small amounts of cholesterol added to films of DPPC elevate the surface pressure of the LE-LC transition and suggest some solubility of the neutral lipid in the condensed phase (Albrecht et al., 1981). The content of cholesterol was estimated to be only 2-5%. This small increase in the fraction of condensed constituents seems unlikely by itself to explain the observed increase in the condensed area of our films according to estimates based on our experimental measurements. The fraction f of constituents located in domains with molecular area $\overline{A}_c$ that occupy the fraction ϕ_c is:

$$f = \phi_c \cdot \frac{\overline{A}}{\overline{A}_c}$$

for a film with average molecular area $\overline{A}$ (Knobler, 1990). The molecular area of LC DPPC provides a first approximation for $\overline{A}_c$. According to our measurements, the neutral lipids would then increase the calculated condensed constituents from 19% for SP&PL to 32% for CLSE. Two other possibilities seem more likely. The domains may contain a limited amount of phospholipids other than DPPC that increases the solubility for cholesterol. Or the domains might represent a phase of mixed DPPC-cholesterol that is more expanded than LC DPPC but still sufficiently dense that its solubility for the fluorescent probe is much less than in the surrounding film of mixed phospholipids. The composition other than LC DPPC for the domains would also explain why the line tension is different in films with and without neutral lipids. It remains to be determined if the critical point observed in CLSE and N&PL resulted from partitioning of components other than DPPC inside the domains. It does seem likely, however, that the characteristics of the domains are more affected than those of the surrounding film.

The proteins have the opposite effect on the area of the condensed phase. The additional presence of the proteins decreased the condensed area at all pressures up to 35 mN/m independent of the presence of the neutral lipids. These results suggest that the proteins prevent the phospholipids from partitioning into condensed domains. Calculations of the fraction of constituents contained in the domains suggest that the proteins reduce the maximum number of constituents entering domains from 29% for PPL to 19% for SP&PL and from 38% of constituents for N&PL to 32% for CLSE. The ratio of 9.8 μg protein per μmole phospholipid (Hall et al., 1994) then indicates that 1 μg protein prevents 10 nmole

phospholipid from entering the domains in the absence of neutral lipids, or 6 nmole in their presence. A recently published assay for the hydrophobic surfactant proteins suggests the presence of equivalent amounts of SP-B and SP-C (w:w) in extracted surfactant (van Eijk et al., 1995). The average molecular weight resulting from this ratio indicates 36-60 phospholipid interacting with one protein. Similar figures have been published previously for the effect of these proteins on the phase transition in lipid bilayers. Differential scanning calorimetry (DSC) with mixtures of SP-B and DPPC showed that each protein removed 51 lipid molecules from the gel-liquid crystal phase transition (Shiffer et al., 1993). The figure for SP-C was 35 phospholipid per protein. Our results and the findings with DSC suggest that both in monolayers containing the full array of surfactant phospholipids and in bilayers of pure DPPC, the proteins prevented a comparable fraction of phospholipid from condensing to a more ordered state. The effect of surfactant proteins on the nonfluorescent area is possibly also related to the difference between N&PL and CLSE in surface pressure of the critical point.

The pronounced effect of the neutral lipids raises the possibility that phase behavior is a physiologically regulated variable. Levels of cholesterol, which constitutes most of the neutral lipid in surfactant, vary in response to a number of physiological and pathophysiological factors. These include exercise (Doyle et al., 1994), hyperventilation (Orgeig et al., 1995), the development of pulmonary fibrosis (Swendsen et al., 1996), and temperature for reptilian species whose body temperature can vary (Wood et al., 1995). Cholesterol levels appear to be tightly regulated, with changes in breathing patterns for periods as brief as 15 minutes producing significant changes (Orgeig et al., 1995). The marked shifts in condensed area produced by the neutral lipids in our studies and the

physical changes in the characteristics of the film that should result from these alterations suggest that phase behavior may be the important response to the changes in cholesterol levels.

In summary, these studies show that the neutral lipids cause the remixing of the separated phases during compression of interfacial films of pulmonary surfactant (Chapter 2). The large distortions of the domain's shape prior to their disappearance as well as the speed at which the domains remix indicate that remixing occurs at or close to a critical point. Both the termination of phase separation and the presence of a critical point raise interesting issues concerning the physiological function of the surfactant films.

ACKNOWLEDGMENTS

The authors thank Dr. Edmund Egan of ONY, Inc. and Dr. Robert Notter of the University of Rochester for providing extracts of calf surfactant. Miranda Kahn and Walter Anyan provided technical assistant in the preparation of surfactant constituents. This work was funded by grants from the Whitaker Foundation, the American Lung Association of Oregon (SH), and the National Institutes of Health (HL 03502 and 54209 (SBH)).

CHAPTER 5

NEUTRAL LIPIDS PARTITION INTO THE NON-FLUORESCENT PHASE IN PULMONARY SURFACTANT FILMS

Bohdana M. Discher[a], Kevin M. Maloney[c],
David W. Grainger[d], Viola Vogel[b], and Stephen B. Hall[a,e]

Departments of Biochemistry and Molecular Biology[a], Physiology and Pharmacology[e], and Medicine[e], Oregon Health Sciences University, Portland, OR 97201

[b]Department of Bioengineering, University of Washington, Seattle, WA 98195

[c]Department of Chemistry, Biochemistry and Molecular Biology, Oregon Graduate Institute of Science & Technology, Portland, OR 97006

[d]Department of Chemistry, Colorado State University, Fort Collins, CO 80523

Address correspondence to:

Stephen B. Hall

Mail Code UHN-67

Oregon Health Sciences University

Portland, Oregon 97201-3098

Telephone: (503) 494-6667

Facsimile: (503) 494-6670

e-mail: sbh@ohsu.edu

Running title: The domains in pulmonary surfactant films contain DPPC and neutral lipids

ABSTRACT

We have established previously that compression of pulmonary surfactant leads to a phase separation and that the separated phases remix very quickly at a critical point due to the presence of neutral lipids. The mechanism by which the neutral lipids cause remixing of the phases is uncertain because distribution of the neutral lipids between the two separated phases is unknown. We have determined neutral lipid partitioning into the domains by comparison of the film's behavior with results predicted for the two extreme cases in which the neutral lipids partition exclusively into the domains or into the surrounding film. Measurements of surface potential, fraction of the non-fluorescent area, and the radius of the domains allowed us to calculate the interfacial tension between the two phases. The results indicate that only the model that assumes the presence of neutral lipids inside domains predicts that the line tension approaches zero, as it must at the critical point. Therefore our results suggest that at least some of the neutral lipids partition into domains.

INTRODUCTION

Pulmonary surfactant is a mixture of phospholipids, neutral lipids, and proteins that adsorbs to a thin liquid layer on the alveolar surface. During exhalation the size of alveoli is decreasing and the surfactant film is compressed. Compression of functional pulmonary surfactant reduces the interfacial tension and thereby prevents alveoli from collapsing. The ability to reduce the surface tension requires very dense films that can achieve very high surface pressures without collapse from the interface. In single component films, the only constituent that is able to form such stable, dense films and to reduce the interfacial tension to the levels observed in the lung (Schürch, 1982) is dipalmitoyl phosphatidylcholine (DPPC). In order to form the stable film, DPPC has to undergo a phase transition from liquid-expanded (LE) phase to liquid-condensed (LC) phase. Therefore a phase transition from the LE to the LC phase was speculated to be a key step for surfactant function.

We have established previously that a phase transition does occur in pulmonary surfactant films. As the film is compressed, a new, presumably LC phase separates from the otherwise LE film (Chapter 2 and Chapter 4). In films containing only the purified phospholipids (PPL), from which the proteins and neutral lipids were removed, the domains contain only LC DPPC (Chapter 3). Since it has been shown that the surfactant proteins reside outside the domains (Nag et al., 1996; our preliminary data), in films containing both the surfactant proteins and phospholipids (SP&PL) the domains should be pure DPPC as well. A similar condensed phase also occurs in films containing neutral lipids. In these films, however, the phases remain separated only temporarily. Further compression leads to a critical point at which the two phases remix back into a single phase (Chapter 4). The characteristics of two phases that are approaching a critical point must become progressively similar prior to the remixing. The critical behavior therefore requires that at least one of the phases must differ from those observed in PPL and SP&PL films.

Therefore the neutral lipids must alter substantially the characteristics of at least one of the phases, making the domains more expanded and/or the surrounding film more condensed.

To establish qualitative estimates of the content of neutral lipids in the domains and in the surrounding film we have calculated line tension for the alternative extremes in which neutral lipids are either completely inside or outside the domains. The experimentally observed critical point provides a test of these calculations. Since the two phases become miscible, line tension must vanish. The balance between line tension and electrostatic repulsions, and specifically the difference in dipole moment densities between the two phases, together determine the size of the individual domains. Line tension favors large domains that minimize the length of the interface, while the electrostatic repulsions tend to disperse the condensed phase, producing smaller domains. Since the surface potential is proportional to the average dipole moment density, line tension can be calculated from the size of the domains obtained by fluorescence microscopy and measurements of surface potential if the composition of one phase is known. The results suggest that the line tension can approach zero only if the condensed domains contain significant amounts of the neutral lipids.

MATERIALS, METHODS, AND THEORY

Materials:

Extracted calf surfactant (calf lung surfactant extract, CLSE) obtained from Dr. Edmund Egan of ONY, Inc. (Amherst, NY) and Dr. Robert Notter of the University of Rochester were prepared as described previously (Hall et al., 1992). CLSE was then fractionated to exclude specific components using column chromatography by a slight modification of a previously published protocol (Hall et al., 1994). Gel permeation chromatography separates the proteins, phospholipids, and neutral lipids into three separate peaks (Takahashi and Fujiwara, 1986). Pooling selected fractions provides preparations which contain the purified phospholipids (PPL), the neutral and phospholipids (N&PL), and the surfactant proteins and phospholipids (SP&PL). Each of these preparations then contains the complete set of surfactant phospholipids with or without the surfactant proteins and neutral lipids. Although in the original protocol (Hall et al., 1994) the protein and phospholipid peaks overlapped, a longer column achieved complete separation on a single pass for the materials studied here. Preparations were eluted from the LH-20 matrix (LKB-Pharmacia, NJ) with a solvent of acidified chloroform-methanol (0.1 N $HCl:CHCl_3:CH_3OH$; 1:9:9 v:v:v) (Bizzozero et al., 1982; Takahashi et al., 1986), followed by extraction of the constituents into chloroform (Bligh and Dyer, 1959). Samples of SP&PL suffered variable losses of proteins and were supplemented with protein purified separately to obtain the protein/phospholipid ratio found for CLSE (Hall et

al., 1994). The ratio of cholesterol to phospholipids (μmole : μmole) varied from 0.053 to 0.074 for CLSE and from 0.045 to 0.071 for N&PL.

DPPC was obtained from Avanti Polar Lipids, Inc. (Alabaster, AL) and used without further analysis or purification. N-(Lissamine rhodamine B sulfonyl)-1,2-dihexadecanoyl-sn-glycero-3-phosphoethanolamine (Rhodamine-DPPE) was purchased from Molecular Probes (Eugene, OR).

Reverse-osmosis grade water for these studies was obtained from purification systems purchased either from Millipore (Bedford, MA) or Barnstead (Dubuque, IA) and had resistivity of approximately 18 Mohm·cm. All glassware was acid-cleaned. All solvents were at least reagent-grade and contained no surface active stabilizing agents.

Methods:

A. *Biochemical Assays*:

Phospholipid concentrations were determined by measuring the phosphate content (Ames, 1966) of measured aliquots of extracted material. Protein assays used the amido black method of Kaplan and Pedersen (Kaplan and Pedersen, 1989), with bovine serum albumin as a standard. Cholesterol (free and esterified) was measured by reduction with ferrous sulfate (Searcy and Bergquist, 1960).

B. *Compression Isotherms*

Surface pressure - area (π-A) isotherms of interfacial monolayers were measured on a commercially available trough (KSV-3000, KSV Instruments, Helsinki, Finland).

Monolayers were compressed at a rate of 2.8 $Å^2$/phospholipid molecule/minute. Water pumped through the base of the trough regulated subphase temperature at 20 °C. Monolayers were created by spreading solutions in chloroform at the air-liquid interface. A 10 minute waiting period before beginning compression allowed for evaporation of the spreading solvent. π-A curves reported in Fig. 5.2 were selected from a group of three reproducible isotherms in which deviations in molecular area and surface pressure between different experiments were less than 2 $Å^2$/phospholipid molecule and 0.4 mN/m respectively. Molecular areas were expressed in terms only of phospholipid for reasons of simplicity and accuracy, with no attempt to correct for the presence of neutral lipid and protein molecules. All experiments used a subphase of 10 mM Hepes pH 7.0, 150 mM NaCl, and 1.5 mM $CaCl_2$ (HSC).

C. *Fluorescence Microscopy*

Epifluorescence microscopy used a Zeiss-ACM microscope (Meller, 1988) with a 50x objective to visualize lipid monolayers (Lösche et al., 1983; McConnell et al., 1984; Peters and Beck, 1983) on the surface of the previously described home-built Wilhelmy balance. The Teflon trough had a surface area of 108 cm^2 and subphase volume of 100 ml (Maloney and Grainger, 1993), the temperature of which was regulated to ± 1°C with water pumped through jackets surrounding the trough. Samples of surfactant preparations containing 1% (mol/mol phospholipid) of rhodamine-DPPE were spread in approximately 80 µl of chloroform to give an initial molecular area of 150 $Å^2$/phospholipid molecule. Films were then compressed at 2.8 $Å^2$/phospholipid molecule/minute to specific surface pressures at which images were recorded on the static film. In experiments at different temperatures the films were compressed at 2.8 $Å^2$/phospholipid molecule/minute until domains appeared. A Hamamatsu C2400 SIT camera recorded fluorescence images either

to VHS video tape for later analysis or directly to computer (Quadra 650, Apple, Inc., Cupertino, CA with LG-3 frame grabber, Scion Corp, Frederick, MD). A C-shaped Teflon mask placed directly in the trough and extending through the interface minimized movement of the monolayer (Grainger et al., 1989; Meller, 1988). Images obtained inside and outside the mask at frequent intervals ensured that the mask created no artifacts.

D. *Surface potential measurements*

Surface potential was measured by the ionizing electrode method (Gaines, 1966). The layer between the electrode and the air-liquid interface was rendered conducting by an ^{241}Am electrode that was placed about 1-2 mm above the subphase. The reference electrode was dipped in the subphase behind the compression barrier. The surface potential was recorded by using a pH meter with a high impedance amplifier. The measured surface potential, ΔV, corresponds to the difference between surface potential for the air-liquid interface with and without a surface monolayer. Drift of surface potential due to water condensation on the electrode occurred when the experiments were done in a closed chamber. Maintaining the doors open to the ambient atmosphere eliminated the drift and reduced the noise of the signal when the domains were present. Chloroform solutions of preparations were spread at 20 °C on HSC. Surface potential was recorded simultaneously with isotherms during compression at 2.8 $Å^2$/phospholipid molecule/minute.

Theory:

A. *Dipole moment densities*

When a film separates into condensed and fluid phases, the normal component of the dipole moments for molecules in the two phases, m_c and m_f, and the average normal component of dipole moments for the total film, m, are related by:

$$m = f_c * m_c + f_f * m_f, \qquad (1)$$

where f_c and f_f are the fractions of molecules in each phase. The dipole moment density for these normal components is then given by

$$\mu_x = m_x / \tilde{A}_x, \qquad (2)$$

where $\tilde{A}$ is molecular area and x refers to the particular phase or average film. The fraction of molecules in each phase is related to the experimentally determined fraction of the interface, ϕ_x, by

$$f_x = \phi_x * \tilde{A} / \tilde{A}_x \qquad \text{(Knobler, 1990)}, \qquad (3)$$

where

$$\phi_c + \phi_f = 1 \ . \qquad (4)$$

Substituting equations (2), (3), and (4) into equation (1) yields a relationship between the dipole moment densities, μ_c and μ_f, and the fraction of interface ϕ_c occupied by the condensed phase:

$$\mu = \mu_c * \phi_c + \mu_f * (1 - \phi_c). \qquad (5)$$

The average dipole moment density μ is related to the surface potential ΔV by the Helmholtz equation,

$$\mu = \varepsilon_0 * \Delta V, \qquad (6)$$

where ε_0 is permittivity of vacuum ($\varepsilon_0 = 8.854 * 10^{-12}\ C^2N^{-1}m^{-2}$).

Given the fraction of the interface occupied by the condensed phase and the dipole moment density of one phase, we can use equations (5) and (6) to calculate the dipole moment density of the other phase from measurements of the surface potential ΔV:

$$\mu_f = (\varepsilon_0 * \Delta V - \phi_c \mu_c) / (1 - \phi_c) \quad (7)$$

$$\mu_c = \{\varepsilon_0 * \Delta V - \mu_f * (1 - \phi_c)\} / \phi_c \quad (8)$$

B. *Line tension*

The balance between the line tension λ and the difference in dipole moment density $\Delta\mu$ determines the radius R of the domains (McConnell, 1991). Consequently, line tension can be determined from R and $\Delta\mu$. Relationships between these three quantities have been derived previously, but only in terms of "ansatz" equations (de Koker and McConnell, 1993). The experiments here require an exact expression. The general approach is to express the energy for a condensed phase with fixed total area distributed among domains with uniform but variable radii. Minimization of the system energy then provides an expression relating R, $\Delta\mu$ and λ at equilibrium. The free energy of the system consists of the electrostatic energy, E_{el}, which results from dipolar repulsions, and the line tension energy, E_λ. Under the assumption that the dipoles do not rotate with respect to each other, the electrostatic energy for two normal components of dipole moments inside the domain, m_c and m_c', is

$$E_{el}(m, m') = \frac{m_c * m_c'}{4 * \pi * \varepsilon_0 * |r - r'|^3}, \quad (9)$$

where $|r - r'|$ is the distance between the dipoles (Israelachvili, 1994). Since the distribution of the condensed phase into domains does not affect the energy of the fluid phase, the dipole moment density μ_f does not contribute to the free-energy change. Therefore we can consider μ_f to be "background" dipole moment density and subtract it from the dipole moment densities of both phases (McConnell, 1991). Then $\mu_f = 0$ and the dipole moment density of the domains is $\mu_c = \Delta\mu + \mu_f = \Delta\mu$.

From equation (2) then

$$E_{el}(m,m') = \frac{(\Delta\mu)^2}{4 * \pi * \varepsilon_0 * |r - r'|^3} * \tilde{A}_c * \tilde{A}_c'. \quad (10)$$

To obtain the electrostatic energy of a complete domain, $E_{el}(\text{domain})$, we have to integrate over all pairs of area elements within the domains:

$$E_{el}(\text{domain}) = \frac{1}{2}\frac{1}{4\pi\varepsilon_0}(\Delta\mu)^2 \iint |r - r'|^{-3} d\tilde{A}_c d\tilde{A}_c'. \quad (11)$$

The factor of $\frac{1}{2}$ comes from a double counting of pairs of elements in the integrand. The line tension energy of each domain is $E_\lambda = 2\pi R\lambda$, where R is equilibrium radius of the domain and λ line tension. The derivation of the line tension from minimization of the total energy $E = E_{el} + E_\lambda$ then proceeds as published previously (McConnell, 1991). When the energy of the system is at a minimum,

$$R_{eq} = \frac{e^3\delta}{4} e^{4\pi\varepsilon_0\lambda / (\Delta\mu)^2} \quad (12)$$

and therefore

$$\lambda = \frac{(\Delta\mu)^2}{4\pi\varepsilon_0} \ln\left(\frac{4R_{eq}}{e^3\delta}\right), \quad (13)$$

where e = 2.718 is the base of Naperian logarithm and δ is an effective distance between neighboring dipoles at the interface ($\delta \approx 10$ Å) (Benvegnu and McConnell, 1992).

RESULTS

To make qualitative estimates of the content of neutral lipids inside the domains and in the surrounding film, we have analyzed the behavior expected for the extreme cases in which neutral lipids partition either completely inside or outside the domains. To distinguish which of the two cases more accurately predicts the actual location of neutral lipids, we have compared our results to the well known behavior of line tension at critical point. We have shown previously that the two phases in our surfactant preparations which contain neutral lipids remix at a critical point. Therefore our calculated line tension should approach zero for the conditions at which remixing occurred. We have calculated line tension from the size of individual domains and the difference in dipole densities between the two phases (McConnell, 1991).

Fluorescence microscopy provides the size of the domains. We have previously determined the fraction of the area covered by the non-fluorescent phase, ϕ_c, as well as the density of the domains in terms of number per area, ρ, (Chapter 4) which allowed us to calculate the average radius of the circular domains, R:

$$R = \sqrt{\frac{\phi_c}{\pi * \rho}}. \qquad (14)$$

Domains in CLSE, N&PL, and SP&PL films were circular and therefore we could use equation (14) directly without any assumptions (Fig. 5.1). The shape of domains in PPL films was not circular, but we have shown previously that the irregular shape represented non-equilibrium forms (Chapter 3). The area of the condensed phase does not change more than 5% when the domains achieved equilibrium circular shapes. Therefore we applied the same equation to PPL films to obtain an approximate equilibrium radius (Fig. 5.1). Initially, the radius of the domains increased in size for all four preparations. With the exception of N&PL, the radius reached a maximum value at 30 mN/m and then slowly decreased. The radius reached maximum values of 9.1 μm for PPL, 5.7 for SP&PL, and

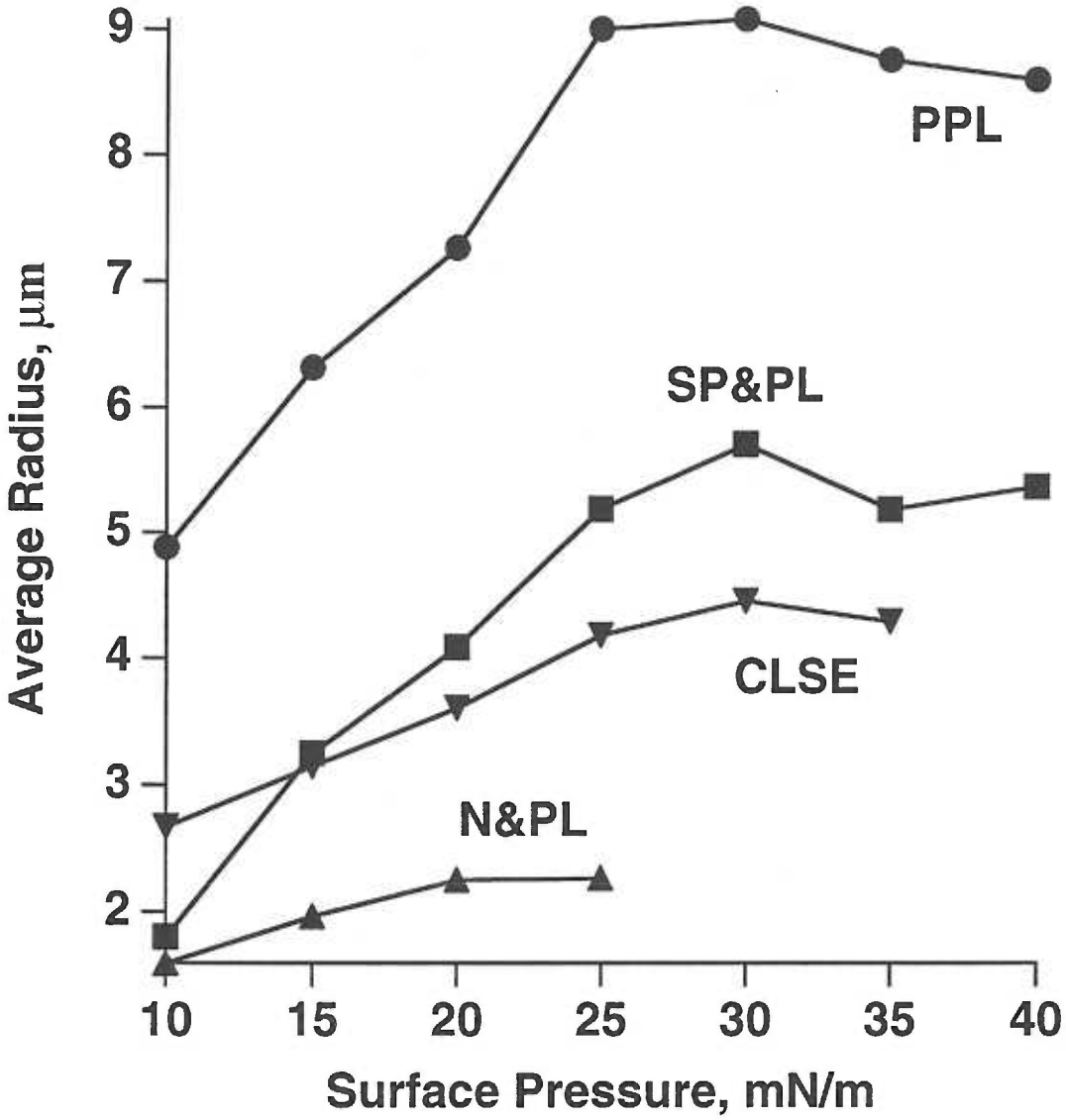

5.1. Radius of the domains versus surface pressure for different preparations of surfactant constituents. Fluorescence microscopy determined the number of domains and the total nonfluorescent area in films of PPL, SP&PL, N&PL, and CLSE. The radius of the average circular domain was then calculated (equation 14).

4.5 for CLSE. We have used the average estimates of radii obtained from the fluorescence micrographs in the calculations of line tension.

We have used the measurements of surface potential to obtain the difference in dipole moment densities. The Helmholtz equation indicates that surface potential is directly proportional to the average dipole moment density, and therefore it provides the basis for establishing electrostatic interactions between the two phases. We have found that the surface potential of CLSE varies significantly from its most abundant component, DPPC, particularly at areas below approximately 70 $Å^2$/phospholipid molecule where the slope of DPPC surface potential increases steeply (Fig. 5.2). The slope of surface potential for all surfactant fractions stayed relatively constant. Above 15 mN/m the surface potential was slightly lower in films containing either surfactant proteins or neutral lipids. These measurements indicated that the average dipole densities for the different preparations were quite similar.

Calculations of line tension, however, require not the average dipole moment density μ but rather the difference in dipole moment densities $\Delta\mu$. Determination of $\Delta\mu$ from the directly measured μ then requires knowledge of the dipole moment density for one of the two phases, and the relative area occupied by each phase (equations (7) and (8)). The fluorescence measurements provided the fraction of the interface occupied by the domains. Therefore the remaining variable that is needed to calculate line tension is the dipole moment density for one phase.

Obtaining the dipole moment density for the condensed phase in PPL and SP&PL is straightforward. Since we know that in these films the domains contain only DPPC (Chapters 3 and 4), we can directly determine the dipole moment density of the LC phase from the surface potential of DPPC at pressures above the coexistence region:

$$\mu_c = \mu_{DPPC} = \varepsilon_0 \Delta V_{DPPC}.$$

The values of the dipole moment density for DPPC, and therefore also for the condensed phase in PPL and SP&PL, are approximately between 1.4 and 1.5 D/100 $Å^2$/molecule.

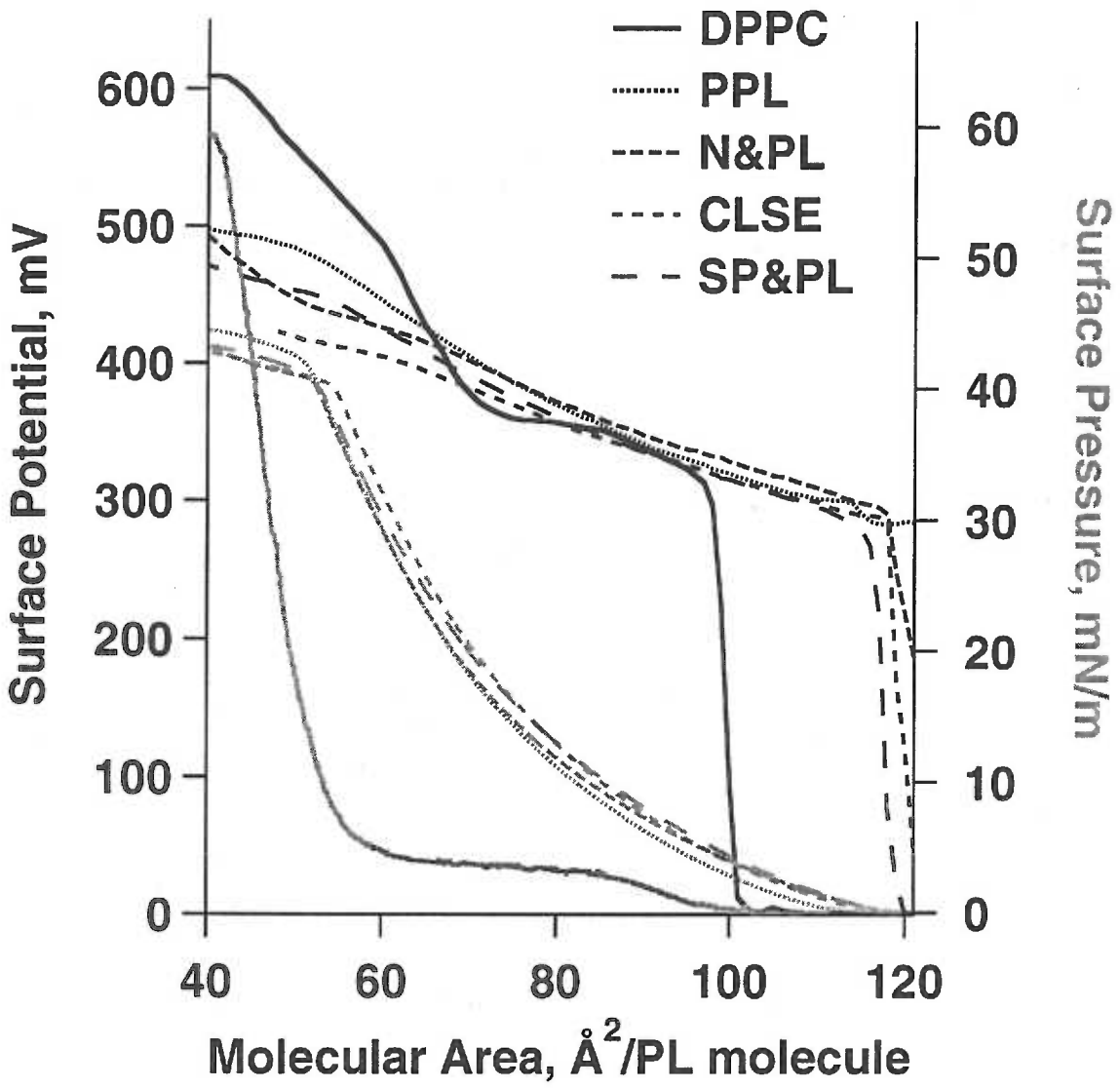

5.2. Surface potentials (left axis, black) and surface pressure (right axis, gray) versus molecular area of films containing: DPPC, PPL, SP&PL, N&PL, and CLSE. Chloroform solutions of preparations were spread at 20°C on HSC. Both surface potential and surface pressure were recorded during compression at 3 $Å^2$/phospholipid molecule/minute. The molecular area is the average molecular area per phospholipid molecule, uncorrected for the presence of cholesterol and surfactant proteins.

With μ_c established, we have also determined the dipole moment densities of the LE phase, μ_f (equation (7)). The values of μ_f for both PPL and SP&PL were similar, ranging from 0.90 to 1.05 D/100 Å^2/molecule. These calculations of dipole moment densities gave us accurate values for both dipole moment densities because we did not use any assumption concerning the composition of the two phases.

For N&PL and CLSE, the location of the neutral lipid is uncertain, and therefore the dipole moment density for both phases is unknown. We can, however, at least calculate what values of dipole moment densities would be predicted by our experimental data if the neutral lipids partition exclusively in one phase. With this assumption the other phase does not contain the neutral lipids and therefore it has the same composition as the corresponding phase in films from which the neutral lipids were removed. The dipole moment density of that phase then would be the same as the already determined density in either PPL or SP&PL film. If the neutral lipids partition into the surrounding film, the domains would contain pure DPPC, allowing us to calculate μ_f in the manner used for PPL and SP&PL. In this case the μ_f determined for N&PL and CLSE (equation 7) is within the range of values obtained for PPL and SP&PL or, at surface pressures above 20 mN/m, lower by less than 0.1 D/100 Å^2/molecule (Fig. 5.3A). $\Delta\mu$ would remain above 0.46 D/100 Å^2/molecule at all surface pressures. In contrast, if all neutral lipids partition inside the domains, the values of μ_f calculated for PPL and SP&PL would provide μ_f for N&PL and CLSE respectively, allowing calculation of μ_c according to equation 8 (Fig. 5.3B). During the course of compression, values of μ_c for CLSE decreased from 1.37 to 1.33 D/100 Å^2/molecule and from 1.33 to 1.26 D/100 Å^2/molecule for N&PL. The difference in dipole moment densities between the phases would then decrease during compression to a minimum of 0.3 D/100 Å^2/molecule prior to disappearance of the domains (Fig. 5.3B). The two models therefore predicted significantly different behavior for $\Delta\mu$ during compression, with films in which the neutral lipids are in the domains having more similar dipole densities for the two phases.

These predicted dipole moment densities then provide $\Delta\mu$ for the two extreme cases, which together with the radii of the domains allow calculation of the line tension, λ. For SP&PL and PPL films, the calculated line tension increased during compression. In PPL, the values changed from 0.14 to 0.19 pN during compression from 10 to 40 mN/m (Fig. 5.4, filled symbols). The change was smaller for SP&PL which increased from 0.13 to 0.17 pN during the same interval of compression. In films containing the neutral lipids, the model in which the domains also contain only DPPC produced similar results. The line tension for N&PL increased from 0.12 to 0.15 pN during compression from 10 to 25 mN/m and for CLSE from 0.14 to 0.21 pN between 10 and 35 mN/m. For the second model, however, for which all neutral lipid would partition into the domains, the results were quite different. The line tension in N&PL films would drop from 0.09 pN at 10 mN/m to 0.02 pN at 25 mN/m and in CLSE films from 0.13 pN at 10 mN/m to 0.06 pN at 35 mN/m. The line tension was always lower for N&PL than for CLSE. The low line tensions that are expected near the critical point were predicted only by the model in which the neutral lipids reside inside domains.

A.

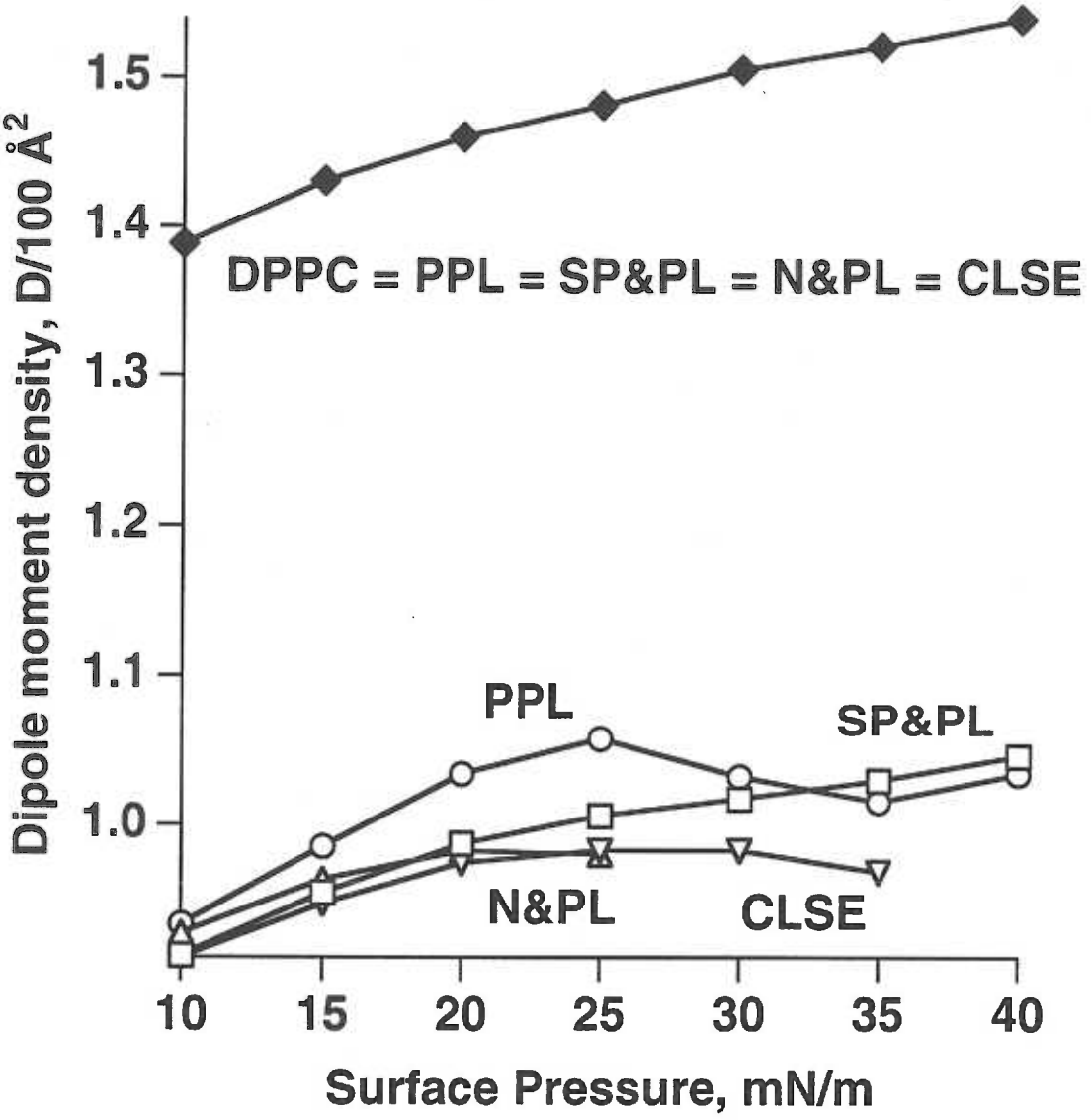

5.3. Dipole moment densities calculated for the condensed domains (filled symbols) and the surrounding phase (open symbols) at different surface pressures for films containing PPL, SP&PL, N&PL, and CLSE. The calculations for PPL and SP&PL films use the dipole moment density of DPPC, obtained in separate experiments, for the condensed phase. For N&PL and CLSE films, the calculations make the following alternative assumptions: A: the domains have the dipole moment density of DPPC; B: the film surrounding the domains has the same dipole density as in films with the same composition but without the neutral lipids.

B.

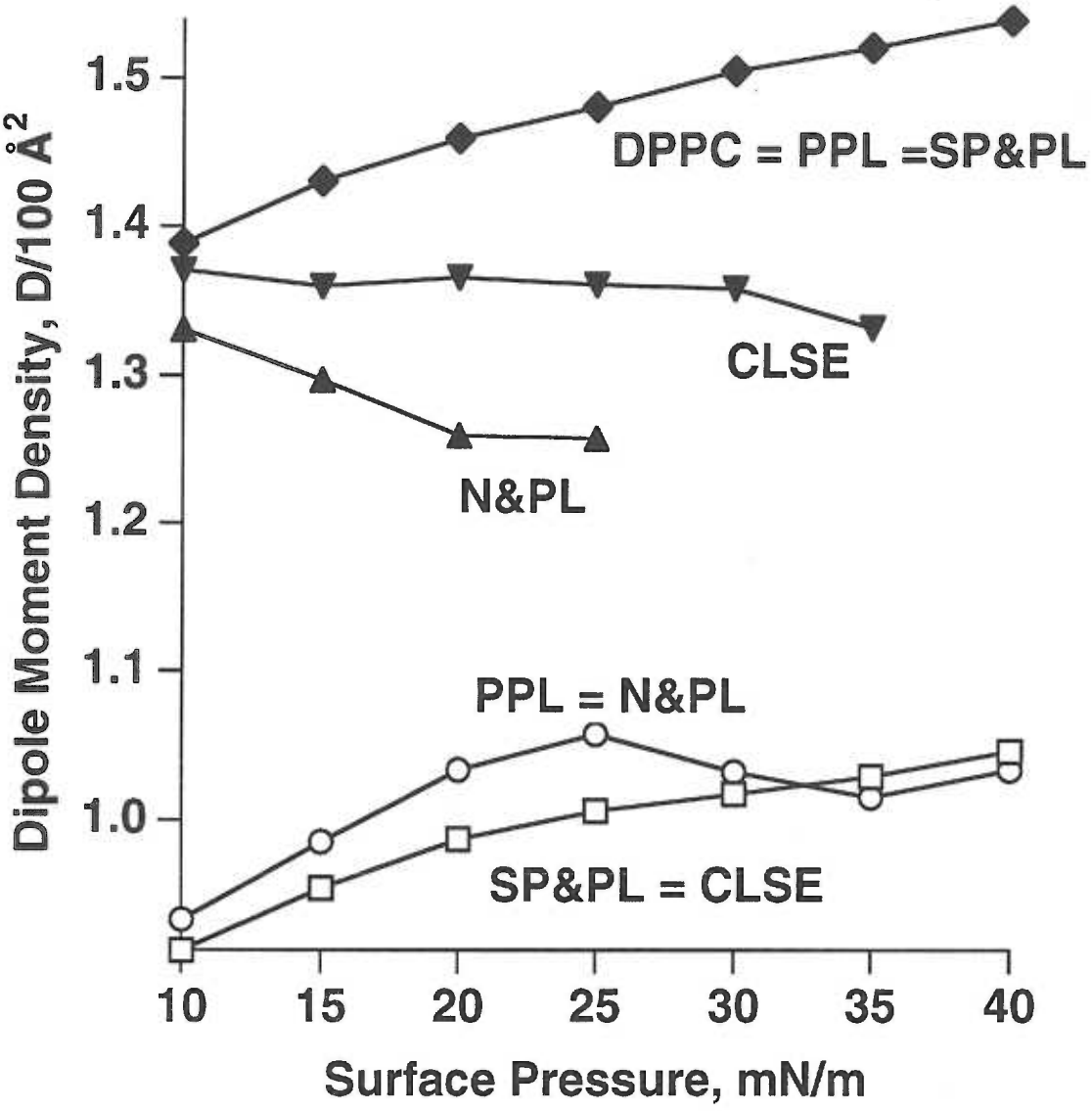
Dipole Moment Density, D/100 Å²
1.5
1.4
1.3
1.2
1.1
1.0
DPPC = PPL =SP&PL
CLSE
N&PL
PPL = N&PL
SP&PL = CLSE
10
15
20
25
30
35
40
Surface Pressure, mN/m

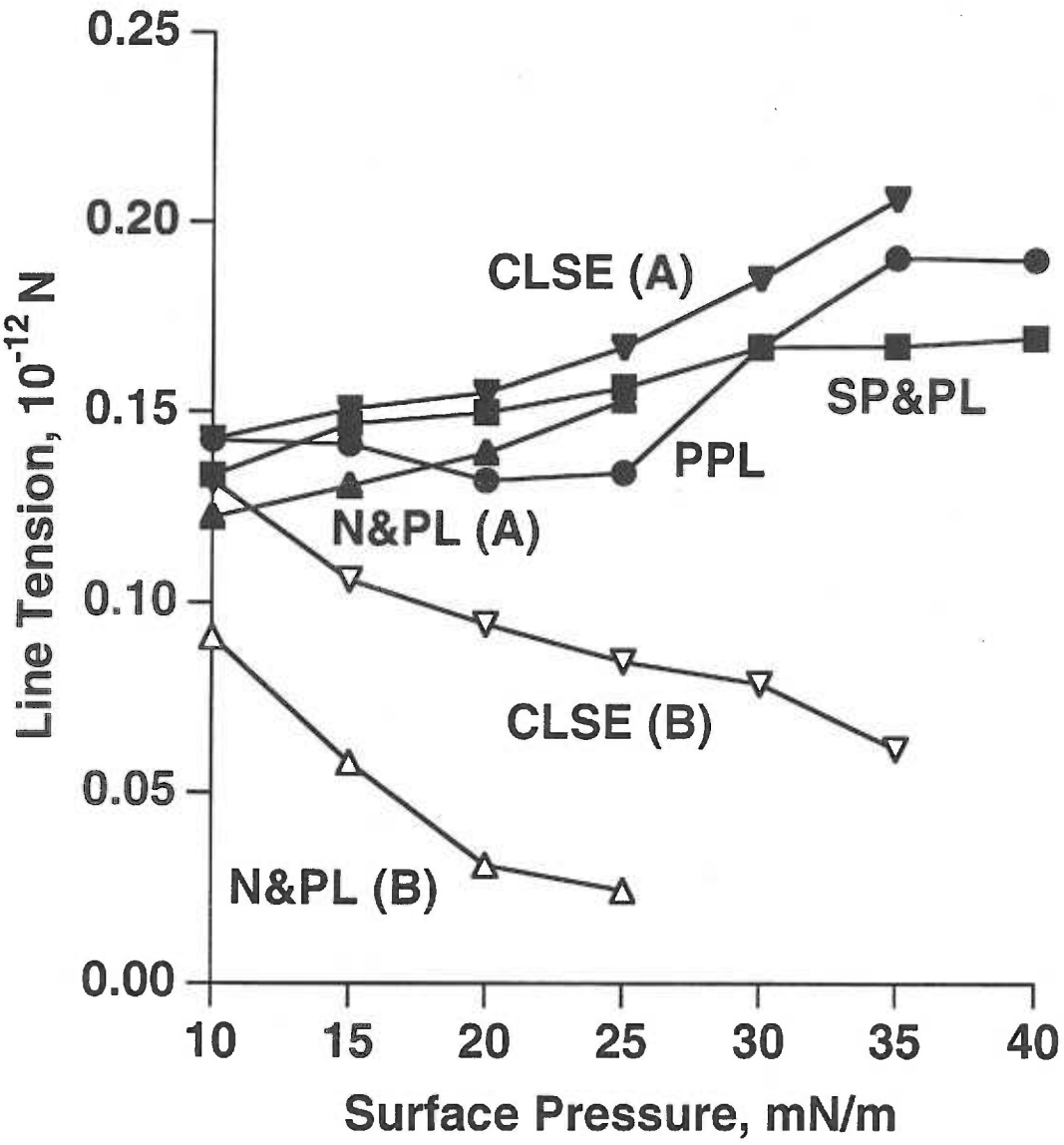

5.4. Line tension calculated at different surface pressures for PPL, SP&PL, N&PL, and CLSE films. Calculations used the experimentally determined radii of domains (Figure 1) and the dipole moment densities shown in Fig. 3A (filled symbols) and 3B (open symbols) according to equation (13).

DISCUSSION

In this study we address the qualitative composition of the domains in the films of surfactant preparations that contain neutral lipids. Phase separation occurs during compression of films containing any fraction of pulmonary surfactant that includes the surfactant phospholipids. We have shown previously that the phase which separates out of the PPL film is pure DPPC (Chapter 3). The same should be true for SP&PL films because the surfactant proteins reside outside the domains (Nag et al., 1996; Nag et al., 1997; our preliminary data). In films containing neutral lipids, however, the composition of the separated domains is unknown. The neutral lipids have a particularly large impact on the behavior of the separated phases. In the presence of the neutral lipids, further compression of films with the separated phases leads to a critical point at which the phases abruptly remix into a homogeneous film (Chapter 4). The critical behavior indicates that the phases must become progressively similar prior to remixing. Therefore the neutral lipids must alter at least one of the two phases. The neutral lipids must make the condensed domains substantially more fluid than LC DPPC, or they decrease the fluidity of surrounding phase, or both. To distinguish between these possibilities, we need to know the distribution of neutral lipids between the two phases.

To predict the location of the neutral lipids, we have analyzed the two extreme cases in which these compounds partition exclusively into one phase. We have selected line tension as a variable that can predict which of the two extreme distributions is closer to the actual behavior of the film. Near the critical point, line tension must decrease and approach zero when the domains disappear (Chapter 4).

The calculations of line tension are based on equilibrium conditions when the system has minimum energy. There are two major energies associated with the phase separation that contribute to the total energy of the film: line tension energy and electrostatic energy. These two energies have opposite effects on the size of the domains. Line tension

energy achieves a minimum when domains are large because it is proportional to the length of the total boundary between the two phases. The electrostatic energy is lower when the domains are small because the average distance between the dipoles is bigger. The balance between line tension and electrostatic repulsions then determines the size of the individual domains. To calculate line tension we therefore have to know the size of the domains and the difference in dipole moment densities. The size of the domains was calculated from the fraction of the non-fluorescent area, ϕ_c, and the density of the domains in terms of number per area, ρ. Both ϕ_c and ρ were obtained by fluorescence microscopy. The difference in dipole moment densities $\Delta\mu$ can be calculated from the average dipole moment density μ and the fraction of non-fluorescent area ϕ_c if either μ_c or μ_f is known (equations (7) and (8)). In PPL and SP&PL films, μ_c is known because the domains contain pure DPPC and the dipole moment density can be calculated directly from measurements of surface potential for pure DPPC (equation (6)). In N&PL and CLSE films, however, both dipole moment densities are unknown. Therefore we can only evaluate the composition of the domains qualitatively from the behavior expected for the alternative extremes in which the neutral lipid is either completely inside or outside the domains. If we assume that the domains contain only DPPC, then we can obtain μ_c the same way as in PPL and SP&PL films. If the LE phase does not contain the neutral lipid, then the compositions of the LE phases in N&PL and CLSE are the same as in PPL and SP&PL respectively and we can use the corresponding μ_f's. Using these assumptions, we can determine the line tension for the two models.

Our calculated line tensions are within the range of the values measured or calculated previously. Line tensions determined in other systems vary from 0.1 to 2 pN for films with an LC-LE interface (Rivière et al., 1994; Rivière et al., 1995), with a higher value of 5 pN found for solid-LE phase coexistence (Muller and Gallet, 1991). These values were obtained in systems that do not reach a critical point. The calculated line tensions in the surfactant preparations are at the lower end of the values reported by others

as expected for films that approach a critical point. Line tension has been determined previously for one other system with a critical behavior. For the binary mixture of 30% cholesterol/ 70% dimyristoyl phosphatidylcholine, line tension decreases from 1.75 pN to zero during compression from 0 to 10 mN/m (Benvegnu et al., 1992). The actual values cannot be compared directly because our data are at surface pressures above 10 mN/m, but the previously reported line tensions agree in general with the values calculated here.

For the films that contain only LC DPPC domains, the calculated line tensions are the correct values obtained without assumptions on the composition of the phases. In these films the line tension is constant or slightly increasing. These values accurately predict that the domains in PPL and SP&PL remain immiscible at all surface pressures. The line tension for films containing neutral lipids represent hypothetical values based on assumptions that the neutral lipids partition only into one phase. The variation of line tension during the compression is appropriate, but only for the model that assumed that neutral lipids are in the domains. For that case, line tension decreases and that it reaches relatively low values (Fig. 5.4, opened symbols). If the neutral lipids instead reside in the surrounding film, the calculated line tension increases during compression and fails to predict the experimentally observed critical point (Fig. 5.4, filled symbols). These results suggest that at least some of the neutral lipids must partition into the domains in order to induce the critical point.

The predicted line tension, however, fails to reach zero even if all the neutral lipids partition into domains. This disagreement could result either from experimental error in one of the measured variables used to calculate line tension or from some additional factors that are involved in the process of phase separation and were not considered in the calculations. Among the possibilities is inhomogeneous distribution of neutral lipids within the domains. The most abundant neutral lipid in pulmonary surfactant is cholesterol or one of its derivatives. Cholesterol has been found edge active in binary mixtures of 2:98 (mol:mol) cholesterol:DPPC. It partitions preferentially to the boundaries of the DPPC

domains where it can dramatically reduce line tension (Weis, 1991; Weis and McConnell, 1985). Because the derivation of equation (13) assumes uniform distribution of dipole moment densities, the presence of cholesterol at the domain's boundaries would require modification of the equations used to calculation line tension.

In films containing neutral lipids, the surfactant proteins significantly affect the predicted line tension. The higher line tension in CLSE films relative to N&PL (Fig. 5.4, open symbols) is in agreement with the larger size of the domains in CLSE films (Fig. 5.1) and with the observation that the critical point in CLSE occurs at surface pressure 10 mN/m higher than in N&PL (Chapter 2 and Chapter 4). The difference between line tension for N&PL and CLSE therefore seems unlikely to result from experimental error.

In summary, we have calculated line tension between the separated phases in subfractions of pulmonary surfactant. Calculations accurately predict that preparations lacking the neutral lipids should maintain non zero line tension and retain immiscible phases. For the subfractions containing the neutral lipid, the model in which the expanded phase contains all neutral lipid indicates a line tension that increases during compression, and fails to approach zero at the experimentally observed critical point. The model in which the domains contain the neutral lipid does yield a line tension that approaches zero at the critical point, although the predicted values remain significantly above zero. These results suggest that the neutral lipids induce critical behavior by partitioning into the condensed domains and expanding that phase to the point that it becomes miscible with the surrounding film.

CHAPTER 6

SUMMARY AND CONCLUSIONS

The presence of pulmonary surfactant in the lung is vital for breathing. Pulmonary surfactant is a mixture of phospholipids, neutral lipids, and very hydrophobic proteins. It adsorbs to the surface of a thin fluid layer that lines alveoli where it very effectively reduces the surface tension of the air-liquid interface. By decreasing the surface tension to extremely low levels, pulmonary surfactant prevents collapse of the small alveoli at the end of exhalation. To stabilize the alveoli, films of pulmonary surfactant have to be compressed above equilibrium spreading surface pressures. That means that pulmonary surfactant must form a film that is very stable upon compression. Dipalmitoyl phosphatidylcholine (DPPC), the most abundant constituent of pulmonary surfactant, is the only entity that, in single component films, forms stable films above equilibrium spreading surface pressures. The stability of the DPPC films is achieved by a phase transition from a disordered, liquid-expanded (LE) phase, to a very ordered, liquid-condensed (LC), phase. Therefore it has been hypothesized that the functional film at the alveolar surface is LC DPPC and that the other components leave the interface during compression. This hypothesis requires the films of pulmonary surfactant to undergo some process of refinement. The mechanism of the refinement is unknown but a potential basis for it might be a phase separation. The stable LC phase would then separate from the LE phase that would be eliminated from the interface at high pressures, above equilibrium, due to its instability. Previously the phase separation was only speculated, without any direct evidence that would document phase separation in pulmonary surfactant films.

Our studies demonstrate that the phase separation in pulmonary surfactant does occur. We have used two complementary microscopic techniques, fluorescence microscopy and Brewster angle microscopy, to characterize the phase behavior.

Fluorescence microscopy allowed us to detect the different phases due to their different solubilities for fluorescently labeled lipids. To confirm that the addition of fluorescently labeled lipids does not create any artifact, we have used Brewster angle microscopy (BAM). BAM has somewhat lower spatial resolution, but it provides an excellent control for the fluorescence microscopy because it distinguishes between different phases on the basis of differences in optical thickness without the use of fluorescently labeled lipids. Both techniques confirmed that the phase separation, which was expected to provide the basis for refinement, does occur.

Several characteristics of the domains suggest that they contain mostly DPPC. The area occupied by the domains approaches but does not exceed the area expected if all the DPPC would partition into LC domains. The surface pressure at which the domains first emerge during compression over a wide range of temperatures lies just above values for DPPC. For the simplified system containing only the surfactant phospholipids, we have elucidated the exact composition of the domains. Variation of the areas of the phases in response to added DPPC allowed construction of a phase diagram. These studies confirmed that in the phospholipid films the domains are only DPPC, whereas the surrounding fluid phase contains the other phospholipids as well as the remaining DPPC. Information on the structure of the film from quantitative analysis of BAM experiments fits with these compositions. The optical thickness and its variation as well as anisotropy are all in agreement with the composition deduced from the fluorescence measurements. In films that also contain the surfactant proteins, the domains should have the same composition. Studies of films containing DPPC together with surfactant proteins (Nag, 1996; Nag, 1997 #88) confirmed my own preliminary findings that fluorescently labeled proteins reside in the fluid phase, outside domains of LC DPPC. In fact, measurements of condensed area suggest that proteins prevent some DPPC from partitioning into the domains. These results demonstrate that phase separation of LC DPPC which has been hypothesized to be the basis of surfactant function, does occur.

The neutral lipids, however, produce a dramatic and unexpected change in the phase behavior. Although in all studied films the domains initially emerge and grow, in the presence of neutral lipids the phases abruptly remix into a single phase later during the compression. The shape of the domains prior to remixing undergoes large distortions characteristic of a critical point. Such distortions of the shape occur when the film is near the critical point because the two phases become progressively more similar and therefore the line tension approaches zero. Our finding of the critical point indicates that phase separation does not persist to equilibrium spreading pressures, and therefore it can not serve as the basis of refinement.

The presence of the critical point implies that at least one of the two phases is altered by neutral lipids. The critical behavior represents a continuous transition and therefore the phases must become gradually very similar before they remix into a single phase. Since without the neutral lipids the two separated phases are different, at least one of the separated phases in films with neutral lipids must be now different. The major neutral lipid in pulmonary surfactant is cholesterol or one of its derivatives. Cholesterol is known to interact with acyl chains of phospholipids and it can partition into both phases. To determine the extent to which each of the phases is altered, we need to know the distribution of cholesterol between them. Our calculations of line tensions which are based on the surface potential measurements and the radii of domains predict that significant amounts of cholesterol must partition into domains. These findings then suggest that the condensed phase as well as the remixed film are likely to be more fluid then previously thought.

The fluidity of the otherwise very condensed phase might be a key feature of the film for the following three reasons: (1) it can prevent irreversible breaks of the film that are likely to occur at high surface pressures due to fragility of solid domains at their boundaries; (2) a fluid film can be more flexible and therefore more likely to keep the same properties for all the different curvatures of the alveoli, and (3) it can be a prerequisite for

the formation of three dimensional discs (interdigitated bilayers) that form at the surface upon further compression of pulmonary surfactant films at 30 °C (preliminary data). These interdigitated discs were found also in cholesterol/DPPC mixtures. In both systems the bilayer structures were able to respread very quickly back into the surface upon expansion. Such ability may be important because it can prevent tearing of the film during fast expansion that would create open regions and consequently elevate the surface tension. The three dimensional phase is likely to be more stable than one dimensional phase at high surface pressures.

The ability of the neutral lipids to produce a critical point uncovered their large effect on the structure of the film that can be directly related to the ability of pulmonary surfactant to form very stable films. The existence of a single, very dense phase suggests that the original model for the refinement has to be modified. These studies allowed us to provide more specific possibilities for a new model for the surfactant function. (1) Refinement can be based on the characteristics of individual molecules rather than the phase in which they reside. Constituents can leave the interface from a homogeneous film, according to the characteristics of individual molecules such as shape or charge distribution. (2) There is no need for refinement because the mixed film containing all constituents is sufficiently stable. The presence of the critical point in the phase diagram for pulmonary surfactant indicates that the LE phase can be very dense and possibly very stable at high surface pressures. Therefore it is conceivable that pulmonary surfactant can function without refinement. (3) The stability of the film is provided not by the structure of the interfacial monolayer but by the formation of a three dimensional phase. The existence of a surfactant film that consists of more than a monolayer has been already documented (Schürch et al., 1995; Yu and Possmayer, 1996). Our preliminary data demonstrate that further compression of pulmonary surfactant films leads to formation of discs that have bilayer thickness and rest above the monolayer. The same discs form after compression of binary DPPC/cholesterol mixture above equilibrium spreading pressures. Therefore the

structural reorganization of the film at the critical point might be a prerequisite to the formation of the three dimensional film that is more stable at high surface pressures than just a monolayer and functionally important. Distinction among the three mechanisms will require studies of the film at the high pressures and dynamic conditions present in the lung.

REFERENCES

Albrecht, O., H. Gruler and E. Sackmann. Pressure-composition phase diagrams of cholesterol/lecithin, cholesterol/phosphatidic acid and lecithin/phosphatidic acid mixed monolayers: a Langmuir film balance study. J. Colloid Interface Sci. 79: 319-338, 1981.

Ames, B.N. Assay of inorganic phosphate, total phosphate and phosphatases. Methods in Enzymology VIII: 115-118, 1966.

Avery, M. and J. Mead. Surface properties in relation to atelectasis and hyaline membrane disease. Am. J. Dis. Child 97: 517-523, 1959.

Benvegnu, D.J. and H.M. McConnell. Line Tension between Liquid Domains in Lipid Monolayers. J. Phys. Chem. 96: 6820-6824, 1992.

Bizzozero, O., M.M. Besio, J.M. Pasquini, E.F. Soto and C.J. Gomez. Rapid purification of proteolipids from rat brain subcellular fractions by chromatography on a lipophilic dextran gel. Journal of Chromatography 227: 33-44, 1982.

Bligh, E. and W. Dyer. A rapid method of total lipid extraction and purification. Can. J. Biochem. 37: 911-917, 1959.

Caminiti, S.P. and S.L. Young. The pulmonary surfactant system. Hospital Practice. Physiology in medicine : 57-70, 1991.

Bohdana Discher

"Structural Organization of pulmonary surfactant films"

Format: Manuscript

Chu, J., J.A. Clements, E.K. Cotton, M.H. Klaus, A.Y. Sweet, W.H. Tooley, B.L. Bradley and L.C. Brandorff. Neonatal pulmonary ischemia. I. Clinical and physiological studies. Pediatr. 40: 709-82, 1967.

Clements, J.A. Functions of the alveolar lining. Am. Rev. Respir. Dis. 115: 67-71, 1977.

Curstedt, T., J. Johansson, B. Robertson, P. Persson, B. Löwenadler and H. Jörnvall. Structure and function of hydrophobic surfactant-associated proteins. In Surfactant in clinical practice (Bevilacqua, G., Parmigiani, S. & Robertson, B., eds) Harwood Publisher, 1993, p. 55-60.

Daniels, C.B., S. Orgeig and A.W. Smits. The composition and function of reptilian pulmonary surfactant. Respir. Physiol. 102: 121-135, 1995.

de Koker, R. and H.M. McConnell. Circle to Dogbone: Shapes and Shape Transitions of Lipid Monolayer Domains. J. Phys. Chem. 97: 13419-13424, 1993.

Dluhy, R.A., K.E. Reilly, R.D. Hunt, M.L. Mitchell, A.J. Mautone and R. Mendelsohn. Infrared spectroscopic investigations of pulmonary surfactant. Surface film transitions at the air-water interface and bulk phase thermotropism. Biophys. J. 56: 1173-81, 1989.

Doyle, I.R., M.E. Jones, H.A. Barr, S. Orgeig, A.J. Crockett, C.F. McDonald and T.E. Nicholas. Composition of human pulmonary surfactant varies with exercise and level of fitness. Am. J. Respir. Crit. Care Med. 149: 1619-27, 1994.

Evans, D.A., R.W. Wilmott and J.A. Whitsett. Surfactant replacement therapy for adult respiratory distress syndrome in children. Pediatric Pulmonology 21: 328-36, 1996.

Fujiwara, T., H. Maeta, S. Chida, T. Morita, Y. Watabe and T. Abe. Artificial surfactant therapy in hyaline-membrane disease. Lancet 1: 55-59, 1980.

Gaines, G.L. Insoluble monolayers at liquid-gas interfaces. Wiley (Interscience), New York, 1966.

Grainger, D.W., A. Reichert, H. Ringsdorf and C. Salesse. An enzyme caught in action: direct imaging of hydrolytic function and domain formation of phospholipase A_2 in phosphatidylcholine monolayers. FEBS Letters 252: 73-82, 1989.

Gregory, T.J., K.P. Steinberg, R. Spragg, J.E. Gadek, T.M. Hyers, W.J. Longmore, M.A. Moxley, G.Z. Cai, R.D. Hite, R.M. Smith, L.D. Hudson, C. Crim, P. Newton, B.R. Mitchell and A.J. Gold. Bovine surfactant therapy for patients with acute respiratory distress syndrome. Am. J. Respir. Crit. Care Med. 155: 1309-15, 1997.

Haagsman, H.P. and L.M. van Golde. Synthesis and assembly of lung surfactant. Annu. Rev. Physiol. : 441-64, 1991.

Hagen, J.P. and H.M. McConnell. Critical pressures in multicomponent lipid monolayers. Biochim. Biophys. Acta 1280: 169-72, 1996.

Hall, S.B., A.R. Venkitaraman, J.A. Whitsett, B.A. Holm and R.H. Notter. Importance of hydrophobic apoproteins as constituents of clinical exogenous surfactants. Am. Rev. Respir. Dis. 145: 24-30, 1992.

Hall, S.B., Z. Wang and R.H. Notter. Separation of subfractions of the hydrophobic components of calf lung surfactant. J. Lipid Res. 35: 1386-94, 1994.

Hénon, S. and J. Meunier. Microscope at the Brewster angle: direct observation of first-order phase transitions in monolayers. Rev. Sci. Instr. 62: 936-939, 1991.

Hirshfeld, C.L. and M. Seul. Critical mixing in monomolecular films: pressure-composition phase diagram of a two-dimensional binary mixture. J. Physique (Paris). 51: 1537-1552, 1990.

Holub, B.J. and A. Kuksis. Metabolism of molecular species of diacylglycerophospholipids. Advances in Lipid Research 16: 1-125, 1978.

Hönig, D. and D. Möbius. Direct visualization of monolayers at the air-water interface by Brewster angle microscopy. J. Phys. Chem. 95: 4590-4592, 1991.

Hudak, M.L., D.J. Martin, E.A. Egan, E.J. Matteson, N.J. Cummings, A.L. Jung, L.V. Kimberlin, R.L. Auten, A.A. Rosenberg, J.M. Asselin, M.R. Belcastro, P.K. Donohue, C.R.J. Hamm, R.D. Jansen, A.S. Brody, M.M. Riddlesberger, P. Montgomery, C.T.J. Article., M.S.R.C.T. . and J. 100(1):39-50. A multicenter randomized masked comparison trial of synthetic surfactant versus calf lung surfactant extract in the prevention of neonatal respiratory distress syndrome. Pediatr. 100: 39-50, 1997.

Israelachvili, J.N. Intermolecular & Surface Forces. Academic Press., 1994, p. 28.

Jobe, A.H. Pulmonary surfactant therapy. N. Engl. J. Med. 328: 861-8, 1993.

Johansson, J. and T. Curstedt. Molecular structures and interactions of pulmonary surfactant components. Eur. J. Biochem. 244: 675-693, 1997.

Kahn, M.C., G.J. Anderson, W.R. Anyan and S.B. Hall. Phosphatidylcholine molecular species of calf lung surfactant. Am. J. Physiol. 269: L567-73, 1995.

Kaplan, R.S. and P.L. Pedersen. Sensitive protein assay in presence of high levels of lipid. Methods in Enzymology 172: 393-9, 1989.

Kendig, J.W., R.H. Notter, W.M. Maniscalco, J.M. Davis and D.L. Shapiro. Clinical experience with calf lung surfactant extract. In: Surfactant replacement therapy., edited by D. L. Shapiro and R. H. Notter. Alan R. Liss, Inc., New York, 1989. p. 257-271.

Keough, K.M.W. Physical chemical properties of some mixtures of lipids and their potential for use in exogenous surfactants. Prog. Respir. Res. 18: 257-262, 1984.

Keough, K.M.W. Physical Chemistry of Pulmonary Surfactant in the Terminal Air Spaces. In: Pulmonary surfactant: from molecular biology to clinical practice., edited by B. Robertson, L. M. G. Van Golde and J. J. Batenburg. Elsevier Science Publishers, Amsterdam, 1992, p. 109-164.

Klopfer, K.J. and T.K. Vanderlick. Isotherms of dipalmitoylphosphatidylcholine (DPPC) monolayers: features revealed and features obscured. J. Colloid Interface Sci. 182: 220-229, 1996.

Knobler, C.M. Recent developments in the study of monolayers at the air-water interface. Advances in Chemical Physics 77: 397-449, 1990.

Korfhagen, T.R., M.D. Bruno, G.F. Ross, K.M. Huelsman, M. Ikegami, A.H. Jobe, S.E. Wert, B.R. Stripp, R.E. Morris, S.W. Glasser, C.J. Bachurski, H.S. Iwamoto and J.A. Whitsett. Altered surfactant function and structure in SP-A gene targeted mice. Proceedings of the National Academy of Sciences of the United States of America. 93: 9594-9, 1996.

Kuksis, A., L. Marai, W.C. Breckenridge, D.A. Gornall and O. Stachnyk. Molecular species of lecithins of some functionally distinct rat tissues. Can. J. Physiol. Pharmacol. 43: 511-24, 1968.

Kuroki, Y., M. Shiratori, Y. Ogasawara, A. Tsuzuki and T. Akino. Characterization of pulmonary surfactant protein D: its copurification with lipids. Biochim. Biophys. Acta 1086: 185-90, 1991.

LeVine, A.M., M.D. Bruno, K.M. Huelsman, G.F. Ross, J.A. Whitsett and T.R. Korfhagen. Surfactant protein A-deficient mice are susceptible to group B streptococcal infection. Journal of Immunology 158: 4336-40, 1997.

Lewis, J.F. and R.A. Veldhuizen. Factors influencing efficacy of exogenous surfactant in acute lung injury. Biology of the Neonate 67: 48-60, 1995.

Lipp, M.M., K.Y.C. Lee, J.A. Zasadzinski and A.J. Waring. Phase and morphology changes in lipid monolayers induced by SP-B protein and its amino-terminal peptide. Science 273: 1196-1199, 1996.

Lösche, M., E. Sackmann and H. Möhwald. A fluorescence microscopic study concerning the phase diagram of phospholipids. Ber. Bunsenges. Phys. Chem. 87: 848-852, 1983.

Ma, S.-K. Modern Theory of Critical Phenomena. Frontiers in Physics, Lecture Note Series 46, 1982, p. 445.

Maloney, K.M. and D.W. Grainger. Phase separated anionic domains in ternary mixed lipid monolayers at the air-water interface. Chem. Phys. Lipids 65: 31-42, 1993.

McConnell, H.M. Structures and transitions in lipid monolayers at the air-water interface. Annu. Rev. Phys. Chem. 42: 171-195, 1991.

McConnell, H.M., L.K. Tamm and R.M. Weis. Periodic structure in lipid monolayer phase transitions. Proc. Natl. Acad. Sci. USA 81: 8249-3253, 1984.

Meller, P. Computer-assisted video microscopy for the investigation of monolayers on liquid and solid substrates. Rev. Sci. Instr. 59: 2225-2231, 1988.

Montfoort, A., L.M. van Golde and L.L. van Deenen. Molecular species of lecithins from various animal tissues. Biochim. Biophys. Acta 231: 335-42, 1971.

Muller, P. and F. Gallet. First Measurement of the Liquid-Solid Line Energy in a Langmuir Monolayer. Phys. Rev. Lett. 67: 1106-1109, 1991.

Nag, K. and K.M. Keough. Epifluorescence microscopic studies of monolayers containing mixtures of dioleoyl- and dipalmitoylphosphatidylcholines. Biophys. J. 65: 1019-26, 1993.

Nag, K., J. Perez-Gil, A. Cruz and K.M. Keough. Fluorescently labeled pulmonary surfactant protein C in spread phospholipid monolayers. Biophys. J. 71: 246-256, 1996.

Nag, K., S.G. Taneva, J. Perez-Gil, A. Cruz and K.M. Keough. Combinations of fluorescently labeled pulmonary surfactant proteins SP-B and SP-C in phospholipid films. Biophys. J. 72: 2638-2650, 1997.

Orgeig, S., H.A. Barr and T.E. Nicholas. Effect of hyperpnea on the cholesterol to disaturated phospholipid ratio in alveolar surfactant of rats. Experimental Lung Research 21: 157-74, 1995.

Pattle, R.E. Properties, function and origin of the alveolar lining layer. Nature 175: 1125-1126, 1955.

Peters, R. and K. Beck. Translational diffusion in phospholipid monolayers measured by fluorescence microphotolysis. Proc. Natl. Acad. Sci. (U.S.A.) 80: 7183-7, 1983.

Possmayer, F. A proposed nomenclature for pulmonary surfactant-associated proteins. Am. Rev. Respir. Dis. 138: 990-998, 1988.

Poulain, F.R. and J.A. Clements. Pulmonary surfactant therapy. West. J. Med. 162: 43-50, 1995.

Putz, G., J. Goerke and J.A. Clements. Surface activity of rabbit pulmonary surfactant subfractions at different concentrations in a captive bubble. J. Appl. Physiol. 77: 597-605, 1994.

Rice, P.A. and H.M. McConnell. Critical shape transitions of monolayer lipid domains. Proc. Natl. Acad. Sci. (U.S.A.) 86: 6445-6448, 1989.

Rivière, S., S. Hénon and J. Meunier. Phys. Rev. E 49: 1375, 1994.

Rivière, S., S. Hénon, J. Meunier, G. Albrecht, M.M. Boissonnade and A. Baszkin. Electrostatic Pressure and Line Tension in a Langmuir Monolayer. Phys. Rev. Lett. 75: 2506-2509, 1995.

Robertson, B. Pathology and pathophysiology of neonatal surfactant deficiency ("respiratory distress syndrome," "hyaline membrane disease"). In: Pulmonary Surfactant, edited by B. Robertson, L. M. G. Van Golde and J. J. Batenburg. Elsevier Science Publishers, Amsterdam, 1984, p. 383-418.

Rowlinson, J.S. and B. Widom. Molecular theory of capillarity. Clarendon Press, Oxford, 1982.

Schürch, S. Surface tension at low lung volumes: dependence on time and alveolar size. Respir. Physiol. 48: 339-55, 1982.

Schürch, S., R. Qanbar, H. Bachofen and F. Possmayer. The surface-associated surfactant reservoir in the alveolar lining. Biology of the Neonate 67: 61-76, 1995.

Searcy, R.L. and L.M. Bergquist. A new color reaction for the quantitation of serum cholesterol. Clin. Chim. Acta 5: 192-199, 1960.

Seul, M. and M.J. Samon. Competing interactions and domain-shape instabilities in a monomolecular film at an air-water interface. Phys. Rev. Lett. 64: 1903-1906, 1990.

Shiffer, K., S. Hawgood, H.P. Haagsman, B. Benson, J.A. Clements and J. Goerke. Lung surfactant proteins, SP-B and SP-C, alter the thermodynamic properties of phospholipid membranes: a differential calorimetry study. Biochemistry 32: 590-7, 1993.

Slotte, J.P. Lateral domain formation in mixed monolayers containing cholesterol and dipalmitoylphosphatidylcholine or N-palmitoylsphingomyelin. Biochim. Biophys. Acta 1235: 419-27, 1995.

Subramaniam, S. and H.M. McConnell. Critical mixing in monolayer mixtures of phospholipid and cholesterol. J. Phys. Chem. 91: 1715-1718, 1987.

Suchyta, M.R., T.P. Clemmer, C.G. Elliott, J.F. Orme, Jr. and L.K. Weaver. The adult respiratory distress syndrome. A report of survival and modifying factors. Chest 101: 1074-9, 1992.

Swendsen, C.L., V. Skita and R.S. Thrall. Alterations in surfactant neutral lipid composition during the development of bleomycin-induced pulmonary fibrosis. Biochim. Biophys. Acta 1301: 90-6, 1996.

Takahashi, A. and T. Fujiwara. Proteolipid in bovine lung surfactant: its role in surfactant function. Biochem. Biophys. Res. Comms. 135: 527-32, 1986.

van Eijk, M., C.G. De Haas and H.P. Haagsman. Quantitative analysis of pulmonary surfactant proteins B and C. Analytical Biochemistry 232: 231-237, 1995.

Watkins, J.C. The surface properties of pure phospholipids in relation to those of lung extracts. Biochim. Biophys. Acta 152: 293-306, 1968.

Weis, R.M. Fluorescence microscopy of phospholipid monolayer phase transitions. Chem. Phys. Lipids 57: 227-239, 1991.

Weis, R.M. and H.M. McConnell. Two-dimensional chiral crystals of phospholipid. Nature 310: 47-9, 1984.

APPENDICES

A. Protein Assay

The following protocol is based on previously published procedure (Kaplan and Pedersen, 1989).

Solutions:

Distilled water (referred to as water below)

Standard solution: 0.1% (w/v) BSA

10% (w/v) SDS

1 M TRIS / 1% (w/v) SDS, pH = 7.5

104% (w/v) TCA

6% (v/v) TCA

Staining solution: 0.02% (w/v) Amido Black 10B dissolved in
methanol : glacial acetic acid : water 45:10:45 (v/v/v)

Destaining solution: methanol : glacial acetic acid : water 45:1:4

Elution buffer: 25 mM NaOH/0.05 mM EDTA/50% (v/v) ethanol

Preparation:

Turn on spectrophotometer and set to 630 nm.

Wear unpowdered gloves during the entire procedure.

Number HA Millipore filters (HAWP 02500, 0.45 µm pore, Millipore, MA) with pencil (#2). Place them in water.

Set up filter manifold (Millipore, MA). Plug empty holes with rubber stoppers. Keep water in the chambers with filters before the actual assay..

If possible, calculate what volume contains 2 - 24 µg of proteins.

Use 13 x 100 mm glass test tubes for prefiltration steps and 12 x 75 mm for elution.

Pipette 30, 60, 90, 120, 150 µl of standard solution into test tubes.

Assay:

1. Dilute samples and standards to 2 ml with water. Include blank test tube (with 2 ml of water).
2. Add 0.2 ml 10% (w/v) SDS. Vortex vigorously. If sample includes lipid or proteolipid, warm samples for 3 minutes in water bath (about 45 °C). Vortex tubes in rotation during the 3 minutes period.
3. Add 0.3 ml of 1 M TRIS / 1% (w/v) SDS, pH = 7.5. Vortex vigorously.
4. Add 0.6 ml of 104% (w/v) TCA. Vortex vigorously. Incubate at least 3 minutes.
5. Pour sample on filter in Millipore manifold. Filter under vacuum. Tap the tube gently against filter to release the last drop of sample. Add 2 ml 6% (v/v) TCA into the empty tube, vortex, and pour on the same filter in Millipore manifold. Filter under vacuum.
6. Carefully transfer filters to beaker for staining.

7. Add staining solution. Swirl gently for 3 minutes. Note: volumes of staining and destaining solution need only to be enough to cover filters generously (you can use 60 - 80 ml in 150 ml beaker).

8. Pour off the staining solution. It can be reused.

9. Wash for 1 minute with destaining solution swirling gently. Repeat 3 times.

10. Wash with water for 2 minutes swirling gently.

11. Cut the filter into small pieces and place into 12 x 75 mm test tube.

12. Add 0.7 ml elution buffer. Incubate for 20 minutes, vortexing occasionally.

13. Use clean Pasteur pipette to transfer elution buffer from each sample to 1 ml cuvette.

14. Read optical density at 630 nm against air.

15. Determine the linear equation for the protein amount as a function of the optical density from the standards and calculate the amount of protein for the samples. Determine concentration of the samples based on the dilution.

B. Phosphate assay

The following protocol is based on previously published procedure (Ames, 1966).

Take extreme care when handling concentrated acids. Wear protective clothing/gloves.

Solutions:

1. Phosphate standard solution: 0.1 mM KH_2PO_4
2. 10% (w/v) $Mg(NO_3)_2$-6 H_2O in 95% ethanol
3. 0.5 N HCl
4. 0.42% (w/v) Ammonium Molybdate in 1N H_2SO_4
5. 10% (w/v) Ascorbic Acid

Assay:

1. Label seven test tubes (13 x 100 mm): 0, 20, 40, 60, 80, 100, 200. Pipette 0, 200, 400, 600, 800, 1000, 2000 µl of the phosphate standard into respective test tubes. Dry in an oven at 125 °C overnight in a metal test tube rack.
2. Let samples come to room temperature. Label test tubes. Pipette samples into test tubes. Aim for 5 to 20 nmoles in each test tube. Use appropriate pipette for samples in organic solvents. Dry the samples under nitrogen or on heating block.
3. Add 200 µl of 10% $Mg(NO_3)_2$ solution into each test tube (samples and standards).
4. Place all tubes in a drying oven or heat block (100 -125 °C) until all of the ethanol has evaporated leaving white crystals behind (20 - 30 minutes).

5. In hood, heat the base of each tube over a Bunsen burner. Within 2 minutes, yellow-brown fumes appear, then disappear, turning the inside of the tube chalky white (this is called chalking). Wear "heat prove gloves" and use a metal test tube holder.

6. Add 1 ml of 0.5 N HCl to each test tube.

7. Place all tubes in a heat block (85 - 100 °C) for 30 minutes. To prevent evaporation, place a marble on top of each test tube and keep an air stream blowing across the top of the test tubes.

8. Prepare a mixture of 6 parts Ammonium Molybdate and 1 part 10% Ascorbic Acid. Mix it at the last minute. Add 2 ml of this solution to each tube.

9. Place all tubes in a 45 °C water bath for 30 minutes. Vortex once during the incubation.

10. Set spectrophotometer at 820 nm. Vortex each tube before recording the optical density.

11. Determine the linear equation for the phosphate amount as a function of the optical density from the standards and calculate the amount of phosphate for the samples. Determine concentration of the samples based on the dilution.

C. Cholesterol assay

The following protocol is based on previously published procedure (Searcy and Bergquist, 1960).

Solutions:

1. 50:50 (v/v) ethanol:acetone (use 200 proof ethanol)
2. Standard solution: 0.6 mg/ml cholesterol in 50:50 ethanol:acetone
3. Prepare saturated solution of ferrous sulfate (crystal, heptahydrate) in glacial acetic acid. Usually few grams are sufficient since the ferrous sulfate is only slightly soluble in the acid. Stir for an hour and let sit overnight. Filter using Whatman #3 or comparable paper to obtain clear solution.
4. Concentrated sulfuric acid

Assay:

1. Turn on spectrophotometer and set to 490 nm.
2. Pipette 15, 20, 25, 35, and 45 ml of standard solution. Use large volume test tubes to avoid splashing of concentrated acid during vortexing later in the procedure. Include blank tube. Pipette your samples. Aim for 25 μg of cholesterol.
3. Bring all the test tubes to a total volume of 100 μl using the 50:50 ethanol:acetone solution.

Note: The next two steps should be conducted in the hood with gloves. This is a concentrated acid. Neutralize the glass pipettes used to deliver solutions (and any spills) with baking soda.

4. Add 1.5 ml of ferrous sulfate solution to each tube. Vortex.

5. Add 500 µl of sulfuric acid and vortex.

6. Read optical density at 490 nm against air 10 minutes after the addition of sulfuric acid. Use new cuvette for each sample. Neutralize the solutions with baking soda before discarding.

D. Separation of components from CLSE

The proteins, phospholipids, and neutral lipids were separated with LH-20 column chromatography (Hall, 1994). The 2.5 x 100 cm column was pre-equilibrated with elution buffer chloroform:methanol:0.1 N HCl 95:95:10 (v/v/v) that was pumped up against gravity during the equilibration and also during the actual purification. 500 µl of sample was injected into the preequilibrated column and eluted at rate 12 ml/hour into fractions collected every 15 minutes. Fractions were assayed for protein, phospholipid, and cholesterol (Fig. 4.1).

E. Experimental Instrumentation:

The experimental setup has been built with the following components:

I. Constant perimeter ribbon barrier apparatus for confinement of interfacial films

II. Linear variable displacement transducer

III. Epifluorescence microscope with digital imaging equipment

IV. Control box and computer

I. Constant perimeter ribbon barrier apparatus for confinement of interfacial films

The ribbon barrier compression system was manufactured by J - L Automation Ltd., Sunderland, United Kingdom to the following specifications:

1. 2 cm ribbon barrier, teflon coated (Labcon Limited, Darlington, United Kingdom)
2. Initial area 530 cm^2, final area less than 20% of the initial area
3. System mounted on an aluminum base
4. Aluminum components to be anodized
5. Mid-point on the vertical dimension of the ribbon to be approximately 6 cm above bench top
6. External barrier control electronics to move barrier between 0 and 40 cm^2 per second, with stabilized control at low speed
7. 0 - 10 V potentiometer output to indicate barrier position

The final ribbon barrier specifications are shown in Fig. E.1. The teflon trough with tubing underneath for temperature regulation was made by Scientific Instrument Division,

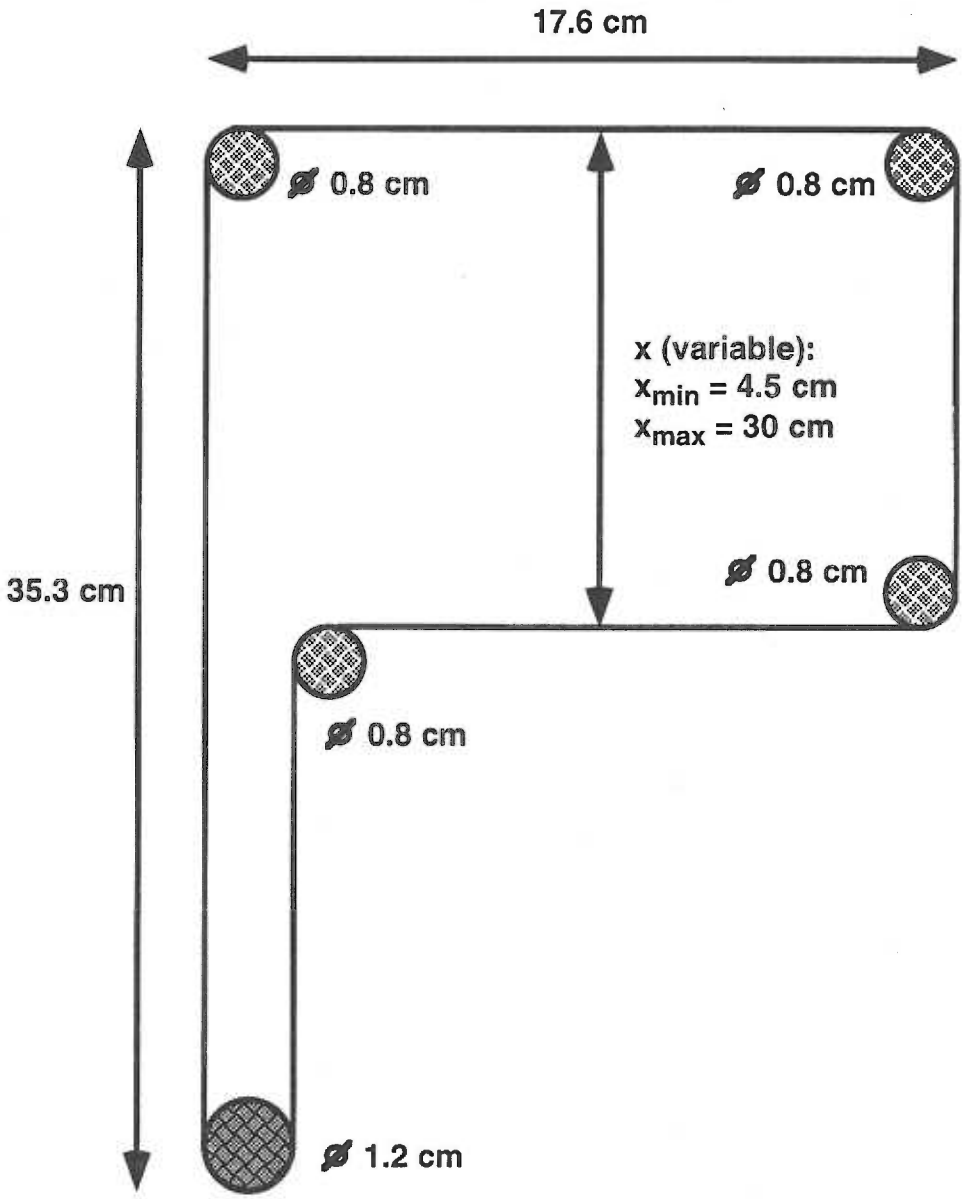

E.1. Ribbon barrier specifications. The circles are profiles of teflon posts, the ribbon barrier is the line surrounding the posts.

University of Washington, Seattle, WA. The temperature was controlled with water pumped by digital programmable temperature controller 070594-VWR, VWR. The subphase temperature was measured by monitoring thermometer 15-077-8C, Fisher.

II. Force measurement: linear variable displacement transducer:

The surface pressure was measured with Wilhelmy plate 1.5 x 2 cm cut out of filter paper using linear variable displacement transducer, Omega, Stamford, CT. The displacement transducer uses a solenoid with magnetic core. By attaching the magnetic core of the solenoid for the displacement transducer to a flat spring (Figure E.2), force on the Wilhelmy plate produces a linear variation in the position of the core and therefore in inductance. The inductance is then calibrated to force units.

III. Epifluorescence microscope with digital imaging equipment

The microscope was assembled by Meridian Instrument Company, Inc., Kent, WA, using the following parts:

1. Episcopic - fluorescence attachment EFD - 3, Nikon, Japan
2. Diascopic DIC Nomarski attachment, Nikon, Japan
3. Optiphot-2, Nikon, Japan
4. Labophot -2A/-2, Nikon, Japan
5. Super High Pressure mercury lamp power supply HB-10101AF and lamp housing, Nikon, Japan
6. Mercury short arc lamp, HBO 100 W/2, made in Germany, purchased from Pacific Lamp Wholesale, Beaverton, OR

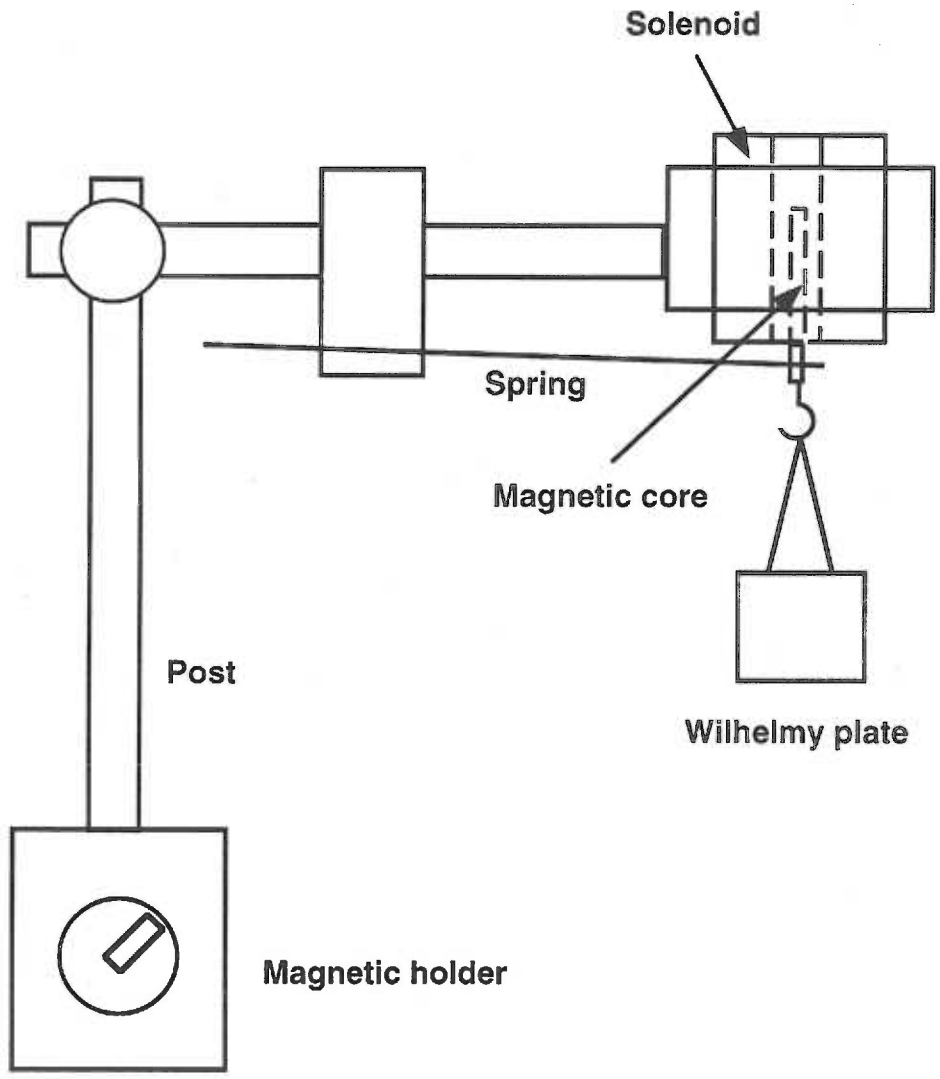

E.2. Scheme of linear variable displacement transducer.

7. Dichroic filters 31001-FITC/Bodipy/Fluo3/DiO and 31002-TRITC/DiO from Chroma Technology Corp.
8. Reflected light infinity corrected, bright field Epi Plan, super long working distance objective MTI SLWD EPI 100, magnification 100x, numerical aperture 0.73, working distance 4.7 mm, focal length 2 mm, resolving power 0.38 μm, depth of field 0.52 μm, Nikon, Japan
9. Monochrome SIT camera Hamamatsu C2400
10. Black and white video monitor PVM-137, Sony
11. VCR M-752 (6 head 19 μ, Pro Drum V3 Technology, Hi-Fi, VHS), Toshiba
12. IsoStation™ vibration isolated workstation NPVH-3036-OPT7, Newport, Irvine, CA

The diagram of the fluorescence microscope is shown in Fig. E.3. The images were recorded to VHS tape or directly to computer with a LG-3 frame grabber, Scion Corp., Frederick, MD. The conversion between pixels and μm was determined using Precision Ronchi Ruling, 300 lines per inch, 1 x 1", G30,518, Edmund Scientific Co., Barrington, NJ. The conversion factor has been found to be 0.6 μm per pixel.

IV. Control box and computer

The control electronics were placed into single control box by Scientific Instrument Division, University of Washington, Seattle, WA. The equipment was controlled by MacIntosh IIci computer, Apple, Cupertino, CA using LabView for Mac: Full development system software, Cat. # 776690-01, Ni-DAQ Software version 4.7, #320103-01, and data acquisition board Lab-NB, #320174B-01, National Instruments, Austin, TX. Our actual LabView program that controlled the equipment is included in Figures E.4. - E.7.

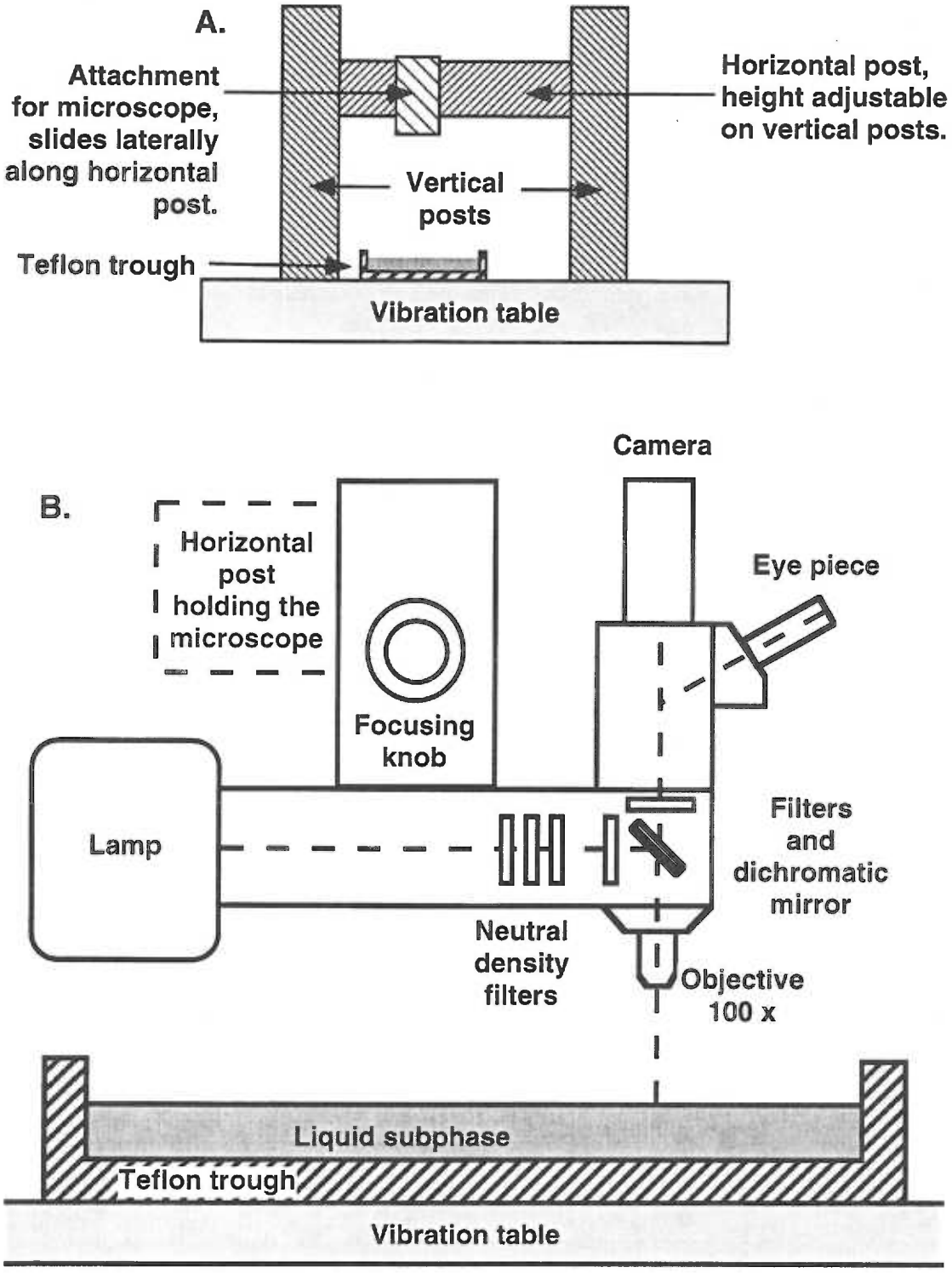

E.3. Schematic diagram of support structure for fluorescence microscope. (A) Front view. (B) Side view.

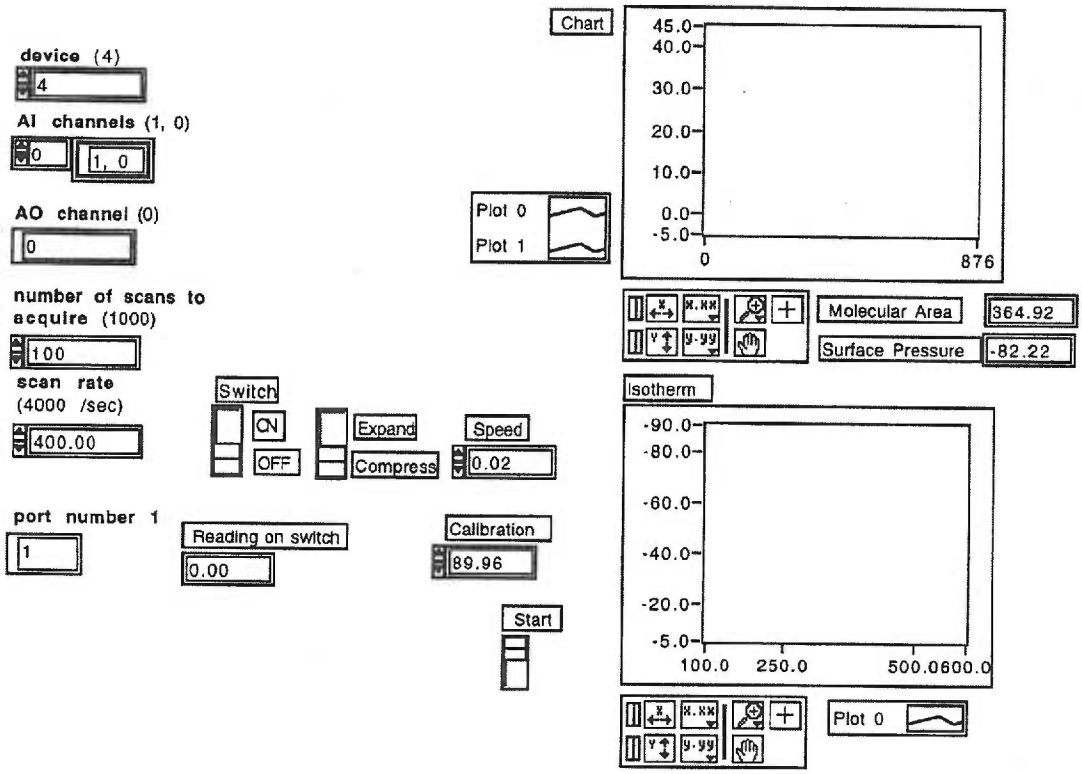

E.4. Front panel of the LabView program that was used to control the equipment. On the left side are input parameters that specify what device, input channels, output channel and port are used, the number of scans required, and the scan rate. The device number identifies the acquisition card, the input channel were linked to the signals from linear variable displacement transducer and potentiometer, and output channel was linked to the motor for barrier movement. The switches in the middle allowed to start and stop the compression or expansion, set the speed of compression, and adjust the surface pressure values based on calibration by palmitic acid. The windows on the left displayed the input values in the chart (top) and compression isotherm (bottom).

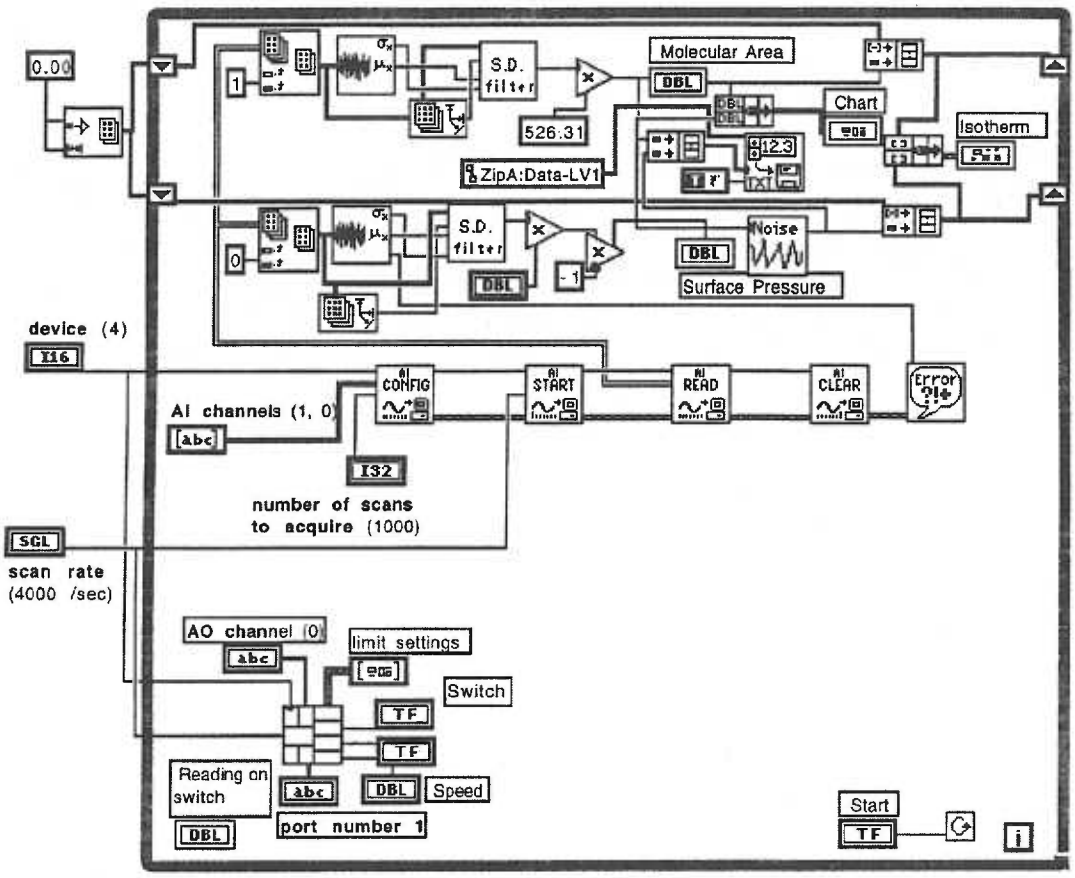

E.5. Block diagram of the LabView program that was used to control the equipment. The core of the program that acquired the analog input data (surface pressure and trough area) was the "Getting Started Analog Input Virtual Instrument" provided by National Instruments (Austin, TX) with the LabView program. The acquired data were assembled into arrays of 1000 data points and filtered for noise by S.D. filter described below. The filtered data were displayed on chart, in graph as isotherm, and recorded by computer into the file Data-LV1. The barrier movement was controlled by "Getting Started Analog Output Virtual Instrument" also provided by National Instruments (Austin, TX) with the LabView software.

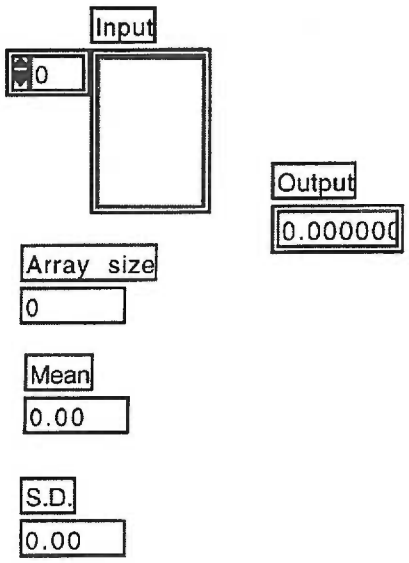

E.6. Front panel of the "S.D. Filter subVI". The following incoming values has to be obtained before executing this subVI: data points to be filtered (input), array size (number of data in points in the array = 1000), mean and standard deviation of the data points in the array. The subVI then filters out the numbers that are outside of mean +/- 1.5 times the standard deviation and calculates the mean of the values inside the specified range.

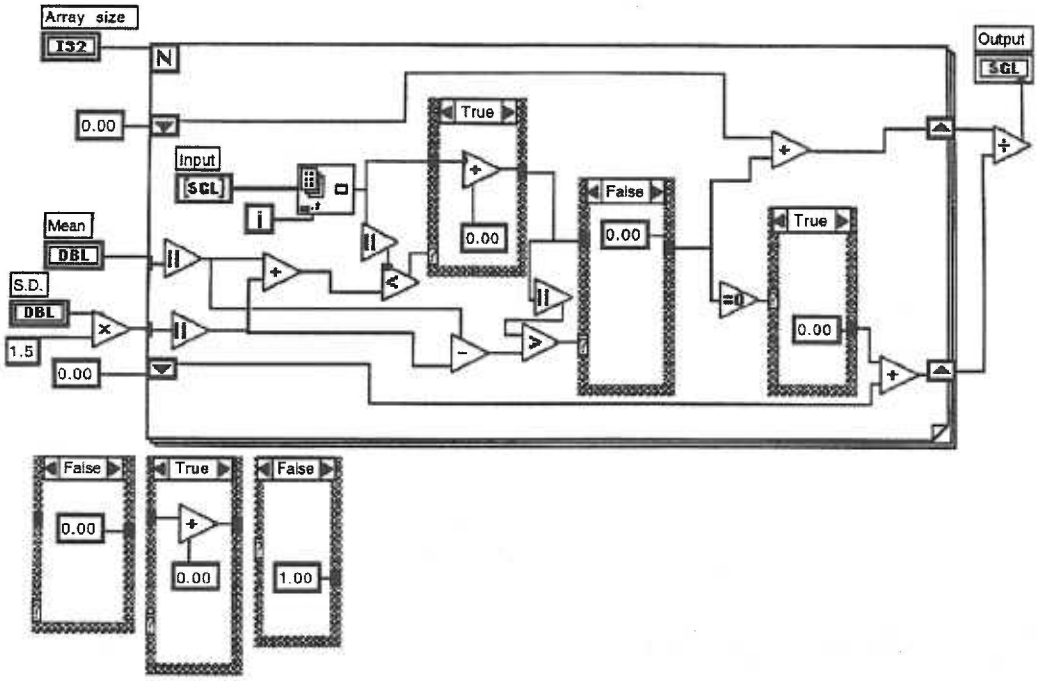

E.7. Block diagram of the "S.D. Filter subVI".